DOE/NV/10150-6
(DE85009464)

(40)
DR-1310-2

Energy

GEOTHERMAL

ANALYSIS OF FLOW DATA FROM THE T-F&S/DOE GLADYS McCALL NO. 1 WELL

Final Report

By
J. W. Pritchett
T. D. Riney

January 1985

Work Performed Under Contract No. AC08-80NV10150

S-CUBED
Maxwell Laboratories, Inc.
La Jolla, California

Technical Information Center
Office of Scientific and Technical Information
United States Department of Energy

DISCLAIMER

DISCLAIMER

Available from the National Technical Information Service, U. S. Department of Commerce, Springfield, Virginia 22161.

Price: Printed Copy A06
Microfiche A01

Codes are used for pricing all publications. The code is determined by the number of pages in the publication. Information pertaining to the pricing codes can be found in the current issues of the following publications, which are generally available in most libraries: *Energy Research Abstracts (ERA); Government Reports Announcements* and Index *(GRA* and I); *Scientific and Technical Abstract Reports (STAR);* and publication NTIS-PR-360 available from NTIS at the above address.

Printed in the United States of America
USDOE Office of Scientific and Technical Information
Oak Ridge, Tennessee

S-CUBED
A Division of Maxwell Laboratories, Inc.

DOE/NV/10150-6
(DE85009464)
Distribution Category UC-66a

ANALYSIS OF FLOW DATA FROM THE T-F&S/DOE GLADYS McCALL NO. 1 WELL

FINAL REPORT

J. W. Pritchett
T. D. Riney

Work Performed under Contract
DE-AC08-80-NV10150

JANUARY 1985

Prepared for
Department of Energy
Nevada Operations Office

P. O. Box 1620, La Jolla, California 92038-1620
(619) 453-0060

FOREWORD

This final technical report describes work performed by S-CUBED, a Division of Maxwell Laboratories, Inc., under a Contract (DE-AC08-80NV10150) with the U. S. Department of Energy. The work consists of well test analysis and reservoir performance simulations for geopressured geothermal systems in the Texas/Louisiana Gulf Coast region. The report summarizes analyses of flow data from geopressured geothermal design wells (Pleasant Bayou No. 2, Amoco Fee No. 1, L. R. Sweezy No. 1) and a parametric study of brine/gas recovery from geopressured systems. These results have been described in detail in earlier formal reports issued under this contract. Analysis of the flow data from the Gladys McCall No. 1 geopressured geothermal well and reservoir simulation history-matching studies are described in detail in this report. The present report together with the four earlier formal reports comprise the Final Report for the subject contract.

ABSTRACT

The flow and bottomhole pressure data have been analyzed for the two sands (Nos. 8 and 9) tested by the Gladys McCall No. 1 Well. The more productive sand (No. 8) appears to be bounded by two linear faults at distances of ~ 740 feet and ~ 1360 feet from the well and there appears to be a decrease in the formation transmissivity away from the well. The formation properties inferred from the well test analysis have been used with a reservoir simulator to match the bottomhole drawdown/buildup history measured during the Reservoir Limits Test of Sand Zone No. 8. Wellhead pressure data measured during the long-term production testing of Sand Zone No. 8 have been employed to estimate the corresponding downhole pressures. The simulation model based solely on the Reservoir Limits Test is found to be in remarkably good agreement with the estimated bottomhole pressures for the first six months of production testing, but enlargement of the reservoir volume, by moving the boundary most remote from the well outward, is required to adequately match the full production history. The added remote volume corresponds to an increase by a factor of three in the estimated reservoir volume. The results for the Gladys McCall well are discussed in the context of earlier results determined from testing the other through geopressured geothermal design wells (Pleasant Bayou No. 2, Amoco Fee No. 1 and L. R. Sweezy No. 1 Well).

TABLE OF CONTENTS

LIST OF ILLUSTRATIONS

LIST OF ILLUSTRATIONS (Continued)

LIST OF ILLUSTRATIONS (Continued)

LIST OF TABLES

I. INTRODUCTION

1.1 BACKGROUND

The U. S. Department of Energy (DOE) has the lead role in determining the technical, economic, and environmental feasibility of extracting energy from the geopressured-geothermal resource located in the northern Gulf of Mexico basin. As part of its geopressured program, DOE has been conducting a deep well drilling and testing program in the Gulf Coast region to help evaluate the resource. Four geopressured test wells have been drilled at sites located in Texas and Louisiana. Testing of two of these "Design Wells" has been completed and long-term production testing of the other two design wells is still underway. In addition, a number of existing nonproductive petroleum and gas wells drilled into geopressured strata by private companies were re-entered and flow-tested under the DOE "Wells of Opportunity" program.

Basically, the ongoing DOE Design Wells Program is intended to test large (e.g., one cubic mile volume), potentially commercial geopressured reservoirs over extended time periods. The now completed DOE Wells of Opportunity Program, on the other hand, was intended to secure fluid samples for determining fluid properties and dissolved gas content and to perform short-term production tests over a wider sample of geopressured reservoirs.

Under the DOE Design Wells Program, the following four production wells have been drilled and tested:

1. Fenix and Scission-DOE, Pleasant Bayou No. 2 Well, Brazoria County, Texas.

2. Magma Gulf-Technadril-DOE, Amoco Fee No. 1 Well, Sweet Lake Field, Cameron Parish, Louisiana.

3. DOW-DOE, L. R. Sweezy No. 1 Well, Parcperdue Field, Vermilion Parish, Louisiana.

4. Technadril-Fenix and Scisson-DOE, Gladys McCall No. 1 Well, Cameron Parish, Louisiana.

Testing of the Amoco Fee No. 1 Well and the L. R. Sweezy No. 1 Well has been completed, and the wells have been plugged and abandoned. Long-term production testing of the Gladys McCall No. 1 Well is still in progress. Since May 1984, the methane produced by the ongoing flow test has been sold commercially. Long-term production testing of the Pleasant Bayou No. 2 Well is planned to restart during 1985. The production test will be performed in conjunction with surface testing of a hybrid electricity generation plant. The Electrical Power Research Institute (EPRI) plans, in cooperation with DOE, to operate a 1 MW system utilizing the hydraulic, thermal and chemical (primarily methane gas) energies of the produced brine. The Pleasant Bayou and Gladys McCall wells are very productive and penetrate very large reservoirs. S-CUBED has performed analyses of the flow data to determine reservoir properties and performed reservoir simulation studies for all four of the DOE design wells under DOE Contract DE-AC08-80-NV10150. Formal DOE reports have been previously issued describing the S-CUBED analyses of data from the Pleasant Bayou No. 2 Well (Garg, et al., 1981), Amoco Fee No. 1 Well (Garg, 1982) and L. R. Sweezy No. 1 Well (Garg and Riney, 1984a). The present report describes the analysis of the flow data and reservoir simulation studies performed on the geopressured sands tested by the Gladys McCall No. 1 Well.

The DOE in cooperation with the U. S. Geological Survey, has also funded studies to define the recoverable energy from the Gulf Coast geopressured-geothermal resource base. S-CUBED has performed calculations under DOE Contract DE-AC08-80-NV10150 in support of this effort. A formal DOE report has been issued describing

parametric calculations performed by S-CUBED to define the brine and gas recovery from geopressured systems (Garg and Riney, 1984b).

The present report together with the four referenced formal reports comprise the Final Report for DOE Contract DE-AC08-80-NV10150. The results of the previous reports will first be summarized and then the contents of the present report will be outlined.

1.2 ABSTRACTS OF PREVIOUS REPORTS

The Phase I flow testing of the Pleasant Bayou No. 2 well at rates up to ~ 19,000 bbl/day was conducted from September 16, 1980 to December 15, 1980. Analysis of the 45-day drawdown/45-day buildup data indicates the presence of a linear barrier at approximately 3,000 ft, and that the skin factor varied during the test (Garg, et al., 1981). No other reservoir boundaries can be identified from the Phase I test data. The reservoir formation parameters (e.g., permeability, ~ 192 md, porosity ϕ = 0.18 and variable skin factor, s) inferred from the downhole pressure buildup data were employed in the MUSHRM reservoir simulator to successfully history match the Phase I downhole drawdown/buildup pressure and flow rate data. Subsequent (Phase II) long-term testing of the Pleasant Bayou No. 2 well has not included downhole pressure measurements.

Sand Zone No. 5 of the sand-shale sequence penetrated by the Amoco Fee No. 1 Well was flow tested during June-July, 1981. Analysis of the downhole pressure buildup data from the well indicates a permeability of ~ 162 md near the wellbore (radius < 200 ft) but a far-field permeability (> 200 ft) of only ~ 12 md (Garg, 1982). An alternate interpretation of the test data would be to assume that the flow to the well is restricted by intersecting faults (graben angle ~ 26°) located at about 200-250 ft from the well. In any case, the well was not able to sustain high production

rates (> 10,000 bbl/day). Subsequent testing of Sand Zone No. 3 gave similar disappointing results, and the well was plugged and abandoned during 1984.

The well test program for the L. R. Sweezy No. 1 well was planned to determine the production characteristics of a small geopressured reservoir from initial fluid withdrawal to final depletion. Production from this well had to be kept below ~ 10,000 bbls/day to avoid excessive sand production. Analysis of the drawdown data indicates a formation permeability of ~ 126 md, and a flow-rate dependent skin (Garg and Riney, 1984a). Conventional analysis techniques were, however, found to be inadequate for analyzing the buildup data. The formation properties inferred from the drawdown data were used for reservoir simulation of the production history of the Sweezy well. The calculated drawdown response matched the measured data; such agreement was not possible for the buildup portion of the tests. Parametric calculations designed to investigate the anomalous buildup response suggest that this nonlinear behavior may be the result of stress-induced hysteresis in formation properties, shale recharge, and/or long-term formation creep. The L. R. Sweezy well was plugged and abandoned after a surge in the sand production had filled the wellbore to ~ 350 ft above the top of the perforated interval.

A series of parametric calculations was run with the MUSHRM geopressured-geothermal reservoir simulator to asssess the effects of important formation, fluid, and well parameters on brine and gas recovery from geopressured reservoir systems (Garg and Riney, 1984b). The Pleasant Bayou reservoir was adopted as the base case and various properties were then varied about their base values to assess their impact on energy recovery. The specific parameters considered were formation permeability, pore-fluid salinity, temperature and gas content, well radius and location with respect to reservoir boundaries, desired flow rate, and possible shale

recharge. It was found that the total brine and gas recovered (as a fraction of the resource in place) were most sensitive to formation permeability, pore-fluid gas content, and shale recharge.

1.3 OUTLINE OF PRESENT REPORT

As part of the DOE Design Wells Program, Technadril-Fenix and Scisson (T-F&S) undertook the drilling, completion and testing of one geopressured production well (i.e., T-F&S/DOE Gladys McCall No. 1) and one brine disposal well in the East Crab Lake Field. This field is located in Cameron Parish, Louisiana, approximately 55 mile southeast of Lake Charles. A description of the geology of the field, well completion, log data and the test plan is presented in a report by T-F&S (1982).

The well test program for the T-F&S Gladys McCall No. 1 well was planned primarily to determine and demonstrate through long-term flow testing the technological and economical feasibility of recovery of natural gas associated with geopressured-geothermal fluids and high-volume brine disposal in shallower aquifers. In addition to the achievement of these primary goals, the test plan was designed to generate sufficient data to: (1) characterize and define adequately the nature and size of the reservoir; (2) characterize the brine and natural gas produced; (3) confirm the adequacy of the test well and surface facilities design; and (4) define the extent of scaling/corrosion problems associated with the long-term high volume production and disposal of geopressured-geothermal brine, and minimize and control such scaling/corrosion.

S-CUBED received the T-F&S Daily Reports on the Gladys McCall well testing activities and the more detailed flow rate and pressure data measured downhole during the Reservoir Limits Tests conducted on two sands (Sand Zone No. 9 and Sand Zone No. 8). S-CUBED performed independent analysis of the well test data and performed

numerical reservoir simulations of the tests under DOE Contract DE-AC 08-80-NV10150. This report summarizes the S-CUBED analysis of the Gladys McCall No. 1 Well flow tests.

It is appropriate to briefly outline here the contents of the rest of this report. The well geology, test instrumentation well completion and laboratory measurements on reservoir samples test are briefly described in Section II. In Sections III and IV, we utiize conventional petroleum engineering techniques to analyze pressure transient data to estimate reservoir formation properties for Sand Zone No. 9 and Sand Zone No. 8, respectively. The fluids from the two sands are essentially identical and the reservoir responses of the two are very similar. The volume of Sand Zone No. 8, however, is much larger than Sand Zone No. 9. In Section V, the estimated formation parameters for Sand Zone No. 8 are utilized to develop a reservoir model that provides in history-match for the simulated Reservoir Limits Test of the sand. In Section VI the production testing of Sand Zone No. 8 is simulated over a period of approximately one year. Finally, the results of the S-CUBED analyses of the Gladys McCall No. 1 Well are summarized in Section VII within the context of the results from testing the other wells under the DOE Design Wells Program.

II. GLADYS McCALL PROSPECT AND TEST WELL

The geologic interpretation of the Gladys McCall prospect was made by Magma Gulf Company based solely on well logs from the subject well and five other nearby deep wells. The prospect lies in one of a series of fault blocks which are successively downdropped towards the coast. The approximate locations of three major growth faults which are considered to control the structure of the prospect are shown at 15,500 feet in Figure 2.1. Fault I cuts the Sun Sturlese well (located approximately one mile north of the Gladys McCall No. 1 well) at ~ 15,500 feet, and cuts out most of the stratigraphic section of the target sand. Fault II cuts the Gladys McCall No. 1 well at ~ 16,350 feet and cuts out about half the target sand. Fault III is interpreted as being located one to two miles south of the Gladys McCall site. Due to the lack of deep well control east and west of the subject well site, the east-west length of the fault block can not be determined from the available geologic information.

The T-F&S/DOE Gladys McCall No. 1 geopressured-geothermal test well was spudded on May 27, 1981, and drilling operations were completed on November 2, 1981. The well was drilled to a total depth of 16,510 feet after a directionally drilled sidetrack from 15,295 feet. The plugged-back total depth (PBTD) of the test well is 15,831 feet. The stratigraphic section of the test well consists of alternating massive sands and shales, with the shales becoming increasingly thick below 11,000 feet. There are approximately 1,100 net feet of sand in the 14,412 - 15,860 foot interval of the target Miocene sand penetrated by the test well.

The open-hole well log in Figure 2.2 shows the eleven potential production zones into which the target sand has been partitioned. Over two-thirds of the productivity appears to be contained in three massive sand zones (Nos. 2, 8 and 9). It was decided to perform the initial testing of the reservoir in Sand Zone

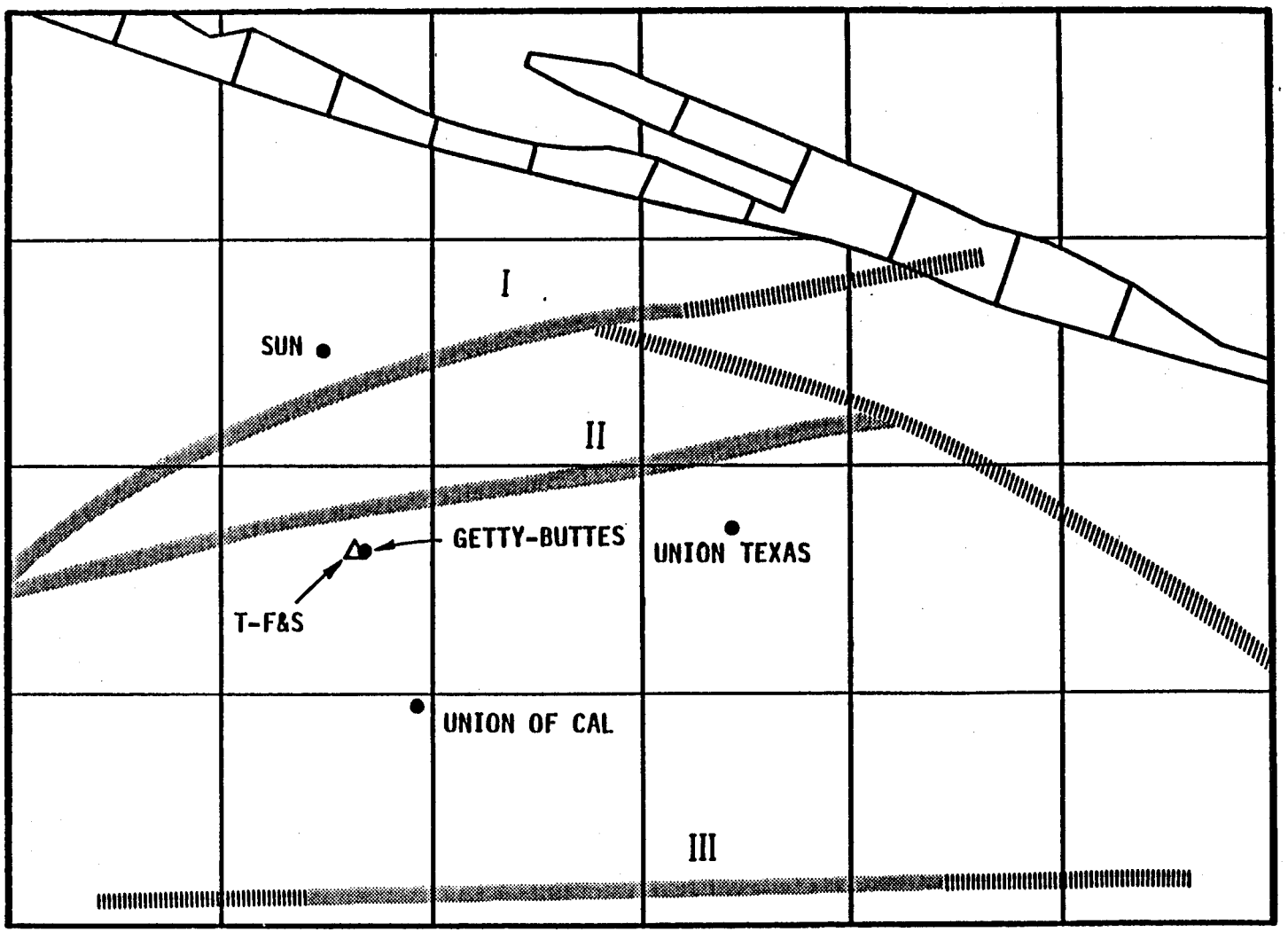

Figure 2.1. Major growth faults at 15,500 feet. Geology map prepared by Magma Gulf Company. Grid squares are 1 mile by 1 mile.

T-F&S/DOE GLADYS McCALL NO. 1 WELL
EAST CRAB LAKE FIELD
CAMERON PARISH, LOUISIANA
LOGS OF POTENTIAL PRODUCTION ZONES

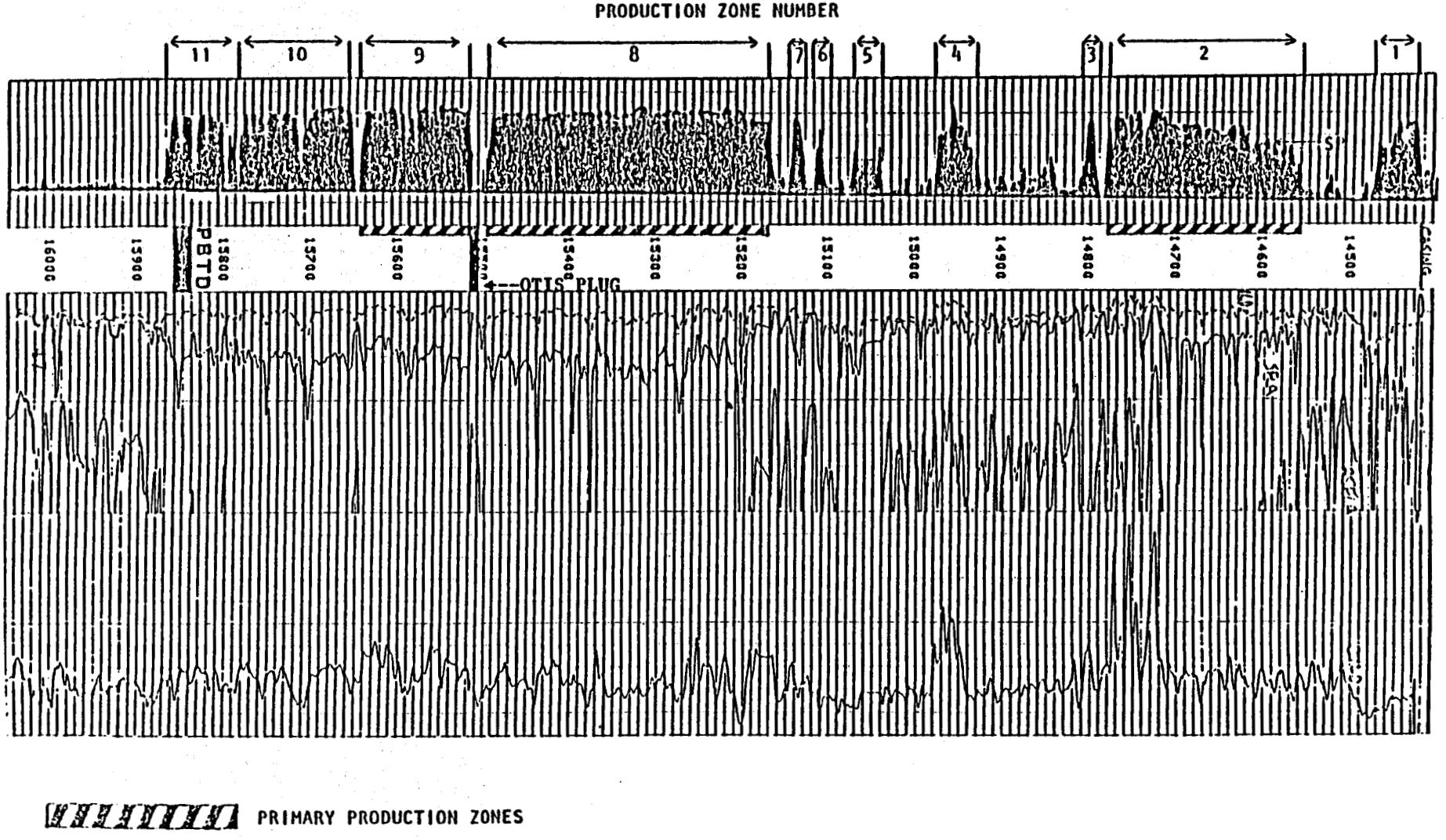

Figure 2.2. Logs of potential production zones of T-F&S/DOE Gladys McCall No. 1 Well, East Crab Lake Field, Cameron Parish, Louisiana.

9 (15,508 - 15,636 feet), with subsequent testing of Sand Zone 8 (15,158 - 15,490 feet) and possibly Sand Zone 2 (14,550 - 14,772 feet). To date, only the two deepest of these three massive sand zones have been tested.

After logging the well, a seven inch (5.5-in I.D.) casing string, run as a liner, was cemented in at 15,958 feet and tied back to the surface. The well was completed with five inch (3.68 in I.D.) tubing as shown in Figure 2.3. A number of mechanical problems were encountered with the well completion (Durrett, 1984). Subsequent to testing Sand Zone No. 9, an Otis wireline packer with an expendable knockout plug was set at ~ 15,500 feet to seal off Sand Zone No. 9 in preparation for testing Sand Zone No. 8. An Otis packer with a ratch-latch seal assembly was used to replace the TIW seal assembly shown in Figure 2.3 since the latter had exhibited a small leak during the testing of Sand Zone No. 9.

The seven inch casing was perforated in the interval 15,511 - 15,627 feet in preparation for the testing of Sand Zone No. 9 (15,508 - 15,636 feet). The interval 15,160 - 15,470 feet was perforated later in order to test Sand Zone No. 8 (15,158 - 15,490 feet).

Sidewall cores were taken over the entire production interval and three diamond cores were recovered within Sand Zone No. 8. The results of laboratory measurements of rock properties on the diamond cores are considered more reliable. Under bench conditions, Core Laboratories, Inc. reported the following arithmetic average values for porosity and horizontal permeability: ϕ ~ 0.154, k ~ 126 md. The porosity value is in good agreement with the average values inferred from the neutron-density and sonic density logs taken in the Gladys McCall No. 1 well.

Terra Tek, Inc. also performed laboratory tests on rock specimens cut from the diamond cores to investigate rock properties

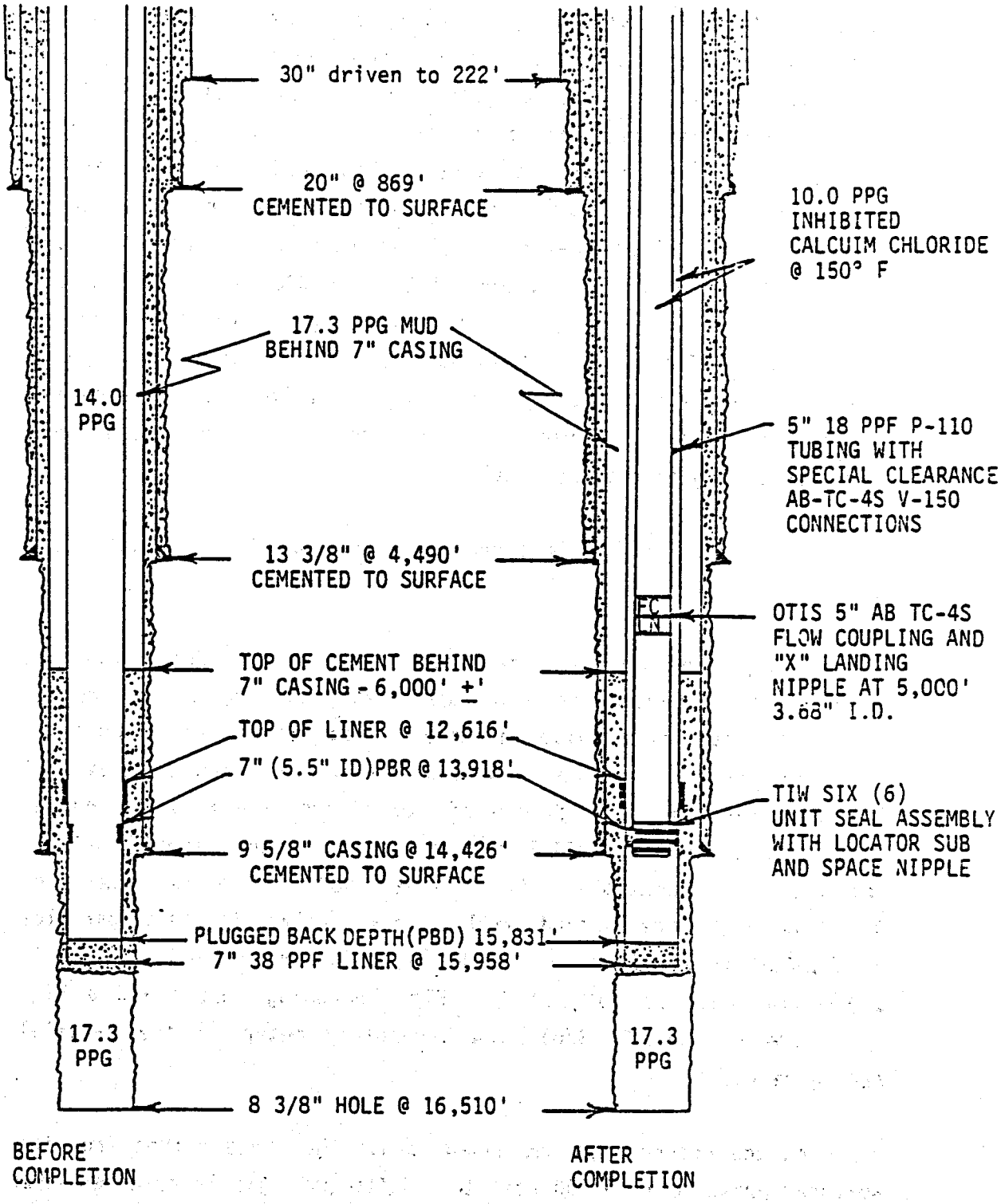

Figure 2.3. Original completion of T-F&S/DOE Gladys McCall No. 1 Well.

(Kelkar, et al, 1982). Under bench conditions, the reported arithmetic average values for rock grain density, porosity and permeability are ρ_{gr} ~ 2.66 gm/cc, ϕ ~ 0.168 and k ~ 83 md respectively. Uniaxial compaction tests, triaxial failure tests, creep tests and ultrasonic tests were also conducted to determine the deformational characteristics of cylindrical specimens (L = 2 in, D = 1 in). The formation rock was found to be quite stiff and strong; extreme pressure drawdowns (Δp > ~ 5,000 psi) were required to produce the large deformations reported. A typical uniaxial compaction coefficient reported was 0.2×10^{-6} psi^{-1}; this value appears to be unrealistically small and may have resulted from the extreme drawdown pressures to which the small specimens were subjected during laboratory tests.

There has been no sand produced from the Gladys McCall test well.

During production of the test well, brine flow from the wellhead is directed through two banks of manually operated adjustable Gray choke valves arranged in series within a manifold. The brine flows from the Gray choke manifold through heavy-wall 10-inch piping and through one of two alternative Flow Technology turbine meters to a parallel bank of Willis choke valves (used for secondary flow control). One Willis choke valve is sized for 0 - 5,500 B/D; the second Willis choke valve in this parallel arrangement is sized for 0 - 45,000 B/D. Correspondingly, there is a low flow rate (0 - 10,000 B/D) Flow Technology meter and a high flow rate (0 - 50,000 B/D) Flow Technology meter in the parallel arrangements.

As the pressure is decreased across the choke valves from the wellhead pressure (~ 5,500 psi) to ~ 1,000 psi, gas is released from solution in the brine. The full-stream flow (two-phase) is measured by the Flow Technology turbine meter. The brine/gas flow from the Willis choke valves is directed to the separator inlet and then

downward by a splash plate at the inlet. The gas and water vapor thereby separated from the brine flows upward and out of the top of the separator. Pressure control on the separator system is maintained through a split range pressure indicator/controller. Low-rate and high-rate Halliburton turbine meters are arranged in parallel for measuring the brine flow rate at the separator outlet. The Halliburton turbine meters measure single-phase liquid flow.

Conventional orifice plates for flow measurement are located downstream of the separator in the gas line to the flare and the line to the gas pipeline. During testing, the instantaneous and cumulative output from both the Flow Technology (two-phase full-stream flow) and the Halliburton (single-phase flow) turbine flow meters were recorded every two hours on the Daily Reports prepared by T-F&S. The flow rate measured on the Flow Technology meter upstream of the separator was also recorded (every ten seconds during the early part of the drawdown and buildup phases) by Reservoir Dynamics, Inc. (RDI).

Brine chemistry studies by Rice University have shown that the fluids produced from Sand Zone No. 8 and Sand Zone No. 9 are essentially identical. This is demonstrated by comparison of the compositions of the liquid brine (Table 2.1) and the production gas (Table 2.2) recovered from the two sands. The fluids from each of the sands were sampled at the same brine/gas separator pressure of 500 psig.

At the conclusion of the Reservoir Limits Test on Sand Zone No. 8, a series of tests were run to determine the variations in composition of the produced gas at separator pressures ranging from 1,000 psig down to 250 psig. As shown in Table 2.3, the recovered gas increases from 22.9 SCF/STB to 29.7 SCF/STB as the separator pressure is reduced over this range. Standard Cubic Feet of gas (SCF) and Stock Tank Barrels of brine refer to standard conditions (14.7 psia, 60°F). The incremental gas production (~ 6.8 SCF/STB),

Table 2.1

Brine Composition of Fluids Produced
from T-F&S/DOE Gladys McCall No. 1 Well (Durrett, 1984)

	Sand Zone	
	No. 8 (ppm)	No. 9 (ppm)
Total Dissolved Solids	97,800	95,500
Chlorides	59,290	58,600
Alkalinity (As HCO_3)	522	527
Calcium	4,040	4,080
Iron (Ferrous)	14	34
Silica	100	140
Specific Gravity	1.064	1.045

Table 2.2

Production Gas Composition at Brine/Gas Separator Pressure of 500 psig for T-F&S/DOE Gladys McCall No. 1 Well (Durrett, 1984)

	Sand Zone	
Component	No. 8 (% Mole)	No. 9 (% Mole)
Methane	85.96	86.52
Ethane	2.34	2.39
Propane	0.52	0.54
Isobutane	0.09	0.08
N-Butane	0.07	0.08
Isopentane	0.02	0.04
N-Pentane	0.01	0.03
Hexanes	0.00	0.01
Heptanes Plus	0.11	0.16
Nitrogen	0.25	0.25
Carbon Dioxide	10.63	9.90
Hydrogen Sulfide	20 ppm	13 ppm

Table 2.3

Gas Production Rate and Composition as a Function of Brine/Gas Separator Pressure for T-F&S/DOE Gladys McCall No. 1 Well (Durrett, 1984)

	Separator Pressure, psig			
	1,000	750	500	250
Brine Production Rate, STB/D	14,451	14,702	14,928	15,032
Gas Production Rate (Recovered), SCF/D	331,720	347,629	392,508	446,110
Gas Production Rate (Recovered), SCF/STB	22.9	23.6	26.3	29.7
Residual Gas in Brine, SCF/STB	6.8	5.7	3.8	1.8
Gas Production from Well, SCF/STB	29.7	29.3	30.1	31.5
CO_2 in Gas Production (Recovered), MOL	6.9	7.9	8.9	13.6
H_2S in Gas Production (Recovered), PPM	6.0	12.0	16.0	35.0

however, contains a large fraction of CO_2. The average for the total gas production from the well is ~ 30.15 SCF/STB. This value is in good agreement with the values of 30.38 SCF/STB (Sand Zone No. 8) and 31.09 SCF/STB (Sand Zone No. 9) reported by Weatherly Laboratories, Inc. (Table 2.4).

Weatherly Laboratories, Inc. (1983a, 1983b) analyzed the physical characteristics of fluid samples from the sand zones tested by the Gladys McCall Well No. 1. The samples were taken at different separator conditions and each sample was recombined to approximate reservoir conditions for the sample. The reported values for fluid density, compressibility and viscosity listed in Table 2.4 are for the recombined (reservoir) fluid.

During the early part ($t < \sim 45$ hrs) of the Reservoir Limits Test of Sand Zone No. 9, the separator pressure was held at ~ 700 psig. The fluid temperature at the separator increased from an initial value of ~ 125°F to 200°F at t ~ 10 hrs, ~ 212°F at t ~ 30 hrs, 215°F at t ~ 45 hrs. At t ~ 45 hrs the separator pressure was lowered to ~ 500 psig and the fluid temperature gradually increased to ~ 235°F. These latter values (~ 500 psig, ~ 235°F) were closely approximated until t ~ 240 hrs when the separator pressure was lowered to ~ 310 psig. At t ~ 405 hrs the separator pressure was returned to ~ 500 psig and maintained at that value for the duration of the drawdown period.

The separator pressure was controlled at 500 psig throughout the drawdown portion of the Reservoir Limits Test of Sand Zone No. 8. The first reported temperature of the fluid at the separator was 204°F at t ~ 0.75 hr. It increased to ~ 236°F at t ~ 1.75 hrs and to ~ 270°F at t ~ 12 hrs. The separator temperature gradually increased to ~ 274°F at t ~ 84 hrs and this temperature was maintained for the duration of the drawdown period.

Table 2.4

Physical Characteristics of Fluids Produced from
Gladys McCall No. 1 Well
(Weatherly Laboratories, Inc., 1983a and 1983b)

	Sand Zone No. 8	Sand Zone No. 9
Separator Conditions	500 psig 268°F	700 psig 212°F
Reservoir Conditions	12,783 psia 290°F	12,936 psia 298°F
Stock Tank Conditions	15.025 psia 60°F	15.025 psia 60°F
Formation Volume Factor (reservoir/stock tank)	1.0426	1.0481
Shrinkage Factor (stock tank/separator)	0.9437	0.9637
Produced Gas-Brine Ratio (based on separator flash)	26.50 SCF/STB	25.59 SCF/STB
Reservoir Fluid Parameters		
Density	1.02255 gm/mL	1.02242 gm/mL
Compressibility	$2.76 \times 10^{-6} psi^{-1}$	$2.75 \times 10^{-6} psi^{-1}$
Viscosity	0.310 cp	0.388* cp
Bubble Pressure	9200 psia	10,030 psia
Solution Gas-Brine Ratio	3.88 SCF/STB	5.50 SCF/STB
Total Gas in Produced Fluid	30.38 SCF/STB	31.09 SCF/STB

* Suspect data measured with old E.L.I. Rolling Ball Viscometer rather than new Ruska Rolling Ball Viscometer.

In this report, we will need to convert from fluid production rates measured at separator conditions to values at reservoir conditions. The product of the formation factor (reservoir volume/stock tank volume) and the shrinkage factor (stock tank volume/separator volume) listed in Table 2.4 for each sand should provide the desired conversion. The corresponding formation factors to convert barrels as measured at the separator to reservoir conditions are as follows:

Sand Zone No. 8: $B = (1.0426)(0.9437) \sim 0.984$
(Separator at 500 psig, 268°F)

Sand Zone No. 9: $B = (1.0481)(0.9637) \sim 1.01$
(Separator at 700 psig, 212°F)

III. SAND ZONE NO. 9 RESERVOIR LIMITS TEST

A Preliminary Flow Test on Sand Zone No. 9 (15,508 - 15,636 feet) was run during December 1982. A total of 22,710 bbl of brine were produced through December 27, 1982. No downhole pressure or temperature measurements were made during this period.

A Panex downhole pressure/temperature gauge was lowered on March 20, 1983 in preparation for the Reservoir Limits Test. The gauge was positioned at 15,460 feet and the pre-test reservoir pressure and temperature recorded

$$p_i = 12{,}911 \text{ psia} \qquad T_i = 298^\circ F \tag{3.1}$$

The well was opened at 18:18:30 on March 21, 1983 and the transient downhole pressure and temperature values recorded. Production continued until the well was closed at 12:56:40 on April 14, 1983; the total production time was $t_p = 570.6$ hrs.

The full-stream flow rate measured on the Flow Technology meter upstream of the separator (and recorded every ten seconds by RDI) was considered to be the primary source of flow rate data. Unfortunately, during the Reservoir Limits Test for Sand Zone No. 9, the indicated flow rate from this two-phase production turbine meter (Flow Technology - Low-Rate) was found to be in error during the early stages of the drawdown portion of the test. Calibration measurements were made by T-F&S which indicated that the Halliburton Low-Rate turbine meter recordings at the outlet from the separator were correct within about two percent. The Flow Technology High-Rate meter was also reported to be accurate and T-F&S switched to this turbine meter at production time $t \sim 92.5$ hrs. The RDI recorder was also switched to the High-Rate meter. There was a gap in the RDI digitized flow rate data from production time $t \sim 349$ to $t \sim 460$ hrs but the Daily Report recordings are sufficiently detailed for this portion of the Reservoir Limits Test.

Figure 3.1a shows the daily-average values for the single-phase flow measured at the separator outlet as reported in the T-F&S Daily Reports. The ratio plot in Figure 3.1b shows that the average full-stream flow rates measured upstream of the separator are in generally good agreement with the values measured at the separator outlet after T-F&S switched to the Flow Technology High-Rate meter ($t > \sim 92$ hrs).

Figure 3.2 illustrates the scatter in the digitized instantaneous flow rates reported by RDI for the Flow Technology High-Rate meter located upstream of the separator. Instantaneous flow rates recorded in the T-F&S Daily Reports for the Halliburton Low-Rate meter located at the separator outlet are also shown. The low values logged for $t < \sim 10$ hrs apparently reflect the fact that the separator temperature is still rising; the values reported at later times show less scatter than the RDI data and cover the full drawdown test period. Since the cumulative flow values recorded on the Daily Reports for the Halliburton Low-Rate meter fall on a straight line of slope

$$q = 4190 \text{ sep bbl/day} \quad , \tag{3.2}$$

we will use this estimate for the flow rate at the separator outlet during the Reservoir Limits Test on Sand Zone No. 9. The actual flow rates during the early stages of the drawdown ($t < \sim 20$ hrs) are not known, but the above estimate is believed to be sufficiently accurate for the longer production times.

The log-log plot of the pressure drawdown against the test time (Figure 3.3) exhibits a very early region of steep slope ($t < 0.01$ hrs) prior to the unit-slope straight-line portion. This is believed to be due to the heating of the wellbore by the produced fluid. This thermal effect on the downhole pressure measurement often swamps the normal wellbore afterflow effects during drawdown testing of geothermal wells. The corresponding plot of the pressure

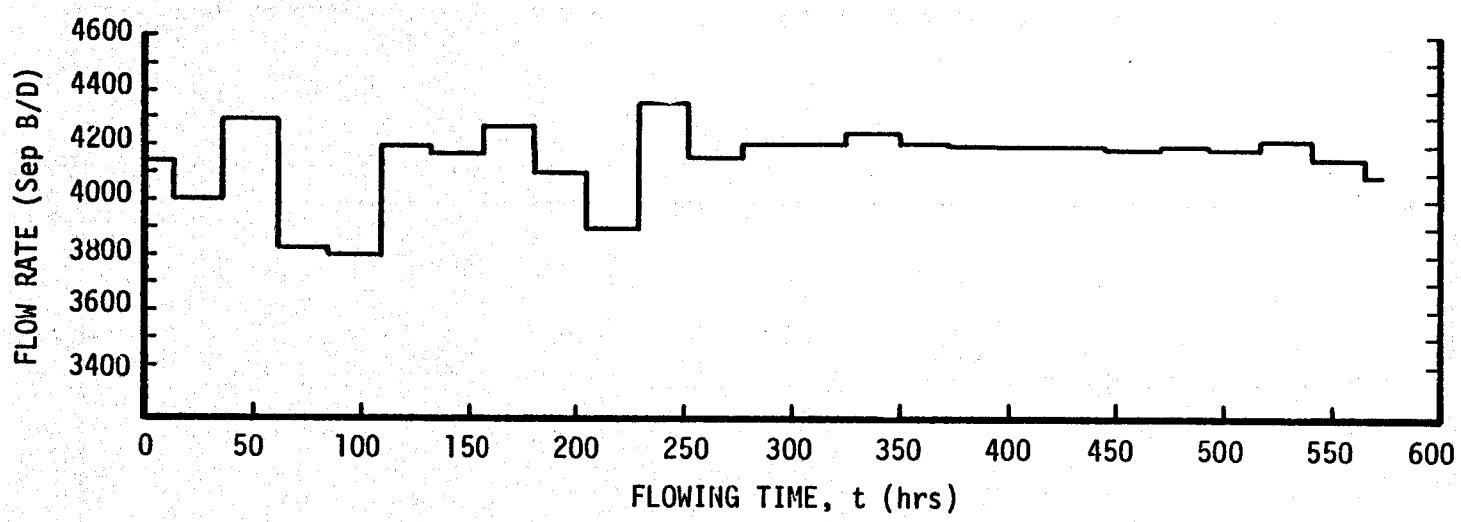

(a) Average Flow Rate at Separator Outlet.

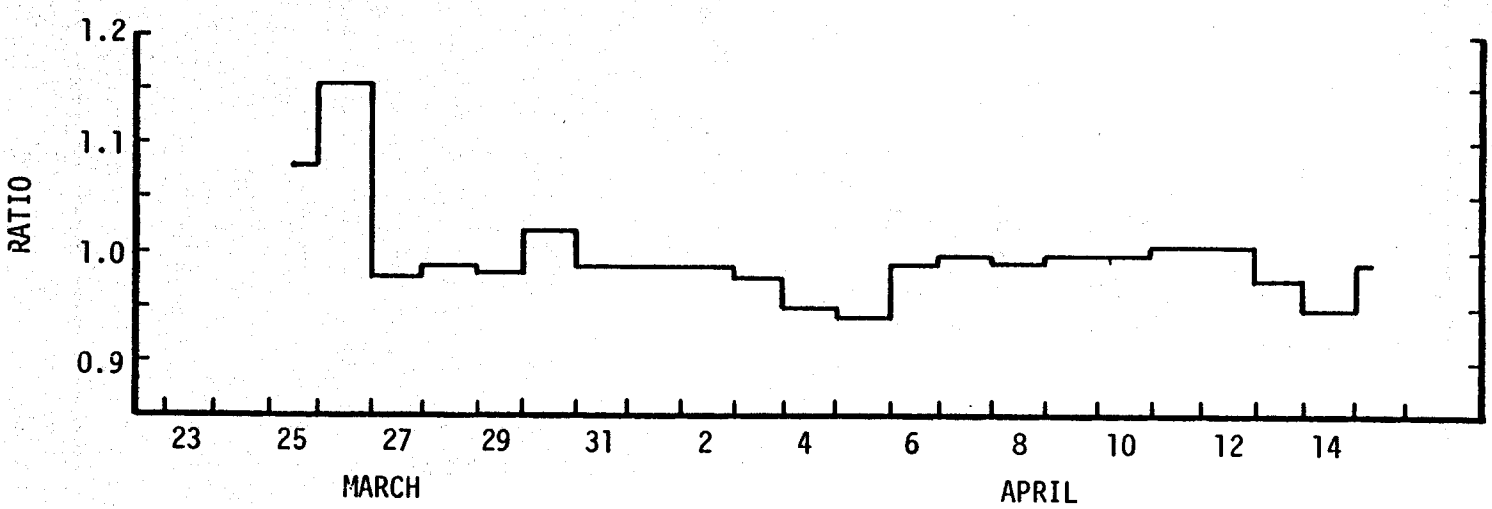

(b) Ratio of Flow Rates: Full Stream B/D to Separator B/D.

Figure 3.1. Comparison of flow rate daily averages from T-F&S daily reports (Sand Zone No. 9).

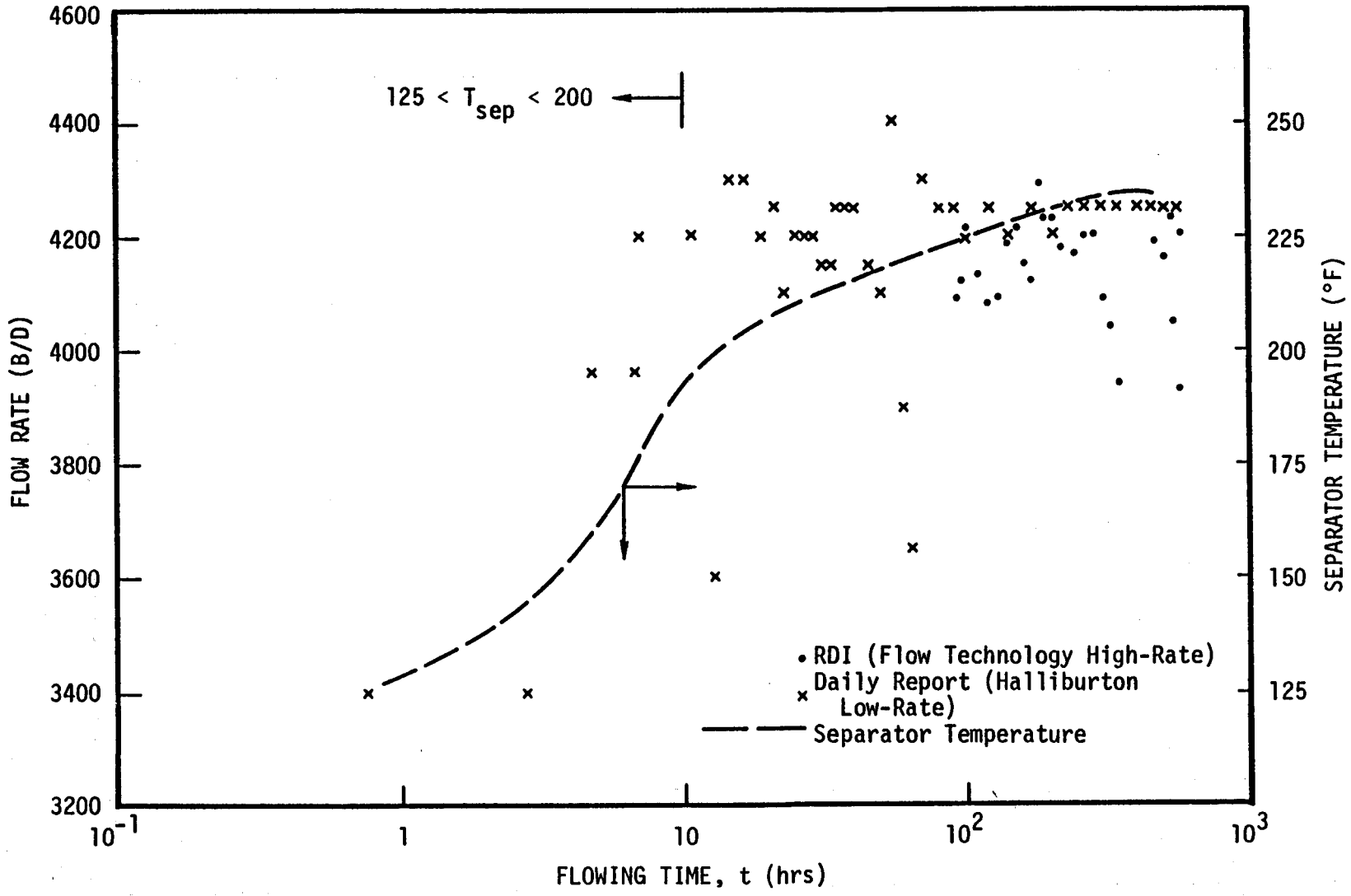

Figure 3.2 Flow-rate and separator temperature data for Reservoir Limit Test on Sand Zone No. 9.

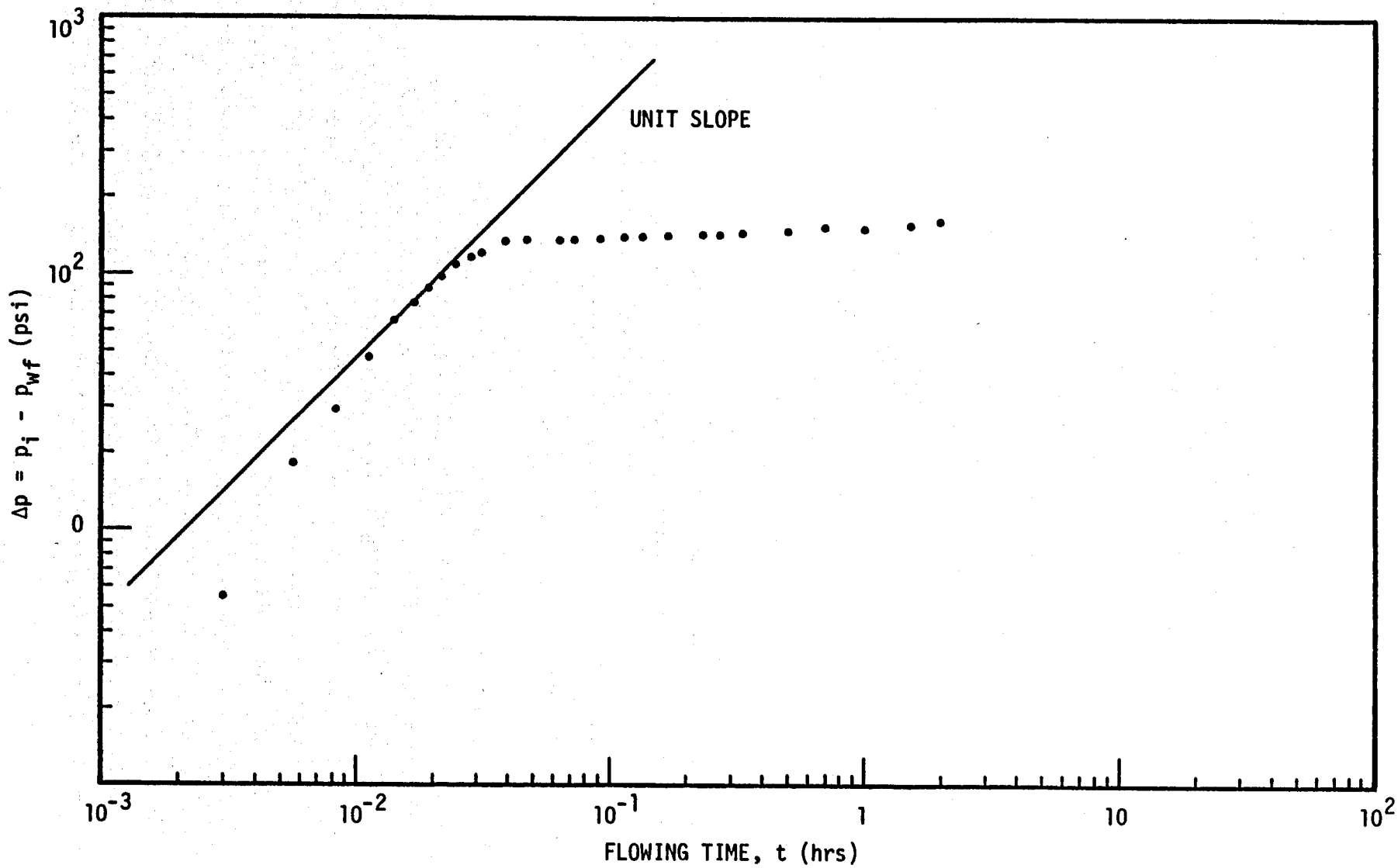

Figure 3.3. Sand Zone No. 9 drawdown type curve.

data for the buildup portion of the Reservoir Limits Test (Figure 3.4) displays the usual unit slope associated with wellbore storage effects. The data start deviating from the unit slope at ~ 0.03 hrs; wellbore effects should be insignificant about 1 to 1.5 cycles thereafter (i.e., for time > ~ 0.3 to 1 hr).

The irregularities in the slope of the semi-log plot of the drawdown bottomhole pressure data (Figure 3.5) are attributed to irregularities in the flow rates but this cannot be definitely established because of problems with the Flow Technology Low-Rate meter. The sudden pressure drop recorded at t ~ 4.2 hrs (Figure 3.5) is probably due to an abrupt increase in flow rate with a corresponding abrupt decrease in pressure due to the skin (formation damage factor, s); this is consistent with the discontinuous increase in the slope of the pressure data which also occurs at t ~ 4.2 hrs. Similarly, there is a sudden pressure drop and a simultaneous discontinuous slope increase at t ~ 7.8 hrs. The earlier pressure variations (~ 0.6 < t < ~ 2.5 hrs) probably also reflect flow rate irregularities. The continuous change in slope at t ~ 29 hrs, however, does not appear to be associated with an abrupt change in flow rate.

There is insufficient reliable early-time flow rate information available to allow reliable estimates of the reservoir parameters for Sand Zone No. 9 to be made from the drawdown data. There are three straight line segments which approximate the semi-log plot of the data for significant drawdown times (Figure 3.5). The line segment of slope m_1 = -25 psi/cycle approximates the data for about half a time cycle during a period (0.2 < t < 0.6 hrs) when the flow rate is unknown and while wellbore storage effects are important. The line segment of slope m_2 = -46 psi/cycle approximates the data for about half a time cycle during a period (8 < t < 25 hrs) when the pressure measurements are still affected by the changing temperature of the fluid in the wellbore.

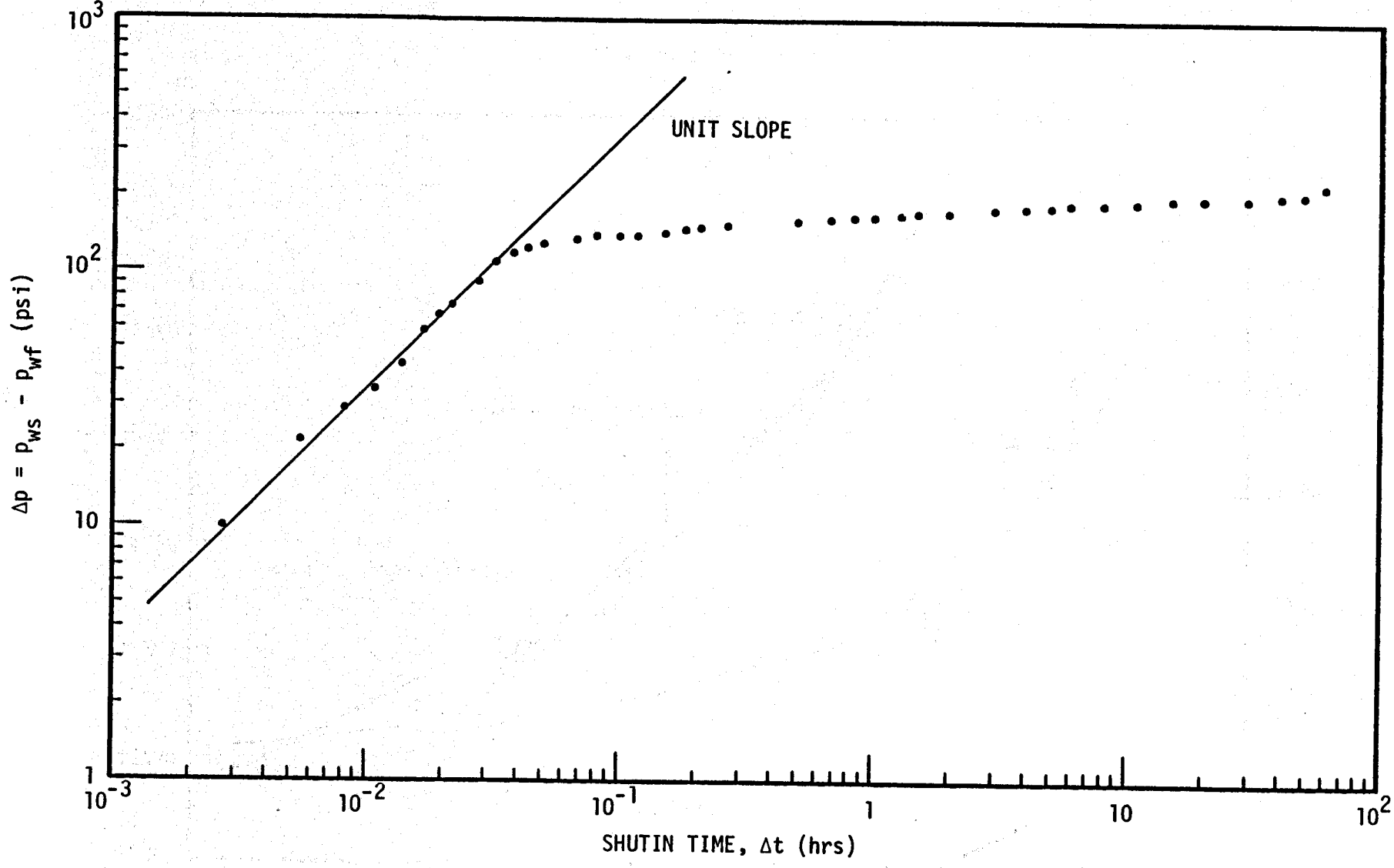

Figure 3.4. Sand Zone No. 9 buildup type curve.

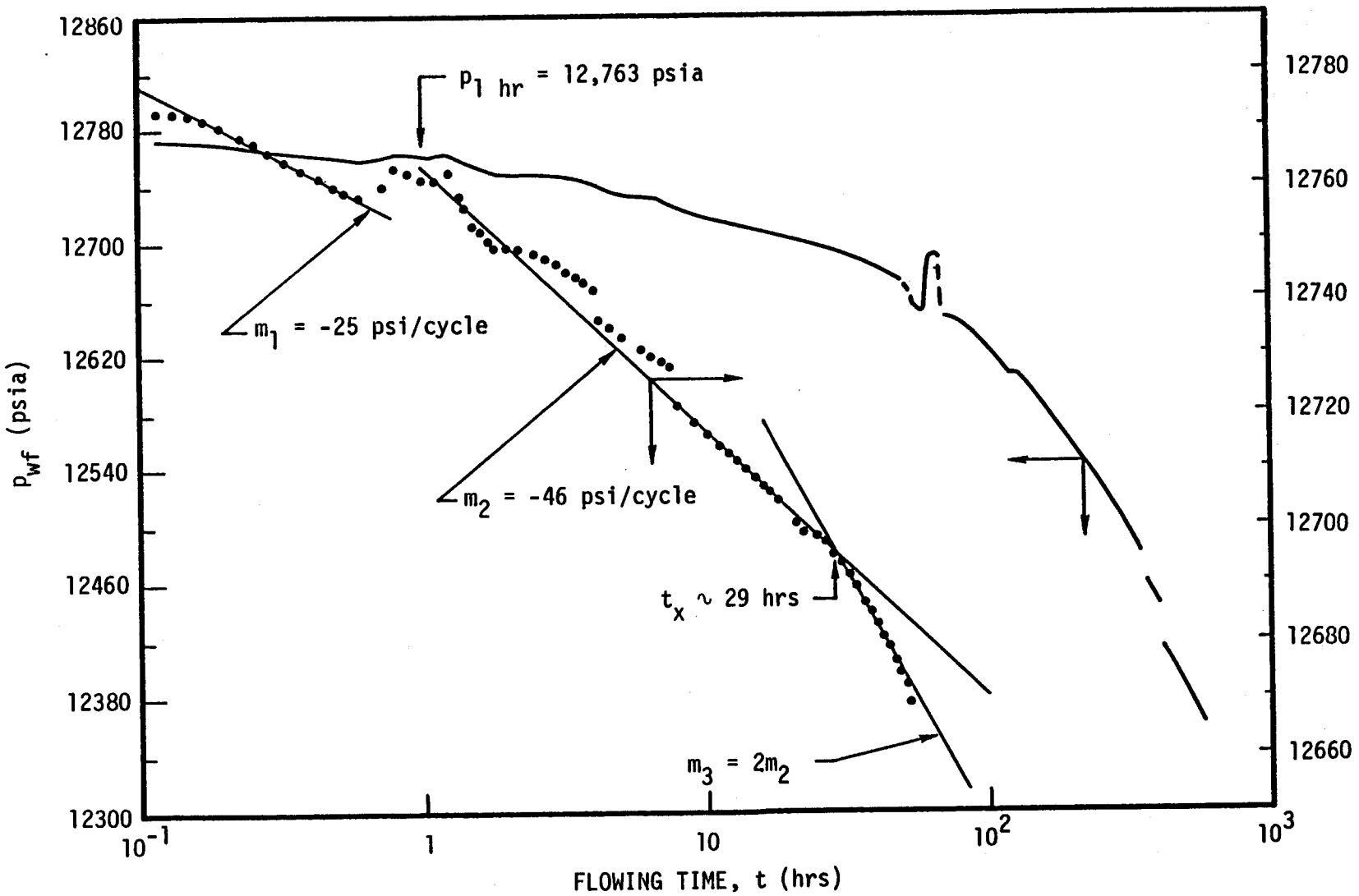

Figure 3.5. Sand Zone No. 9 pressure drawdown semi-log plot.

The third line segment (of slope $m_3 \sim 2m_2$) appears to indicate the presence of a reservoir boundary which causes a doubling of the slope at $t = t_x \sim 29$ hrs.

Figure 3.6 shows a Horner plot of the downhole data for the buildup portion of the Reservoir Limits Test on Sand Zone No. 9. The flow rate during the latter part of the drawdown period is most important in interpreting the buildup data and the flow rate was reasonably stable during that time period. The Horner plot of the buildup pressure data is approximated by a straight line of slope $m_1 = -25$ psi/cycle up to the time at which gauge problems were encountered ($\Delta t \sim 18$ hrs). This fit holds for more than two log cycles and may be used to estimate formation properties.

The slope corresponding to the infinite reservoir portion of the Horner plot is related to the formation permeability through the relation

$$k = \frac{162.6\ q\ \mu\ B}{mh} \qquad (3.3)$$

where

k ~ Formation permeability, md.
q ~ Brine flow rate, sep bbl/day.
μ ~ Brine viscosity, cp.
B ~ Formation volume factor, res bbl/sep bbl.
m ~ Slope of straight line on Horner plot, psi/cycle.
h ~ Formation thickness, feet.

With $q = 4190$ sep bbl/day, $\mu = 0.31$ cp, $B = 1.01$ and $h = 128$ feet, we obtain

$$k = \frac{(162.6)(4190)(0.31)(1.01)}{(25)(128)} = 67 \text{ md} \qquad (3.4)$$

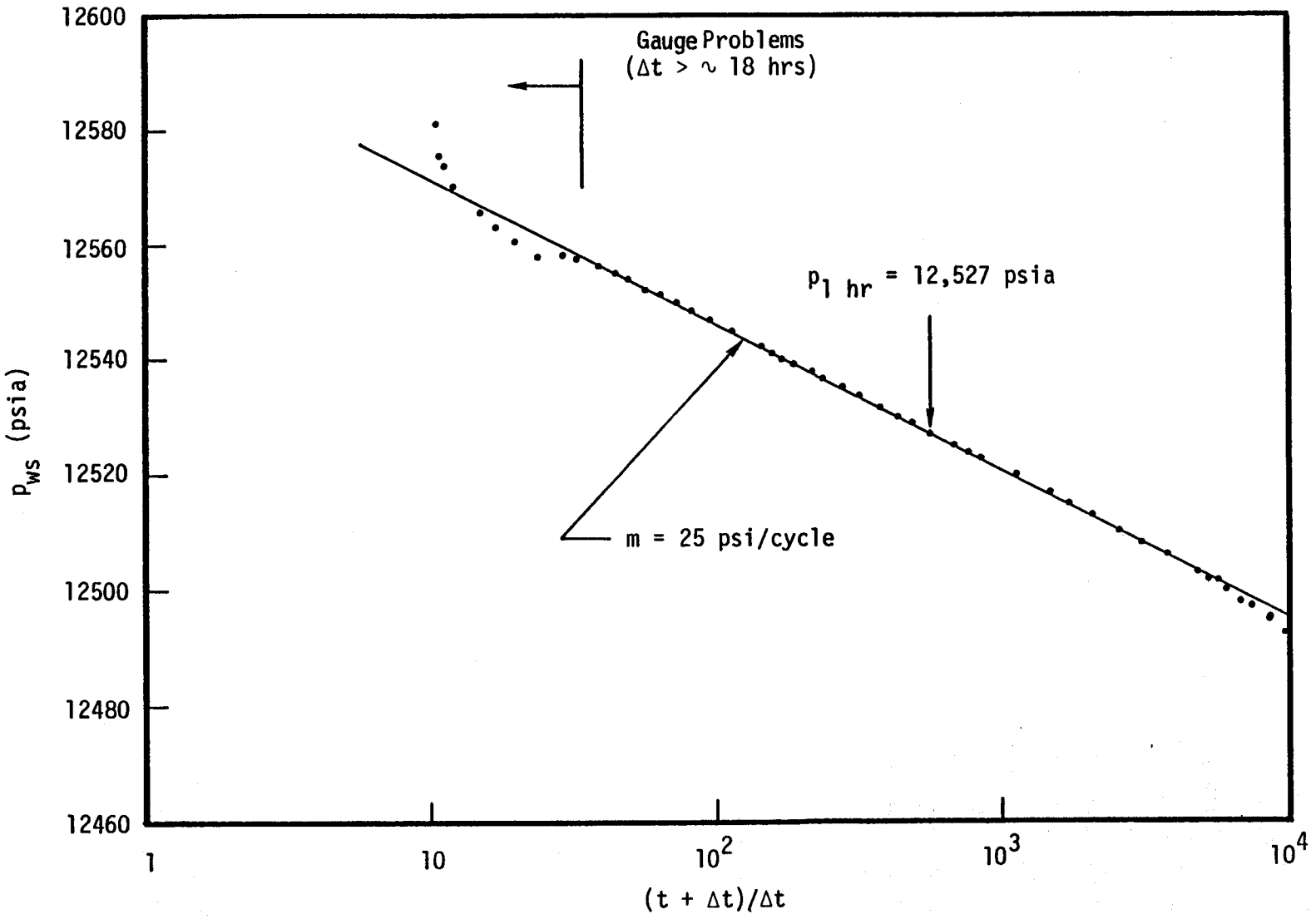

Figure 3.6. Sand Zone No. 9 pressure buildup Horner plot.

The skin factor may also be computed from the buildup data by using the following relation

$$s = 1.151 \left[\frac{p_{1hr} - p_{wf}}{m} - \log \frac{k}{\phi \mu C_T r_w^2} + 3.23 \right] \qquad (3.5)$$

where

m ~ Slope of straight line fit on Horner plot, psi/cycle.

$p_{1\ hr}$ ~ Shutin pressure at Δt = 1 hr from the straight line on the Horner plot, psia.

p_{wf} ~ Flowing pressure just prior to shutin, psia.

r_w ~ Radius of wellbore, feet.

ϕ ~ Formation porosity.

C_T ~ Total formation compressibility ($= C_f + C_w$), $psia^{-1}$.

C_f ~ Formation rock pore-volume compressibility, $psia^{-1}$.

C_w ~ Pore fluid compressibility, $psia^{-1}$

With $m = 25$ psi/cycle, $p_{1hr} = 12{,}527$ psia, $p_{wf} = 12{,}361$ psia, $r_w = 0.2917$ ft, $\phi = 0.16$ and $C_T = 6.27 \times 10^{-6}$ psi^{-1}, we obtain

$$s = 1.151 \left[\frac{12{,}527 - 12{,}361}{25} - \log \frac{67}{(0.16)(0.31)(6.27 \times 10^{-6})(0.2917)^2} + 3.23 \right]$$

$$= +0.54 \qquad (3.6)$$

These values of k and s may be used to re-examine the pressure drawdown data shown in Figure 3.5. A sudden increase in the flow rate (Δq) during drawdown would cause an abrupt pressure drop (Δp_s) due to a skin factor (s) given by

$$\Delta p_s = \frac{141.2\ \Delta q\ B\ \mu}{kh} \qquad (3.7)$$

The pressure drop of $\Delta p \sim 5$ psi observed at $t \sim 4.2$ and 7.8 hrs during drawdown (Figure 3.5) would correspond to a flow rate increase of

$$\Delta q = \frac{kh\ \Delta p_s}{141.2\ B\mu} = \frac{(67)(128)(5)}{141.2(1.01)(0.31)} = 970 \text{ sep bbl/day} \qquad (3.8)$$

The uncertainties in the early time flow rates are at least this large. The effect of two such flow rate increases (changes in choke setting) may have resulted in the transition in slope of the drawdown data from m_1 to m_2 as is indicated in Figure 3.5.

The straight line fit to the buildup data in Figure 3.6 indicates that there are no reservoir boundaries encountered prior to $\Delta t \sim 18$ hrs. The doubling of the slope of the drawdown data at $t = t_x = 29$ hrs (Figure 3.5) can be used to estimate the distance to the nearest fault from the relation

$$L = 0.01217 \left[\frac{kt_x}{\phi\mu C_T}\right]^{1/2} \qquad (3.9)$$

Using $k = 67$ md, $t_x = 29$ hrs, $\phi = 0.16$, $\mu = 0.31$ cp and $C_T = 6.27 \times 10^{-6}$ psi^{-1} we compute

$$L \sim 960 \text{ ft}$$

The Cartesian plot of the recorded downhole pressures over the full drawdown portion of the Reservoir Limits Test for Sand Zone No. 9 is presented in Figure 3.7. As indicated in the figure, there were considerable problems with the downhole gauges during the test period, but the data over the final ~ 145 hrs are closely approximated by a straight line of slope $\tilde{m}^* = -0.332$ psi/hr. If this straight line fit is maintained it would indicate that a semi-steady state flow condition has been attained in the

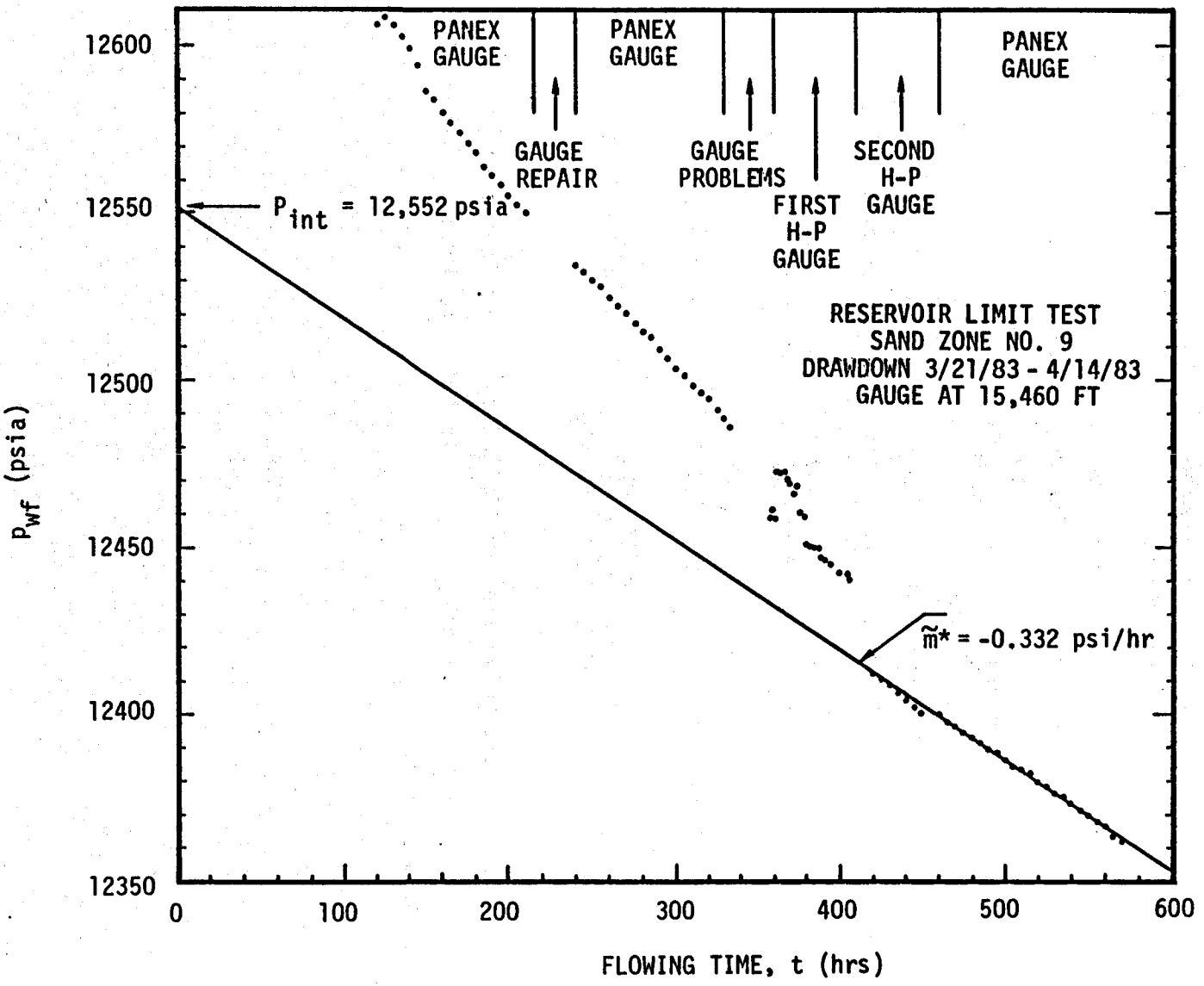

Figure 3.7. Sand Zone No. 9 pressure drawdown Cartesian plot.

reservoir. If it corresponds to late stage transient flow, however, the slope is still decreasing. We can, in any case, use the slope to calculate a lower bound on the connected pore-volume through the relation:

$$V_p = 0.0418 \frac{q\,B}{C_T\,m^*} \qquad (3.10)$$

where

V_p ~ Reservoir volume, res bbls.
q ~ Brine flow rate sep bbl/day.
B ~ Formation volume factor, res bbl/sep bbl.
m^* ~ Slope of a linear plot in semi-steady state flow, psi/hr.
C_T ~ Total formation compressibility, $psia^{-1}$.

In the present case ($-m^* < -\tilde{m}^* = 0.332$ psi/hr) we obtain

$$V_p > 0.0418 \frac{(4190)(1.01)}{(6.27 \times 10^{-6})(0.332)} = 85 \times 10^6 \text{ res bbls} \qquad (3.11)$$

Because of the apparently limited volume of Sand Zone No. 9 it was sealed off with a plug set at ~15,500 feet in preparation for testing Sand Zone No. 8.

IV. SAND ZONE NO. 8 RESERVOIR LIMITS TEST

4.1 WELL TEST ANALYSIS

Subsequent to perforating the seven inch casing of the Gladys McCall No. 1 well within Sand Zone No. 8 (15,158 to 15,490 feet), a stable pressure of 12,799 psia was recorded on a Panex gauge fixed at a depth of 15,100 feet. The test well was opened for a Preliminary Flow Test on September 20, 1983. Well cleanup operations were completed and the well was shutin on September 21, 1983 after flowing at a brine rate of ~ 3,100 bbl/day for ~ 25 hrs.

A Panex pressure/temperature gauge was again lowered on September 26, 1983 in preparation for the Reservoir Limits Test on Sand Zone No. 8. The gauge was fixed at a depth of 15,100 feet and a stable pressure of 12,794 psia recorded. After opening the well on September 27, 1983 and producing brine at a rate of ~ 14,600 bbl/day for ~ 12 hrs, the test was aborted because of mechanical problems. The well was again opened on October 6, 1983 and flowed at a rate of ~ 9,400 bbl/day for ~ 5 hrs before being aborted due to a brine deposal problem. The Reservoir Limits Test was restarted successfully at 13:14:40 on October 7, 1983; the conditions recorded at 15,100 feet prior to flowing the well were

$$p_i = 12{,}784 \text{ psia} \qquad T_i = 289^\circ F \tag{4.1}$$

Production continued until the well was shutin at 13:16:10 on October 18, 1983; the total production time was $t_p = 505.5$ hrs.

During the production period of the test, the full-stream flow rate measured by the Flow Technology turbine meter upstream of the choke was recorded on a Taylor strip chart and digitized by RDI. Readings for these instantaneous flow rates and the cumulative flow measured at this location are given every two hours in the

T-F S Daily Reports as are the instantaneous and cumulative single-phase flow rates measured at the separator outlet on the Halliburton turbine meter.

Figure 4.1 is a comparison of the early averages for the flow rates computed from the cumulative production recorded on the Daily Reports for the full-stream two-phase flow meter (Flow Technology - High-Rate) and the separator single-phase liquid flow meter (Halliburton - High-Rate). There is a significant discrepancy even between these daily averaged rates and the deviation increases from ~ 4 percent to ~ 11 percent during the production period. This increasing discrepancy is also apparent in Figures 4.2 and 4.3 which show, respectively, the two-hour averages for the two flow meters, calculated from the cumulative values recorded in the Daily Reports. The extent of the variations in the instantaneous full-stream flow rates reported by RDI is also illustrated in Figures 4.2, 4.3 and 4.4. Figure 4.4 also illustrates the variation with time of the temperature of the produced fluid.

The single-phase flow measurements at the separator outlet are considered to be more reliable than the full-stream two-phase measurements. During the early drawdown period (Figure 4.2) the measurements at the two turbine locations are in reasonably good agreement and the RDI instantaneous values show very limited scatter. There appears to be no large variations in flow rates during the drawdown period. The average flow rate over the production period is taken to be

$$q = 14{,}170 \text{ sep bbl/day} \qquad (4.2)$$

The log-log plot of the pressure data during drawdown (Figure 4.5) displays a delay in approaching the unit slope line as was the case with Sand Zone No. 9 (see Figure 3.3); wellbore afterflow effects should not be significant for $t > 0.1$ to 0.5 hr, but wellbore thermal effects persist longer. Pressure data for the

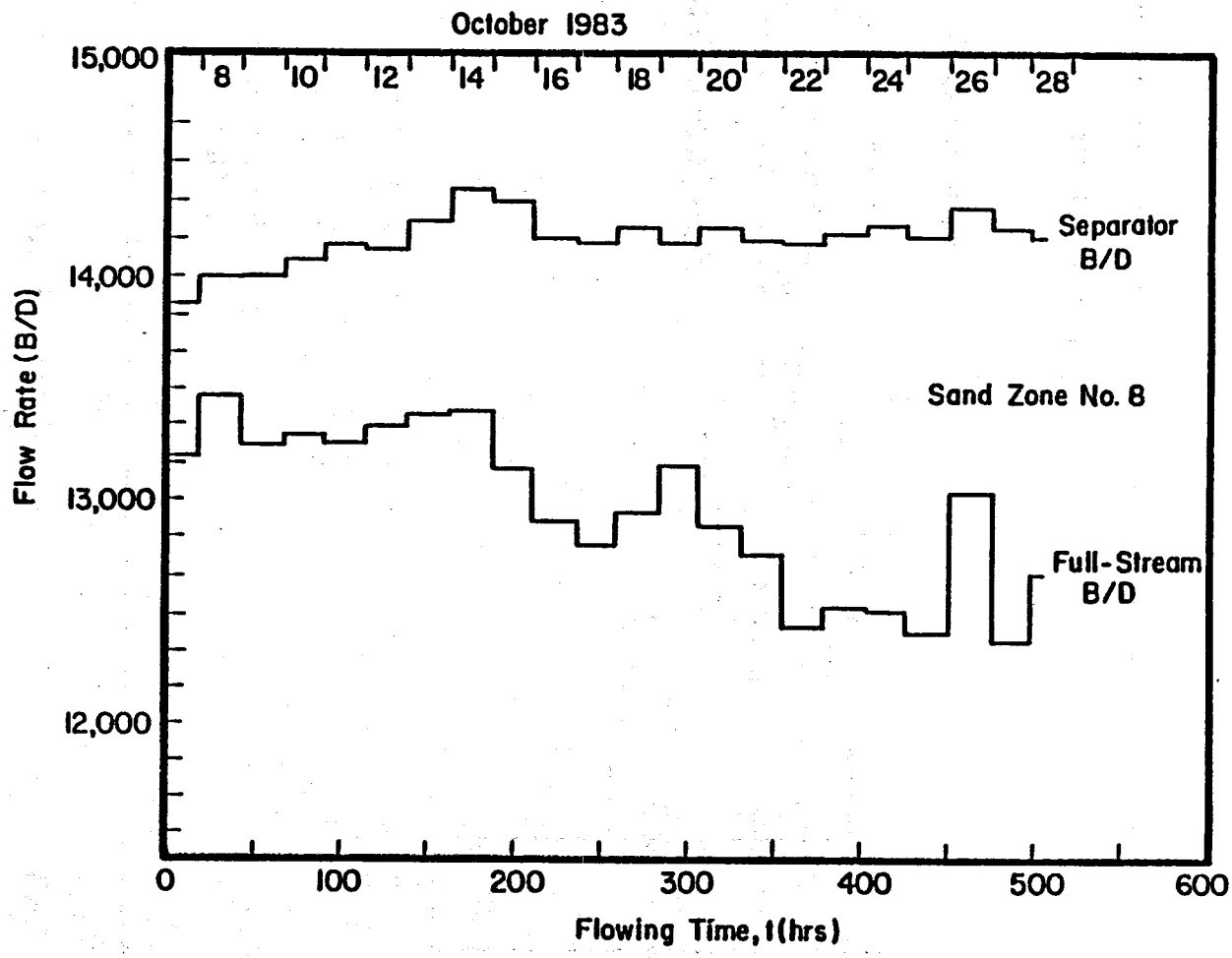

Figure 4.1. Comparison of Gladys McCall flow rate daily averages from T-F&S Daily Reports (Sand Zone No. 8).

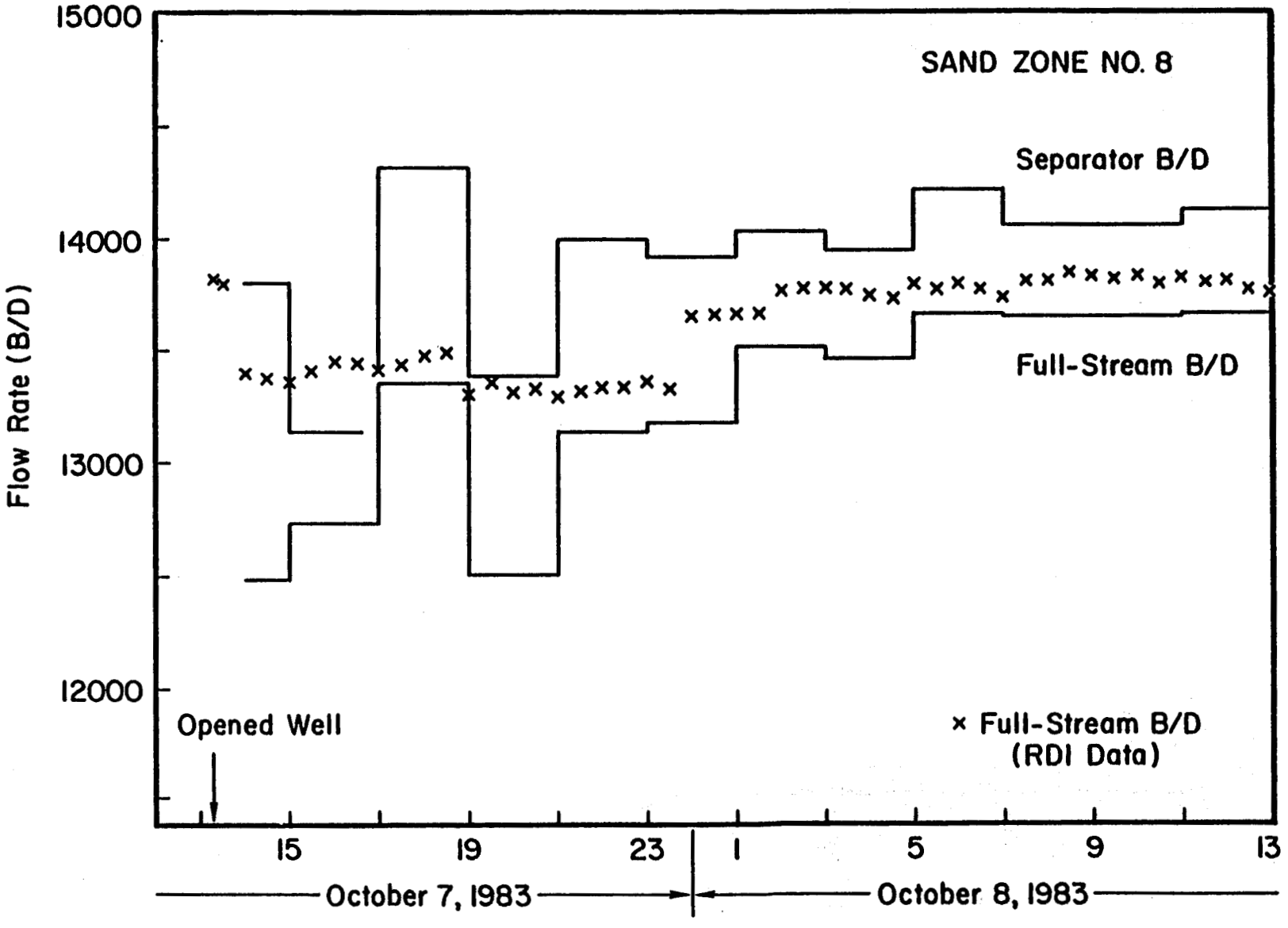

Figure 4.2. Comparison of early-time flow rates computed from cumulative production measured at two turbine locations.

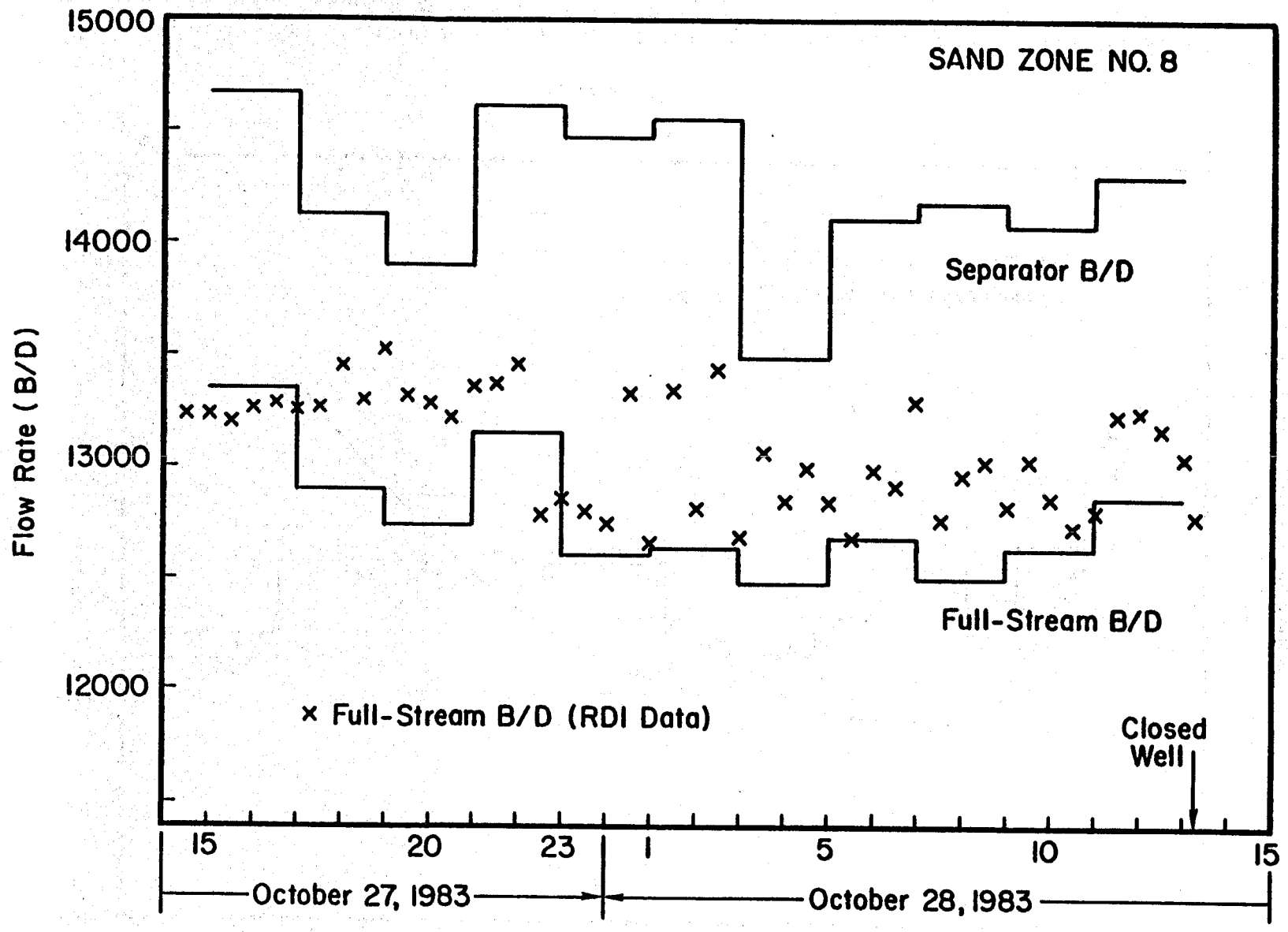

Figure 4.3. Comparison of late-time flow rates computed from cumulative production measured at two turbine locations.

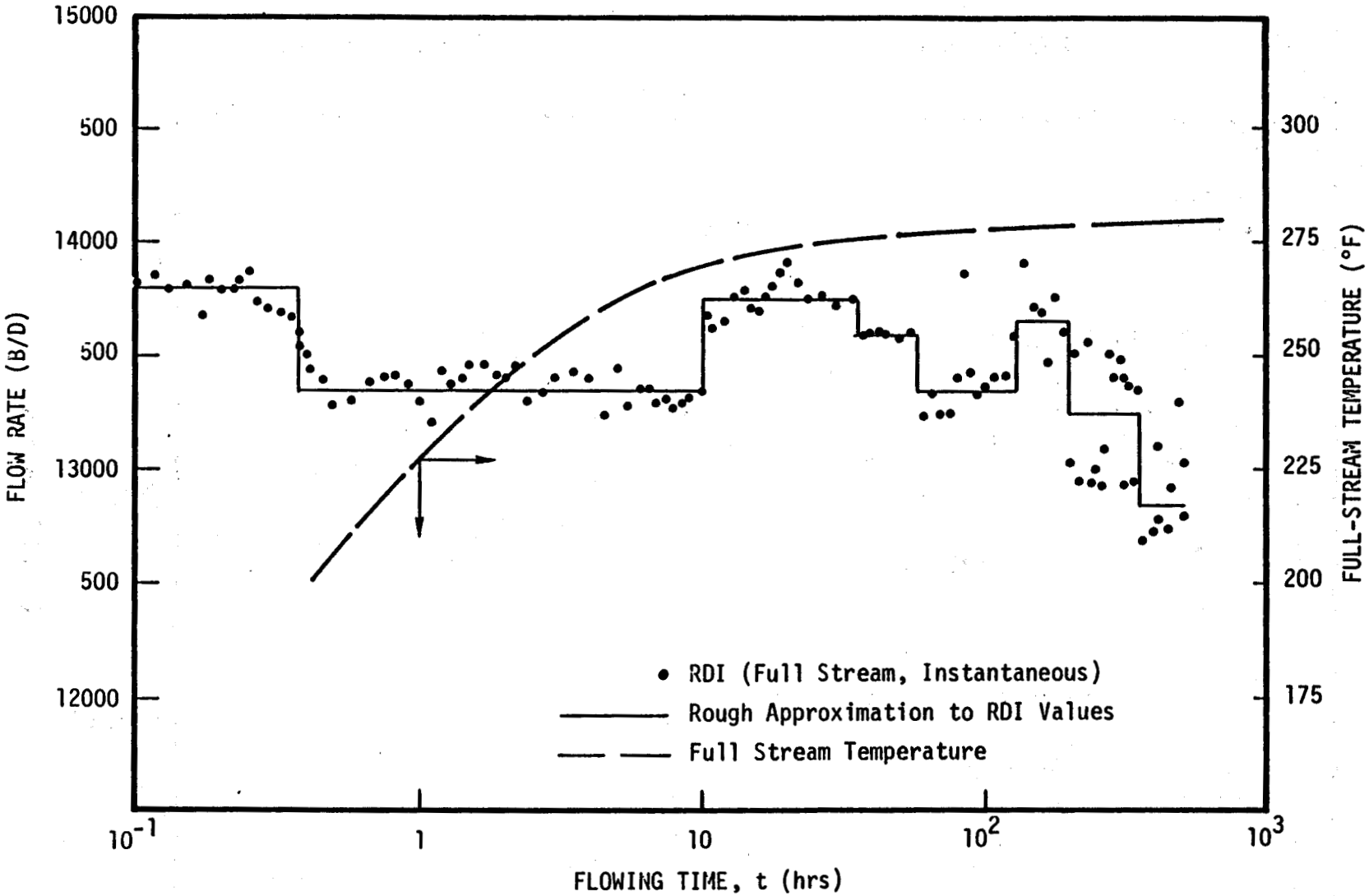

Figure 4.4. Illustration of very early variations in full-stream temperature and the flow-rate data reported by RDI for Sand Zone No. 8.

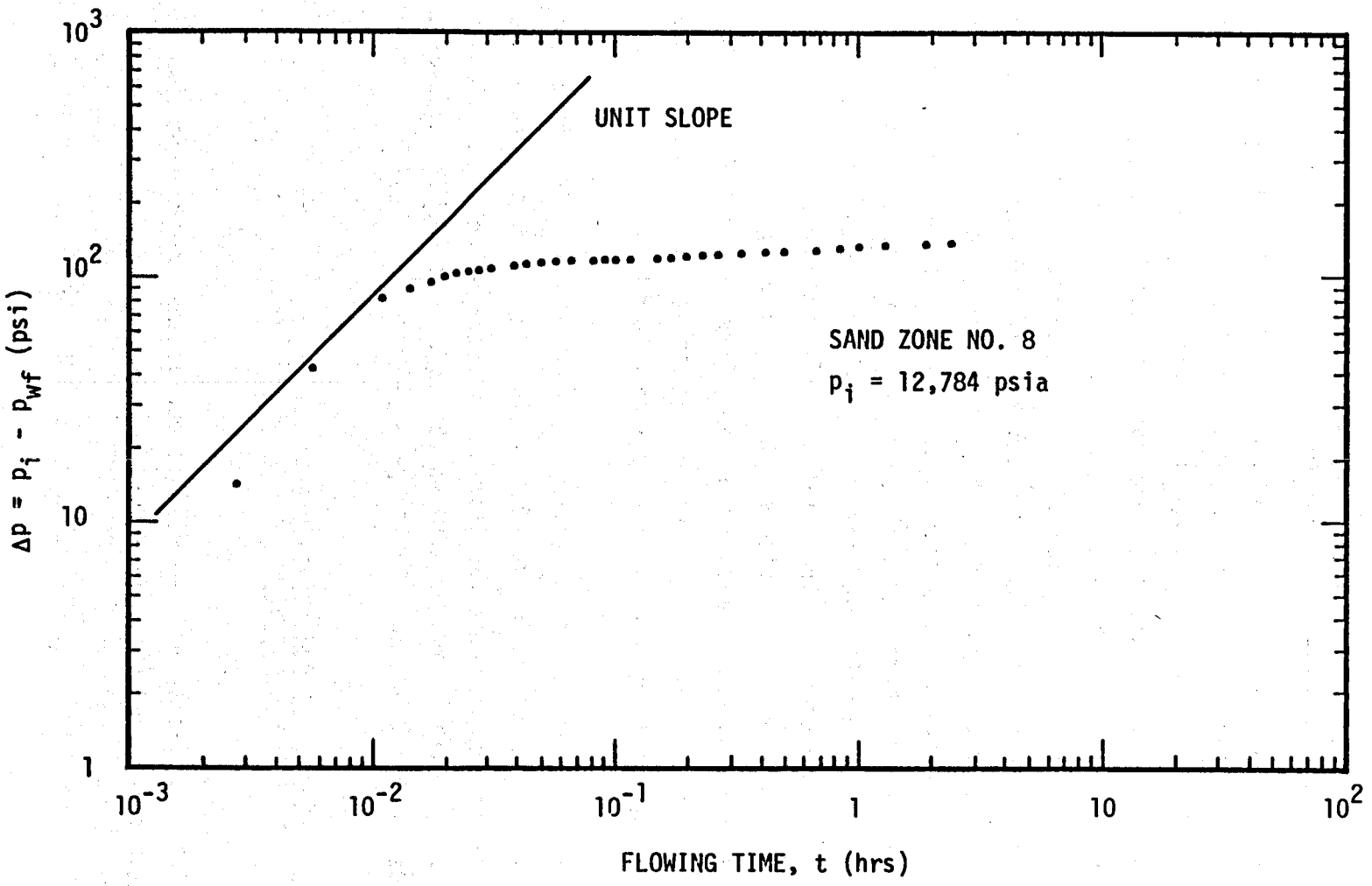

Figure 4.5. Sand Zone No. 8 drawdown type curve.

buildup portion of the Reservoir Limits Test for Sand Zone No. 8 are not available for very short shutin times but the log-log plot of the data (Figure 4.6) is similar over the range where data exist.

Significant portions of the semi-log plot of the bottomhole drawdown pressure data (Figure 4.7) are approximated by four straight line segments. The first line segment, of slope m_1 = -10.6 psi/cycle, fits the data for only about two-thirds of a log cycle and the pressure measurements it approximates are influenced by fluid compression and thermal changes in the wellbore (wellbore storage effects). The second line segment, of slope m_2 = -18.2 psi/cycle, fits the data for a full log cycle and the pressure measurements it approximates should not be significantly influenced by wellbore effects. The value of m_2 is assumed to reflect the reservoir response and will be used to estimate formation parameters. The third line segment (of slope $m_3 \sim 2\, m_2$) appears to indicate the presence of a reservoir boundary which causes a doubling of the slope at t ~ 9.5 hrs. The fourth segment (slope $m_4 \sim 4\, m_2$) beginning at ~ 31.5 hrs probably represents a more distant reservoir boundary.

Using m_2 and relation (3.3), we can estimate the formation permeability for Sand Zone No. 8. During the first ten hours the flow rate is somewhat smaller than the average value of 14,170 sep bbl/day. With q ~ 13,800 sep bbl/day, m = 18.2 psi/cycle, μ = 0.31 cp, B ~ 0.984 and h ~ 332 ft, we obtain

$$k = \frac{(162.6)(13{,}800)(0.31)(0.984)}{(18.2)(332)} = 113 \text{ md} \qquad (4.3)$$

The skin factor at the wellbore during the drawdown portion of the test is computed from the relation

$$s = 1.151 \left[\frac{p_i - p_{1\,hr}}{m} - \log \frac{k}{\phi \mu c_T r_w^2} + 3.23 \right] \qquad (4.4)$$

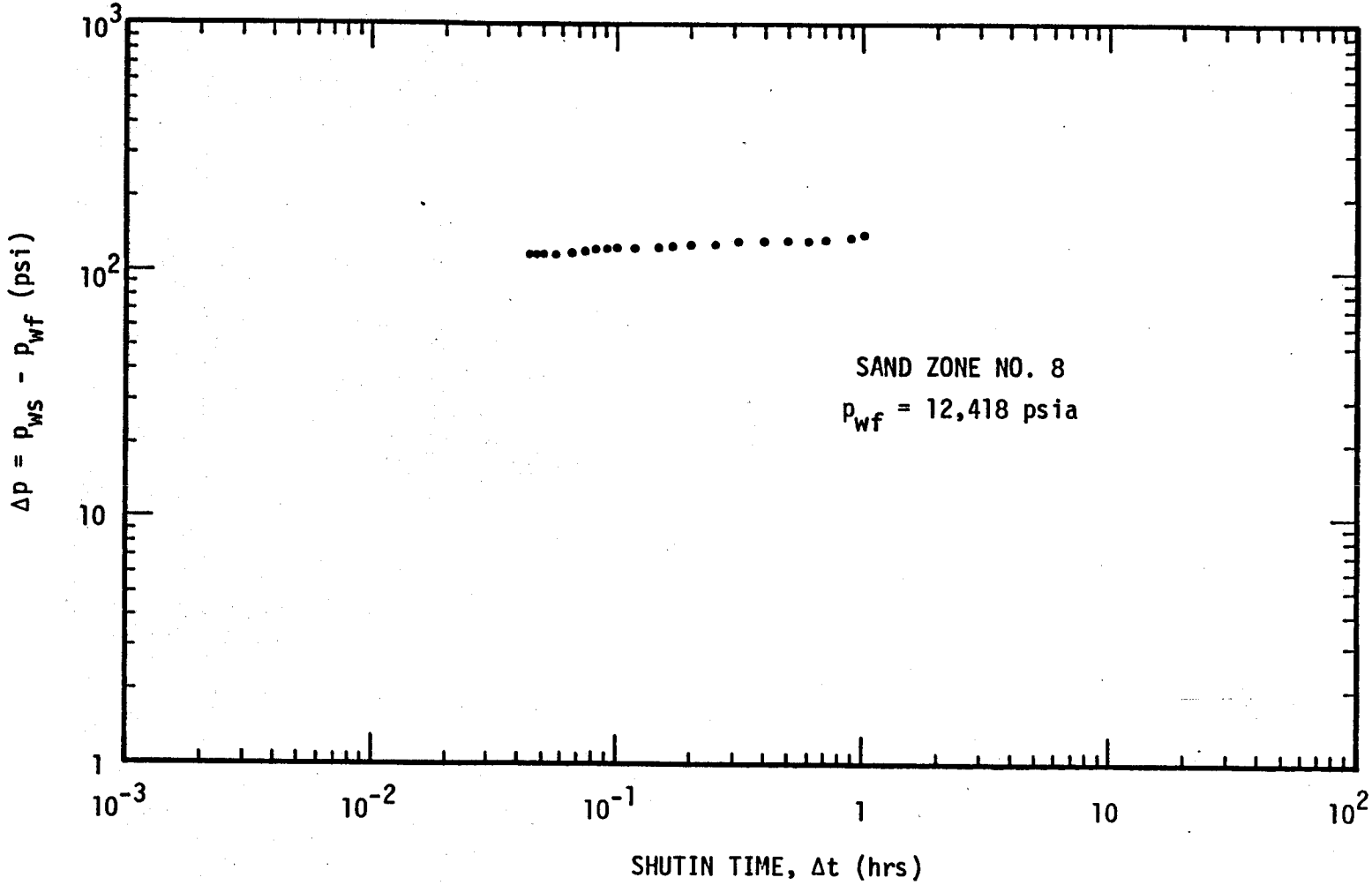

Figure 4.6. Sand Zone No. 8 buildup type curve.

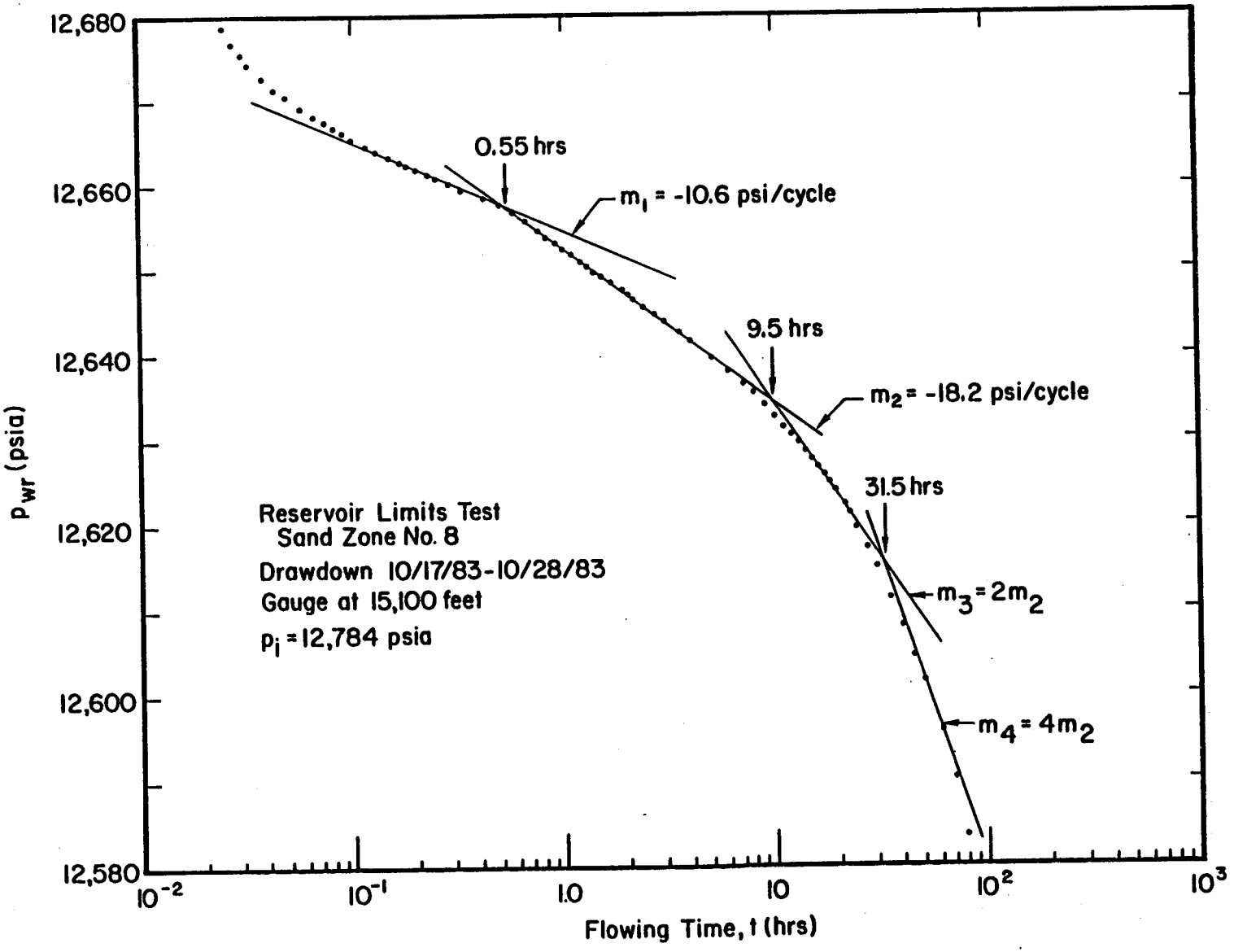

Figure 4.7. Sand Zone No. 8 pressure drawdown semi-log plot.

where

m ~ Slope of straight line-fit on semi-log plot, psi/cycle.

p_i ~ Shutin pressure just prior to drawdown, psia.

$p_{1\ hr}$ ~ Flowing pressure at t = 1 hr from the straight line on the semi-log plot, psia.

r_w ~ Radius of wellbore, feet.

ϕ ~ Formation porosity.

C_T ~ Total formation compressibiity, $psia^{-1}$.

With $m = 18.2$ psi/cycle, $p_i = 12{,}784$ psi, $p_{1\ hr} = 12{,}652$ psia, $r_w = 0.2917$ ft, $\phi = 0.16$ and $C_T = 6.27 \times 10^{-6}$ psi^{-1}, we compute

$$s = 1.151 \left[\frac{12{,}784 - 12{,}652}{18.2} - \log \frac{113}{(0.16)(0.31)(6.27 \times 10^{-6})(0.2917)^2} + 3.23 \right] \quad (4.5)$$

$$= +0.98$$

The semi-log plot of the buildup data (Figure 4.8) is approximated by three straight line segments. The segment of slope $m_1 = 16$ psi/cycle fits the data for one and a half time cycles and persists well beyond the duration of wellbore storage effects; the second segment, of slope $m_2 = 11.9$ psi/cycle, fits the data for about two-thirds of a time cycle. The first segment is assumed to reflect the infinite reservoir response portion of the buildup data and the changes in slope to m_2(at $\Delta t = 1.5$ hr) and to m_3(at $\Delta t =$ 14 hrs) are believed due to reservoir boundaries.

Using Equation (3.3) with $q = 14{,}200$ bbl/day, $\mu = 0.31$ cp, $B = 0.984$, $m = 16$ psi/cycle and $h = 332$ ft, we obtain

$$k = \frac{(162.6)(14{,}200)(0.31)(0.984)}{(16)(332)} = 133 \text{ md} \quad (4.6)$$

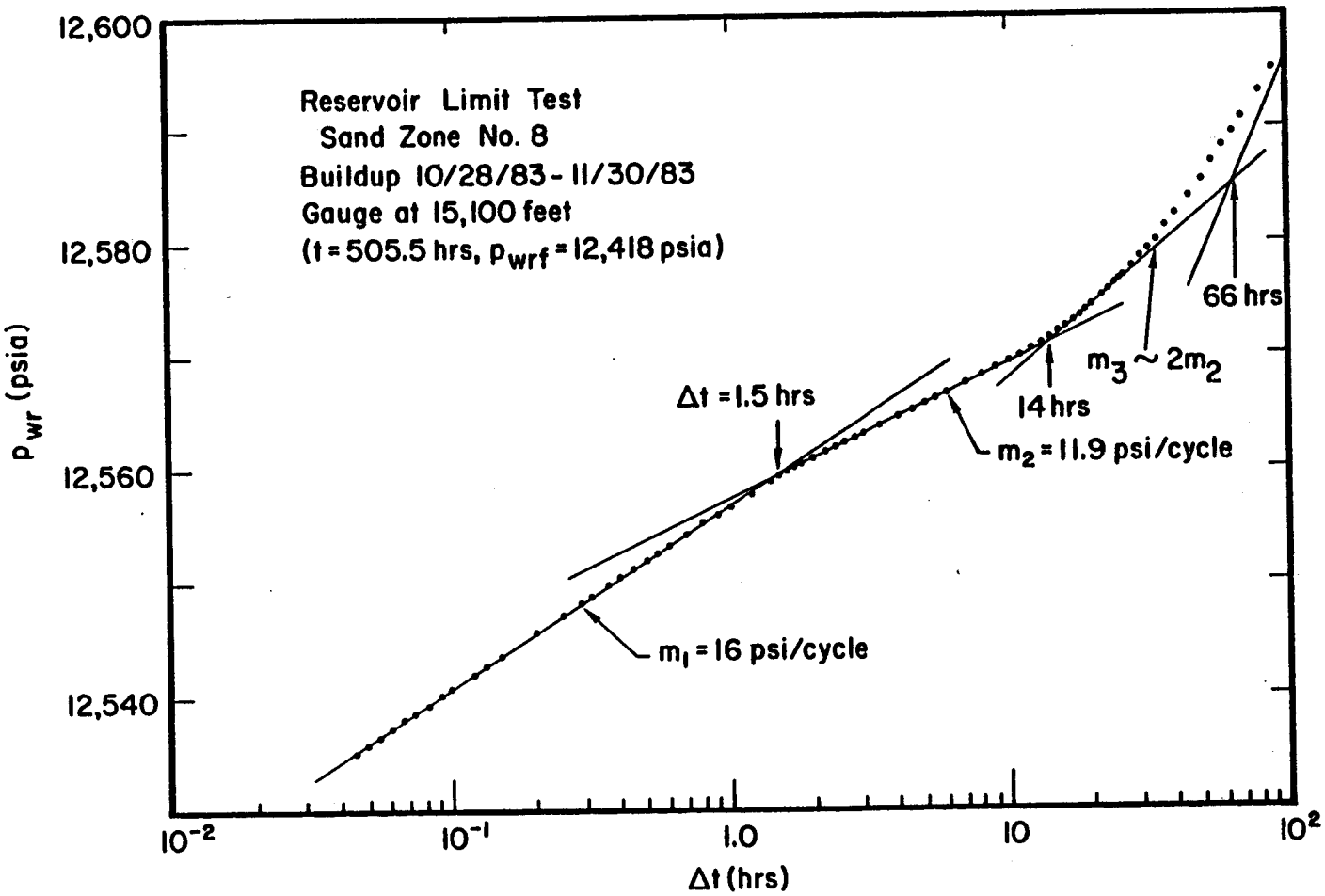

Figure 4.8. Sand Zone No. 8 early pressure buildup semi-log plot.

The corresponding estimate for the skin factor may be computed using Equation (3.5). With $m = 16$ psi/cycle, $p_{1\ hr} = 12{,}557$ psi, $p_{wf} = 12{,}418$ psia, $r_w = 0.2917$ ft, $\phi = 0.16$ and $C_T = 6.27 \times 10^{-6}$ psi^{-1} we obtain

$$s = 1.151 \left[\frac{12{,}537 - 12{,}418}{16} - \log \frac{133}{(0.16)(0.31)(6.27 \times 10^{-6})(0.2917)^2} + 3.23 \right]$$

$$= +2.55 \quad . \tag{4.7}$$

The doubling of the slope of the semi-log plot during drawdown at $t \sim 9.5$ hrs and 31.5 hrs (Figure 4.7) may be used with Equation (3.9) to estimate the distances to the two nearest faults. With $k = 133$ md, $\phi = 0.16$, $\mu = 0.31$ cp and $C_T = 6.27 \times 10^{-6}$ psi^{-1}, we compute

$$L_1 = 0.01217 \left[\frac{(133)(9.5)}{(0.16)(0.31)(6.27 \times 10^{-6})} \right]^{1/2} \sim 780 \text{ ft} \tag{4.8}$$

and

$$L_2 = 0.01217 \left[\frac{(133)(31.5)}{(0.16)(0.31)(6.27 \times 10^{-6})} \right]^{1/2} \sim 1410 \text{ ft} \quad . \tag{4.9}$$

The Cartesian plot of the recorded drawdown pressures over the full drawdown portion of the Reservoir Limits Test for Sand Zone No. 8 is presented in Figure 4.9. The data over the final ~ 200 hrs are closely approximated by a straight line of slope $\tilde{m}^* = -0.347$ psi/hr. This slope is still decreasing and hence corresponds to late-stage transient flow. We can use relation (3.10) to calculate a lower bound for the connected pore volume.

$$V_p > 0.0418 \frac{(14{,}170)(0.984)}{(6.27 \times 10^{-6})(0.347)} = 268 \times 10^6 \text{ res bbls} \tag{4.10}$$

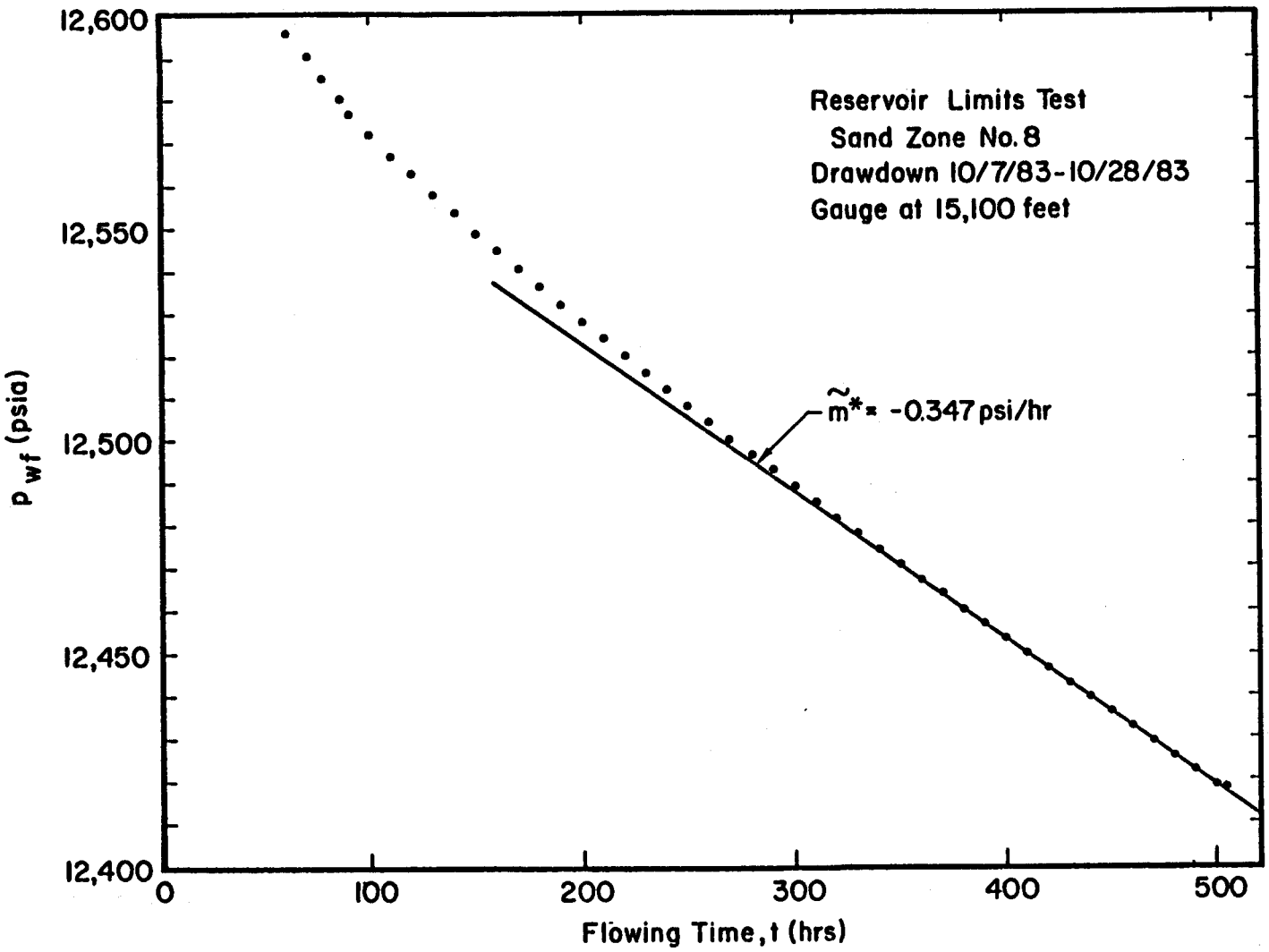

Figure 4.9. Sand Zone No. 8 Cartesian plot of late pressure drawdown data.

If the drawdown of Sand Zone No. 8 had indeed attained semi-steady state flow, the volumetric average pressure within the closed reservoir would be

$$\bar{p} = p_i + t_p m^* \tag{4.11}$$

$$\sim 12{,}784 + (505.5)(-0.347) = 12{,}609 \text{ psia} .$$

In fact, a value of $p_{ws} = 12{,}655$ psia was measured at $\Delta t = 785.5$ hrs and the pressure appears to be still rising at that point. To obtain a better estimate for the reservoir volume than the lower bound given in (4.10), we hypothesize the p_{ws} in approaching $\bar{p}$ exponentially, i.e.,

$$p_{ws} = \bar{p} + p^* \exp(-\Delta t/\tau) .$$

A semi-log plot of $(\bar{p} - p_{ws})$ versus shutin time, Δt, does indeed yield a straight line for

$$\bar{p} = 12{,}676 \text{ psia (874 bars)} \tag{4.12}$$

as is shown in Figure 4.10. The corresponding estimate for the connected pore-volume may be computed from

$$V_p = \frac{QB}{C_T \Delta p}, \quad (\Delta p = p_i - \bar{p}) \tag{4.13}$$

where

Q ~ Total brine volume produced, sep bbl.
B ~ Formation volume factor res bbl/sep bbl.
C_T ~ Total formation compressibility, psia^{-1}.
p_i ~ Initial reservoir pressure, psia.

With

$$Q = 2.98 \times 10^5 \text{ sep bbl and } \Delta p = 12{,}784 - 12{,}676 = 108 \text{ psi},$$

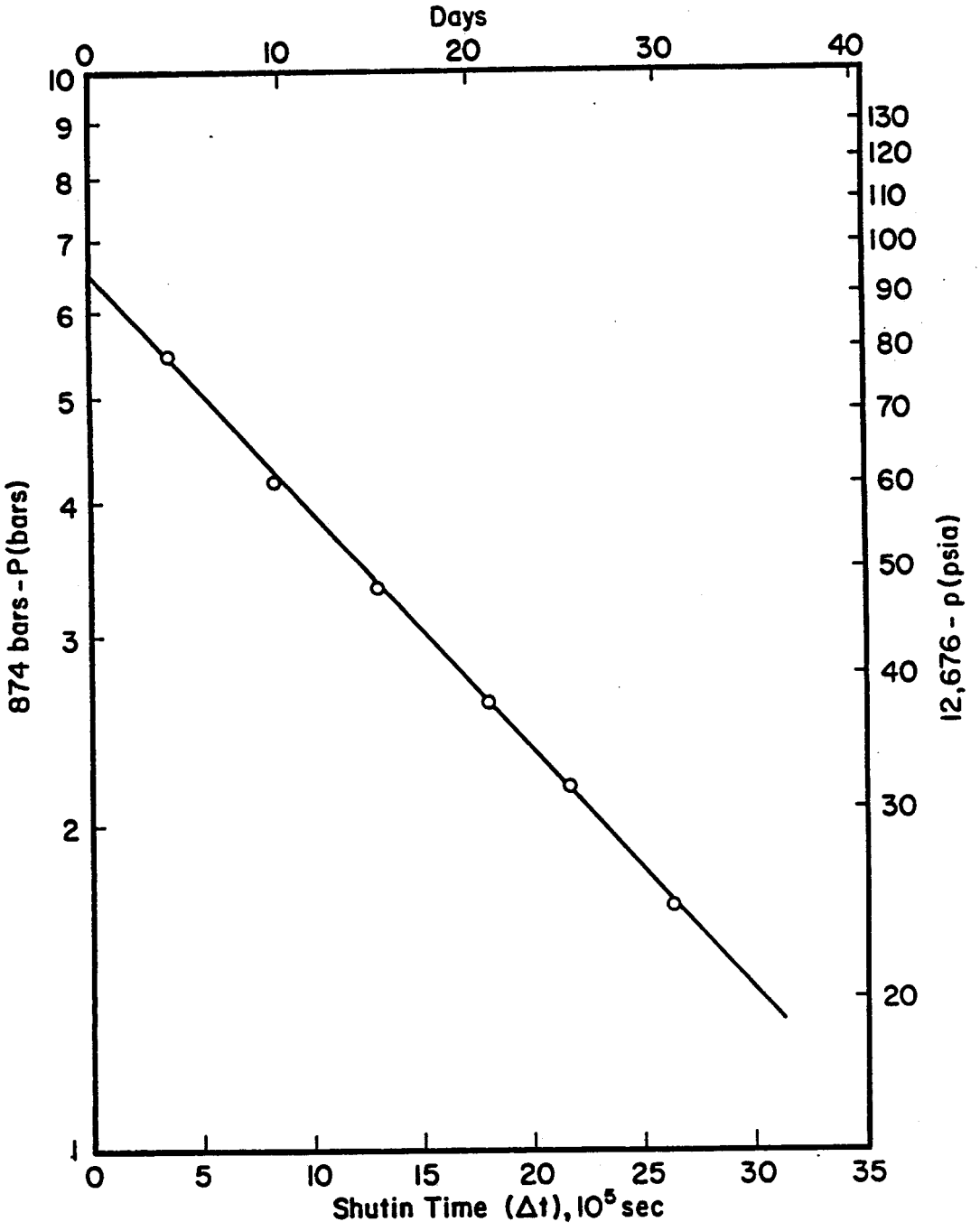

Figure 4.10. Use of late buildup data for Sand Zone No. 8 to estimate average reservoir pressure after limit test.

we calculate

$$V_p = \frac{(2.98 \times 10^5)(0.984)}{(6.27 \times 10^{-6})(108)} \sim 433 \times 10^6 \text{ bbl} \qquad (4.14)$$

4.2 HISTORY MATCHING SIMULATIONS

The geologic map prepared by Magma Gulf Company (Figure 2.1) shows two nearly parallel west-east growth faults (Faults II and III) to the north and to the south of the Gladys McCall No. 1 well. Their locations relative to the subject well could not be fixed from the north-south structural sections based on well correlations. The reservoir boundaries at the distances approximated by Equations (4.8) and (4.9) are probably Faults II and III or other essentially parallel west-east growth faults. Since there are no wells to provide geologic constraints on the reservoir to the east and west of the Gladys McCall No. 1 well, we assume the east and west boundaries are at an equal distance from the well; this distance can be estimated from the reservoir volume approximation in Equation (4.14).

Figure 4.11 depicts the rectangular reservoir configuration used in the history matching simulation of the Reservoir Limits Tests of Sand Zone No. 8. Since the reservoir simulator employs the International System of Units, reservoir dimensions used in the history matching calculations were round numbers in SI units. The distances from the well to the two nearest boundaries (growth faults) are assumed to be

$$L_1 = 240 \text{ m } (787 \text{ ft})$$
$$L_2 = 400 \text{ m } (1312 \text{ ft}) \qquad (4.15)$$

The distances from the well to each of the two most distant boundaries are assumed to be 3300 meters (10,827 ft); the reservoir thickness is assumed to be h = 100 m (328 ft).

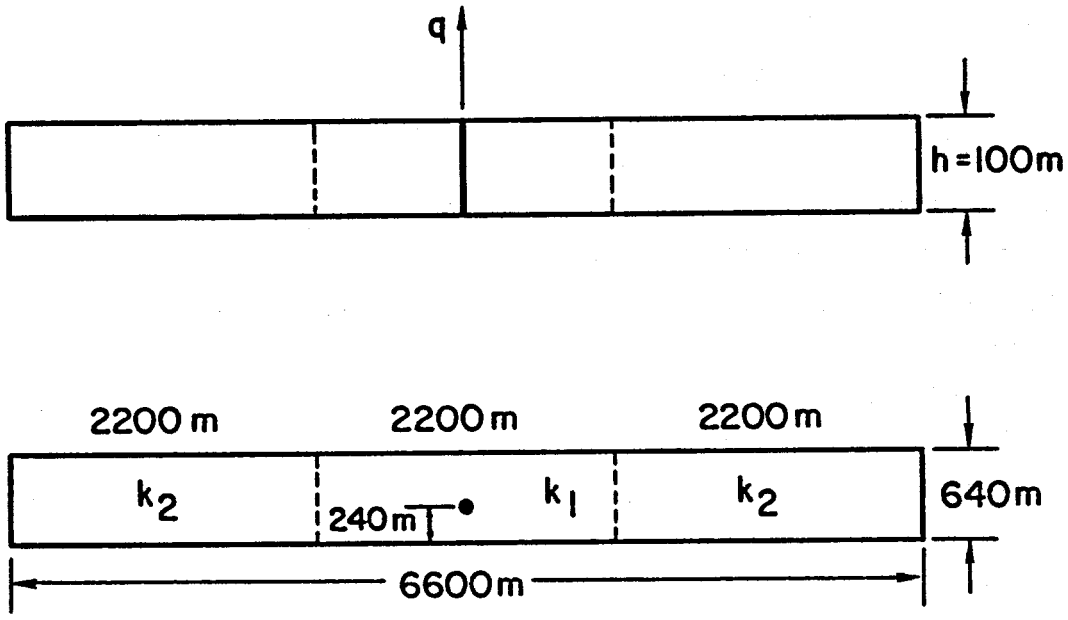

Figure 4.11. Simulation model for Sand Zone No. 8 Reservoir Limits Test pressure history matching.

The simulations employed the following reservoir formation rock and fluid input parameters:

Initial pressure, $p_i = 8.8143 \times 10^7$ Pa (12,784 psia) .

Fluid density, $\rho = 1030.5$ kg/m^3 (64.3 lb/ft^3) .

Fluid viscosity, $\mu = 3.1 \times 10^4$ Pa-sec (0.31 cp) .

Fluid compressibility, $C_w = 4.23 \times 10^{-10}$ Pa^{-1} (2.93×10^{-6} psi^{-1}).

Rock pore-volume compressibility, $C_f = 4.87 \times 10^{-10}$ Pa^{-1} (3.34×10^{-6} psi^{-1}).

Formation porosity, $\phi = 0.16$.

The total compressibility is $C_T = C_w + C_f = 9.1 \times 10^{-10}$ Pa^{-1} ($= 6.27 \times 10^{-6}$ psi^{-1}). The connected pore-volume assumed in the simulation is given by

$$V_p = \phi V = (0.16)(100)(640)(6600) \tag{4.16}$$

$$\sim 67.6 \times 10^6 \text{ m}^3 \ (425 \times 10^6 \text{ res bbl}) .$$

The calculations employed a two-dimensional areal representation of the reservoir. Each half of the symmetrical reservoir configuration is represented by a 13 x 18 numerical grid; the zone penetrated by the well is 20 m x 40 m with the zone dimensions increasing away from the well. During the drawdown period ($t < 505.5$ hrs) of the Reservoir Limits Test the production rate from the well is

$\dot{m} = 26.03$ kg/sec (14,170 sep bbl/day) .

The radius of the well is $r_w = 0.0889$ m (0.2917 ft).

A number of simulations were made in which the choices of the reservoir formation permeability (k) and skin factor (s) were varied. It was necessary to assume a decrease in the reservoir transmissivity (kh product) away from the well to account for the

slowly changing slope in the Cartesian plot of the drawdown pressures (Figure 4.9) and the slow buildup to p in the buildup portion of the test (Figure 4.10). A match to the drawdown/buildup bottomhole pressure history measured during the Reservoir Limits Test of Sand Zone No. 8 can be obtained by simply assuming a "near-well" permeability (k_1) abruptly decreasing to a "reduced" permeability (k_2) at a distance of 1100 meters from the well (Figure 4.11). The simulation performed using

$$k_1 = 160 \times 10^{-15} m^2 \text{ (162 md)}$$

$$k_2 = 20 \times 10^{-15} m^2 \text{ (20.2 md)} \qquad (4.17)$$

$$s = 4.3$$

resulted in the excellent history match over the entire production/injection test period that is presented in Figure 4.12.

The reservoir model described by Figure 4.11 and the above reservoir parameters is by no means unique. An alternative history match simulation of the Reservoir Limits Test of Sand Zone No. 8 has been presented which is based on a conceptual model in which both reservoir thickness (h) and permeability (k) decrease with distance from the well (Ancell, 1984). His conceptual model (a) and two other alternate conceptual models, (b) and (c), are illustrated schematically in Figure 4.13. Model (b) could represent a reservoir with a flow constriction caused by a fault which cuts across and offsets the sand layer. Model (c) could represent vertical flow from overlying or underlying sands at distances where intervening shale layers have pinched out. An alternative (nonlinear) reservoir model would be to assume the compressibility of the rock pore-volume increases as the reservoir pressure declines. Predictions of future long-term reservoir response might differ substantially for simulations that are based on the different conceptual models.

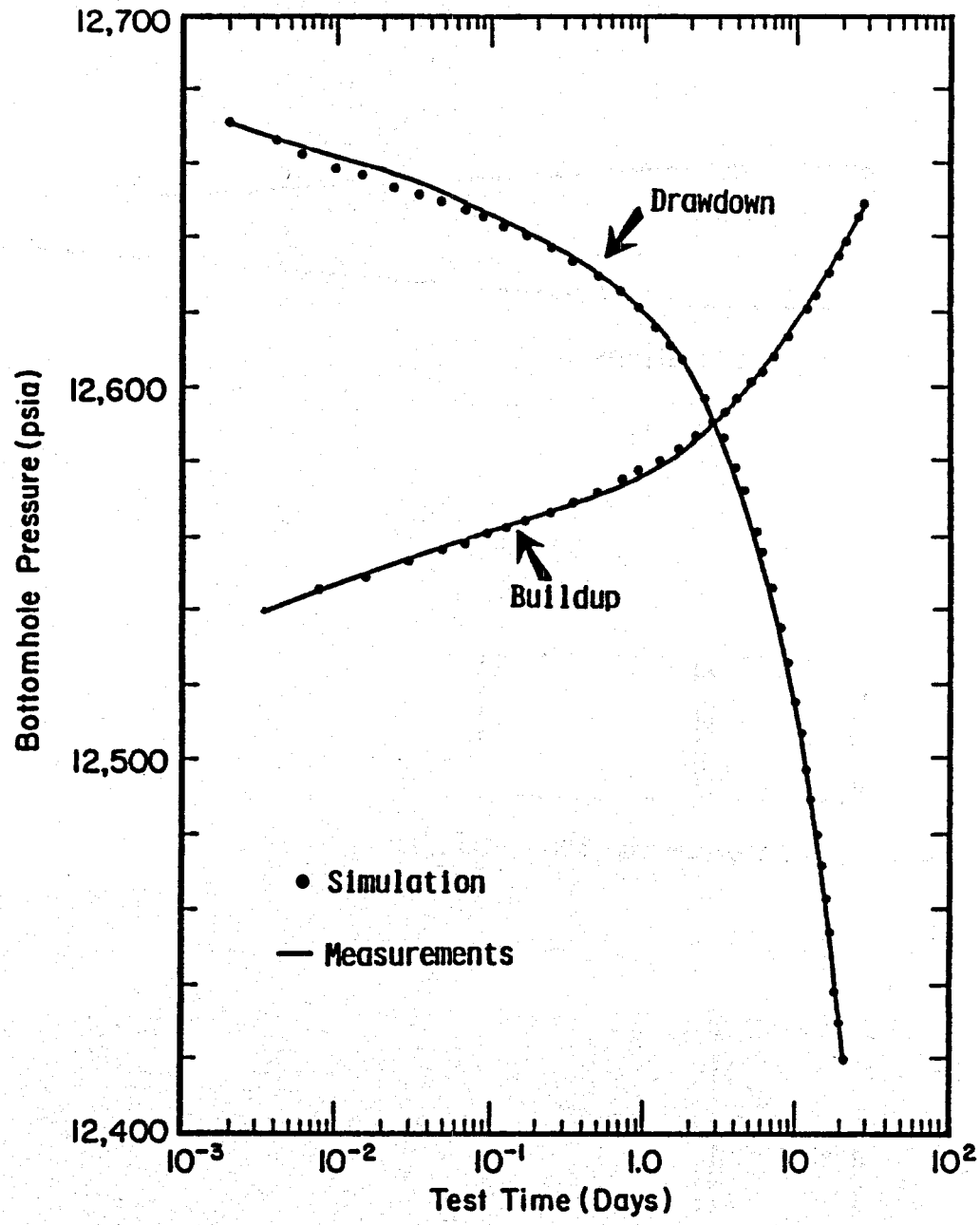

Figure 4.12. Comparison of simulation and measured bottomhole pressures for Sand Zone No. 8 Reservoir Limits Test.

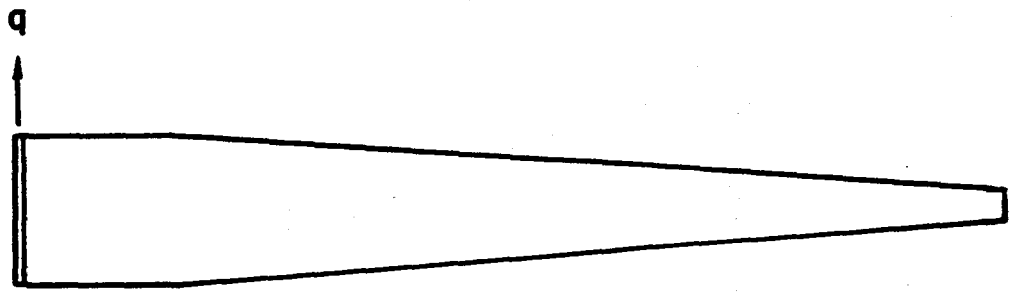

(a) h, k variations

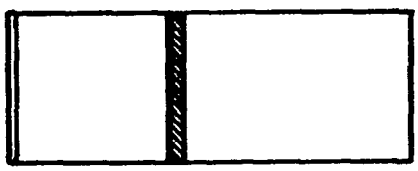

(b) membrane or fault offset

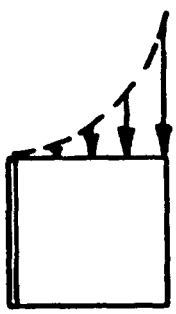

(c) vertical crossflow from adjacent aquifer

Figure 4.13. Symmetrical reservoir vertical sections of alternate conceptual models for Gladys McCall reservoir.

V. SAND ZONE NO. 8 PRODUCTION HISTORY

5.1 WELLHEAD VERSUS WELLBOTTOM DATA

The cumulative production during the Reservoir Limits Test of Sand Zone No. 8 was Q ~ 297,783 sep bbl according to the T-F&S Daily Reports. As of September 4, 1984 the cumulative production from this sand had reached Q ~ 4,510,634 sep bbl. Figure 5.1 presents a plot of the cumulative production over this approximately one year time period; production testing is still in progress. The average for the total gas production from the well is still ~ 30 SCF/STB. Figure 5.1 also shows the approximate variations (over 60 rate changes) in the flow rate of the Gladys McCall No. 1 well during this period.

Since no wellbottom pressures (p_{WB}) have been measured since completion of the Reservoir Limits Test, only wellhead pressure (p_{WH}) measurements are available to estimate bottomhole values. Under semi-steady state flow conditions the two are related by

$$p_{WH} = p_{WB} - \Delta p_{fric} - \Delta p_{hydr} \tag{5.1}$$

where

Δp_{fric} ~ Pressure drop due to wellbore friction

Δp_{hydr} ~ Pressure drop due to elevation change .

Estimation of Δp_{fric} is complicated in the Gladys McCall well by scaling on the inner wall of the production tubing, especially at production rates of > ~ 20,000 bbl/day. This decrease in the inner radius of the tubing is controlled by periodic acid treatments which have proved to be effective in removal of the scale and reduction of Δp_{fric}. When the well is shut, $\Delta p_{fric} = 0$ and it is only necessary to add the hydrostatic pressure drop to p_{WH} in order to

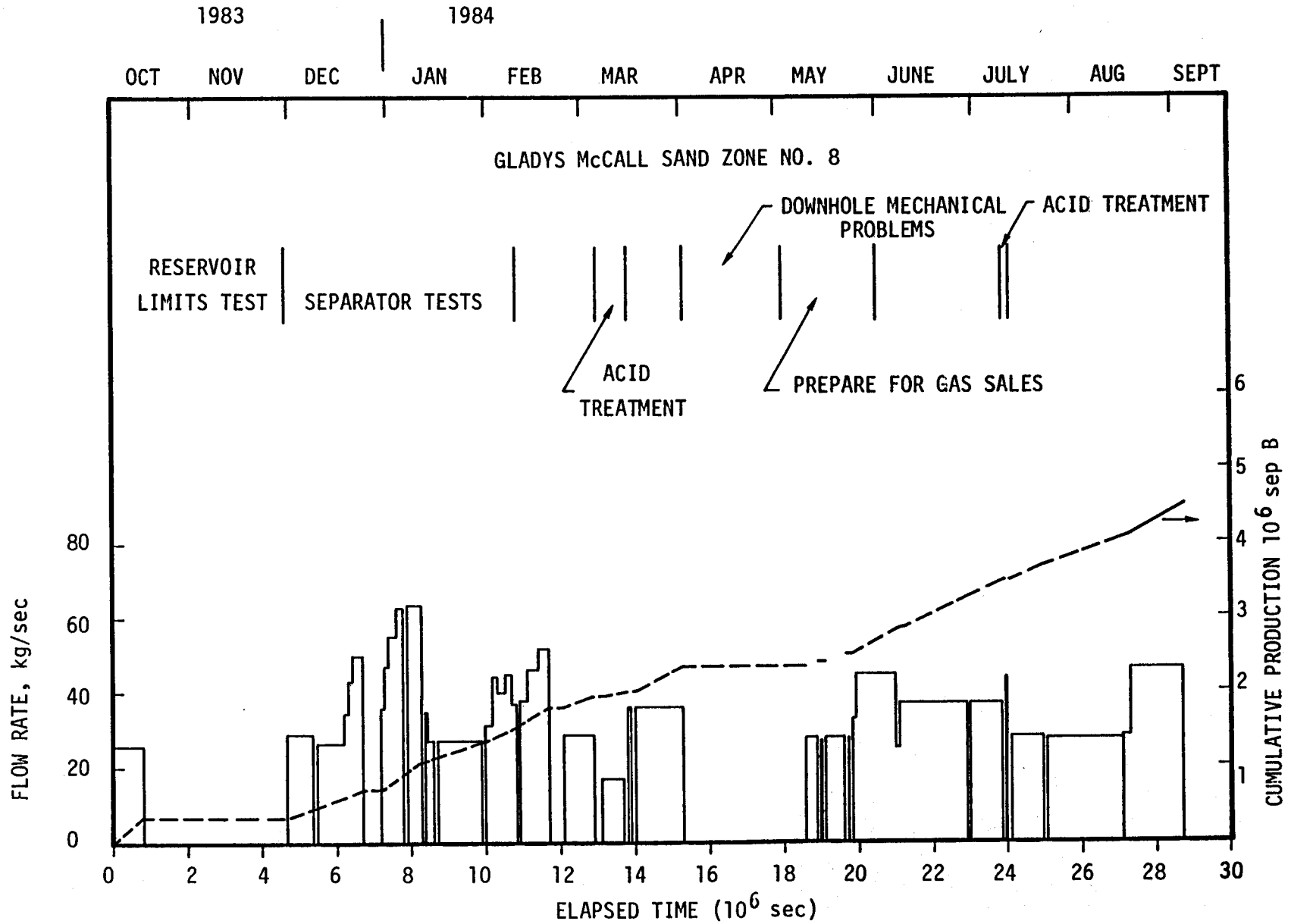

Figure 5.1. Gladys McCall Sand Zone No. 8 production history through September 4, 1984.

estimate p_{WB} from Equation (5.1). Since the relation ignores wellbore storage effects (after flow and cooling in the wellbore), the inferred values for p_{WB} during the transient period following shutting the well, however, may be in significant error. To evaluate the reliability of estimating p_{WB} from p_{WH} measurements made immediately after shutting the well, we refer to the data from the Reservoir Limits Test of Sand Zone No. 8 during which both were measured.

Figure 5.2 shows that during the latter stages of the drawdown portion of the test (q = 14,200 sep bbl/day) the pressure drop from wellbottom (at a depth of 15,100 feet) to wellhead is

$$p_{WB} - p_{WH} = \Delta p_{fric} + \Delta p_{hydr}$$

$$\sim 6992 \text{ psi } (482 \times 10^5 \text{Pa}) \qquad (5.2)$$

Figure 5.3 shows that immediately after shutin, the pressure drop in the wellbore is

$$p_{WB} - p_{WH} = \Delta p_{hydr}$$

$$\sim 6626 \text{ psi } (457 \times 10^5 \text{Pa}) \; . \qquad (5.3)$$

The corresponding estimate for the frictional pressure drop in the wellbore is (prior to significant scaling of the production tubing)

$$\Delta p_{fric} \sim 6692 - 6626$$

$$= 366 \text{ psi } (25.23 \times 10^5 \text{Pa}) \qquad (5.4)$$

at q = 14,200 sep bbl/day. Analogous plots of $p_{WB} - p_{WH}$ for Sand Zone No. 9 (Figures 5.4 and 5.5) yield an estimate of (prior to significant scaling of the production tubing)

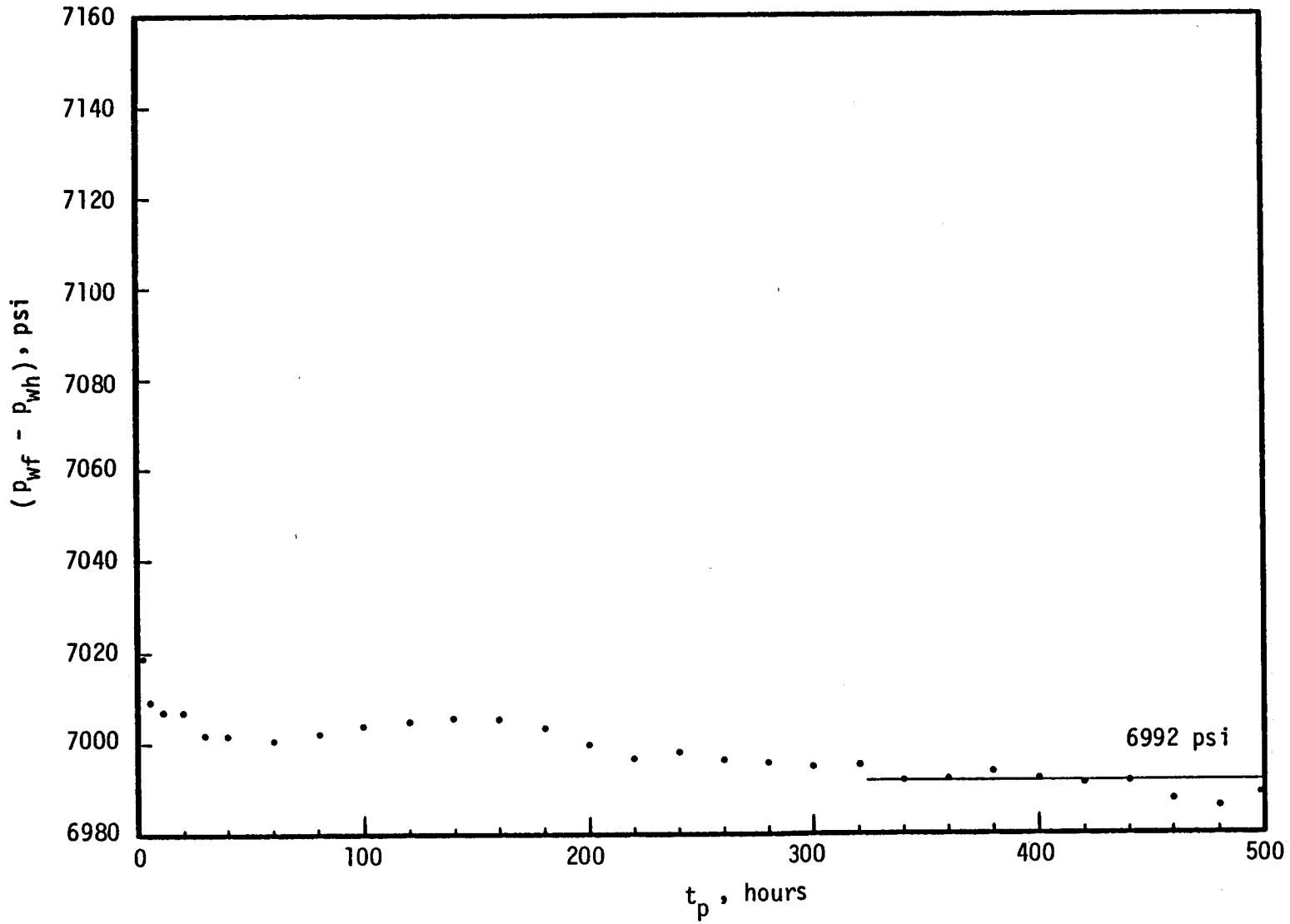

Figure 5.2. Pressure drop in the wellbore during drawdown portion of Reservoir Limits Test of Sand Zone No. 8.

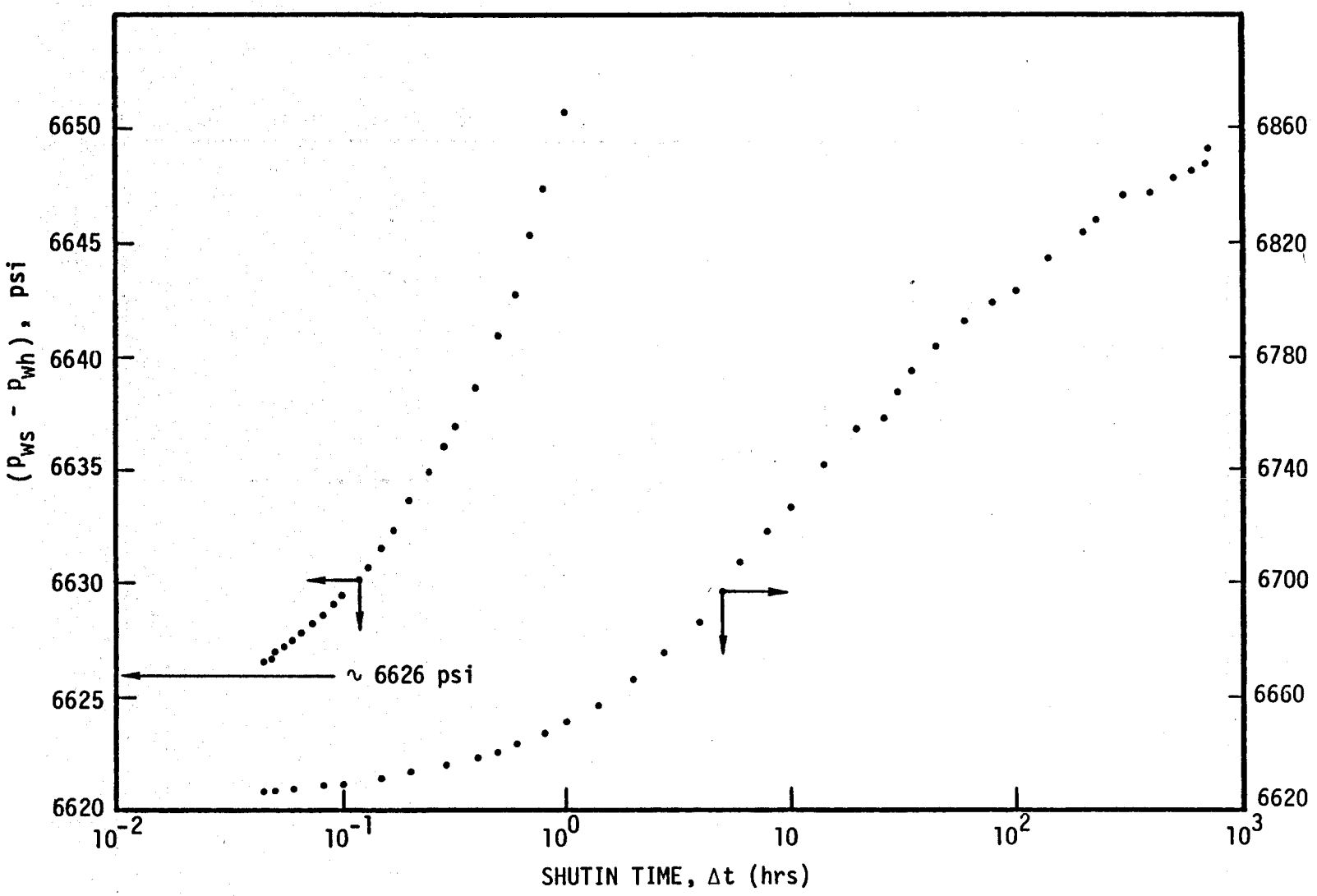

Figure 5.3. Pressure drop in the wellbore during buildup portion of Reservoir Limits Test of Sand Zone No. 8.

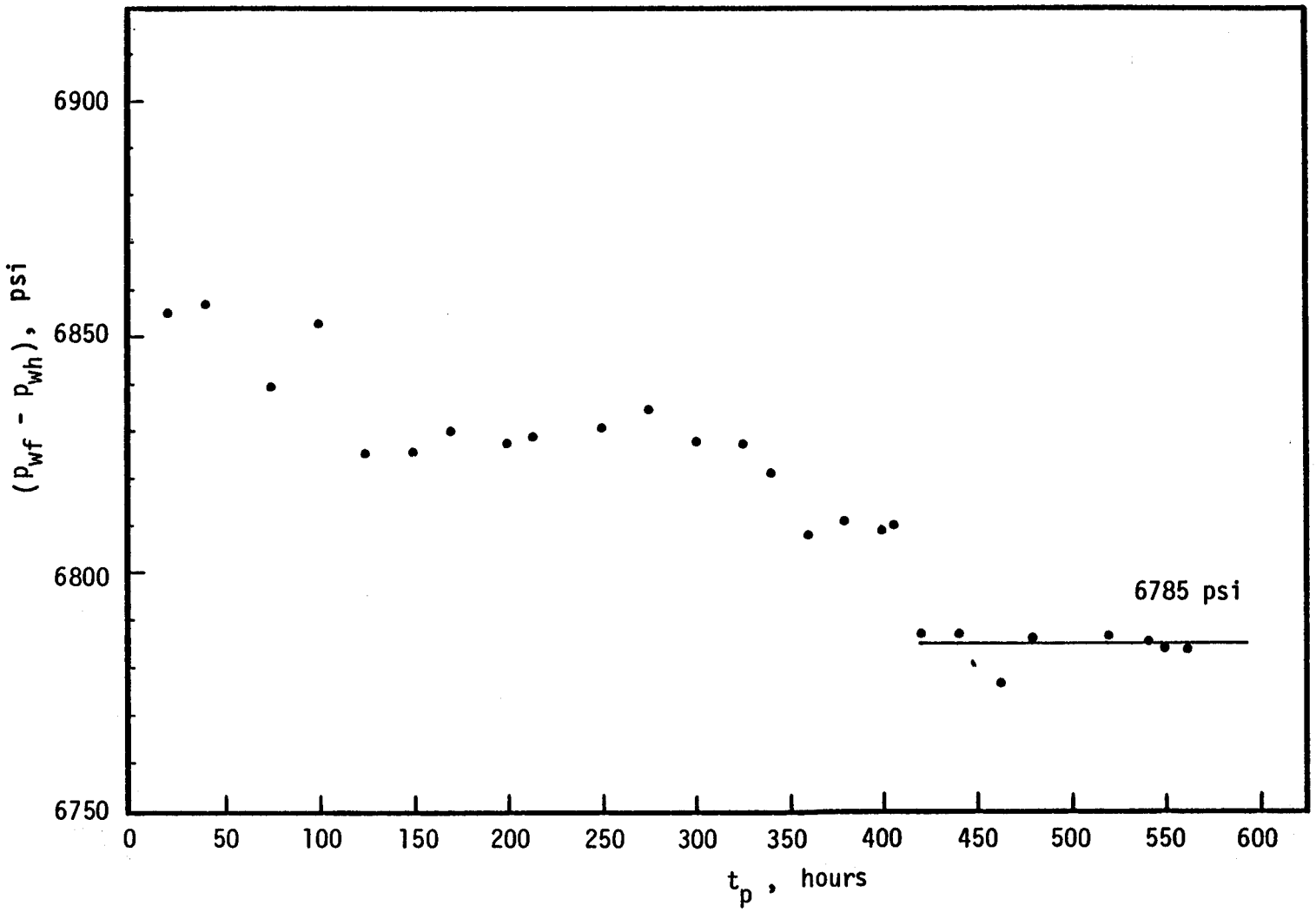

Figure 5.4. Pressure drop in the wellbore during drawdown portion of Reservoir Limits Test of Sand Zone No. 9.

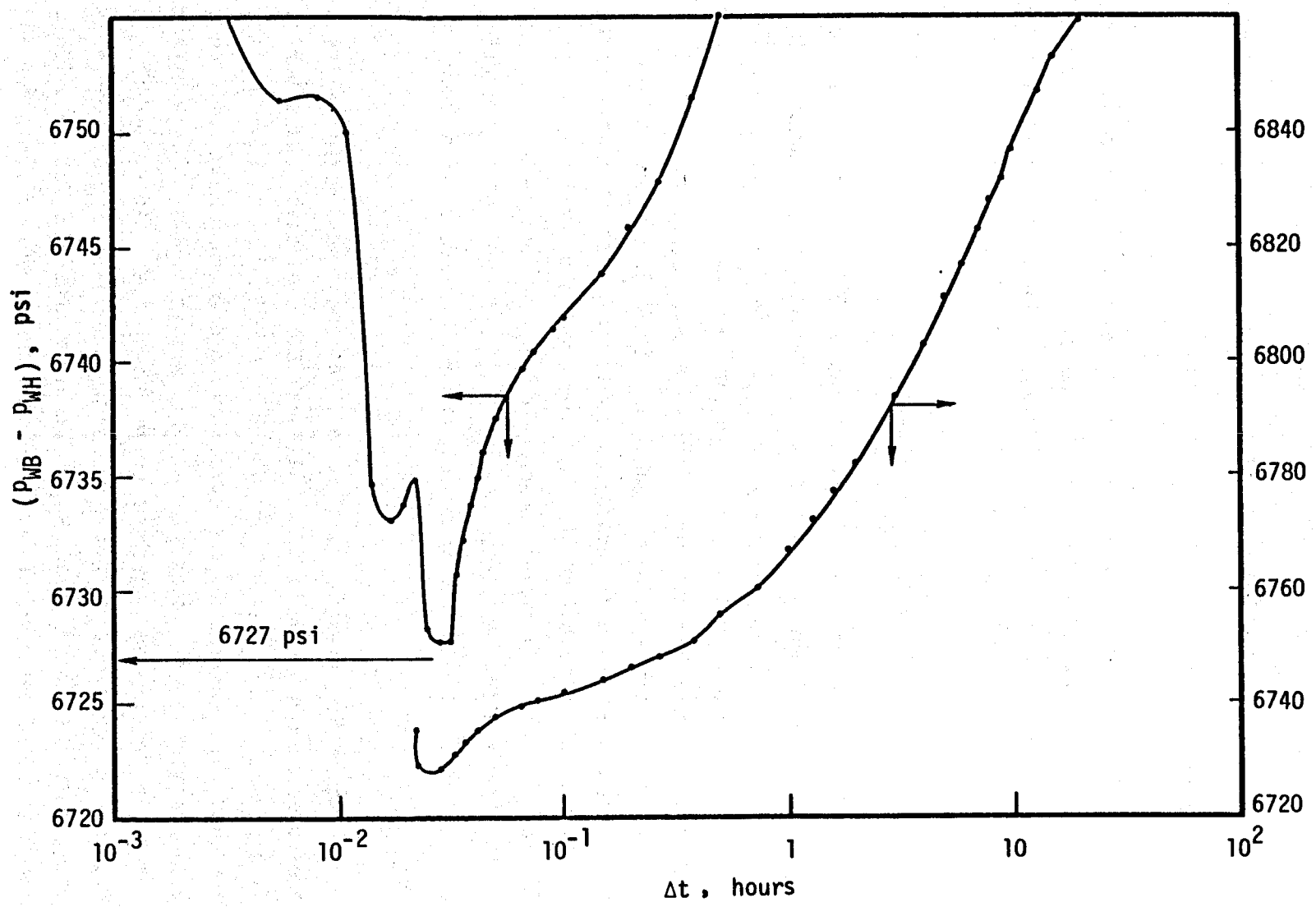

Figure 5.5. Pressure drop in the wellbore during buildup portion of Reservoir Limits Test of Sand Zone No. 9.

$$\Delta p_{fric} \sim 6785 - 6727$$

$$= 58 \text{ psi } (4.0 \times 10^5 \text{Pa}) \qquad (5.5)$$

at q = 4190 sep bbl/day.

From Figures 5.3 and 5.5 it is apparent that the values for $(p_{WB} - p_{WH})$ increase rapidly after shutting the well. Provided that p_{WH} is read at $\Delta t < \sim 3$ min, however, the error in estimating wellbottom shutin pressures from

$$p_{WB}]_{\Delta t = 0^+} = p_{WH}]_{\Delta t = 0^+} + \Delta p_{hydr} \qquad (5.6)$$

should be less than ~ 25 psi. Table 5.1 lists values of $p_{WH}]_{\Delta t=0^+}$ taken from the T-F&S Daily Reports. The shutin time (value of $\Delta t = 0^+$) is generally not given in the reports but are said to be "immediately" after closing the well. The last two wellhead pressure buildup tests did give p_{WH} values for the first few minutes after shutin as shown in Table 5.1. The values at Δt = 1 to 3 minutes are considered to be the best estimates since the afterflow effects should be completed and wellbore cooling should not be significant then. The listed estimates for the wellbottom shutin pressures, $p_{WB}]_{\Delta t = 0^+}$ are obtained by adding Δp_{hydr} = 6626 psi to the wellhead values in accord with Equation (5.3).

Figure 5.6 presents a plot of the recorded shutin wellhead pressures listed in Table 5.1. Although the production rates varied widely during the testing of the Gladys McCall No. 1 well, the averaged rate (slope of the cumulative production curve in Figure 5.1) is very nearly constant through August 1984. The apparent change in the pressure decline curve (at Q ~ 2 x 10^6 sep bbl) in Figure 5.6 would not be anticipated on the basis of the reservoir model described in Section 4.2. The more complete data available for the two more recent wellhead buildup tests (during September and October) are also in reasonable agreement with the later-time slope

Table 5.1

Estimated Shutin Values For Bottomhole Pressures Obtained
By Adding Δp_{hydr} = 6626 psi To Recorded Wellhead Values

Date	Test Time 10^7 sec	$p_{WH}]_{\Delta t=0+}$ psia	Estimated $p_{WB}]_{\Delta t=0+}$ psia	kPa	Cumulative Production sep bbl
10/28/83	0.18198	5908	12,534	86,419	297,783
1/30/84	0.99135	5422	12,048	83,068	1,333,944
2/20/84	1.17341	5200	11,826	81,537	1,783,834
3/5/84	1.29231	5240	11,866	81,813	1,933,346
6/5/84	2.08977	5178	11,804	81,386	2,848,571
6/29/84	2.29563	5070	11,696	80,641	3,303,263
7/11/84	2.39949	5006	11,632	80,200	3,534,376
7/22/84	2.50002	5011	11,637	80,234	3,703,469
8/16/84	2.71077	4962	11,588	79,896	4,057,832
9/20/84	3.01312	4696 (~ 0 min)	11,322	78,062	4,819,911
		4706 (~ 1 min)	11,332	78,131	
		4712 (~ 2 min)	11,338	78,173	
		4716 (~ 3 min)	11,342	78,200	
		4750 (~ 4 min)	11,376	78,435	
10/30/84	3.35914	4536 (~ 0 min)	11,162	76,959	5,414,585
		4667 (~ 1 min)	11,293	77,862	
		4705 (~ 2 min)	11,331	78,124	
		4717 (~ 3 min)	11,343	78,207	

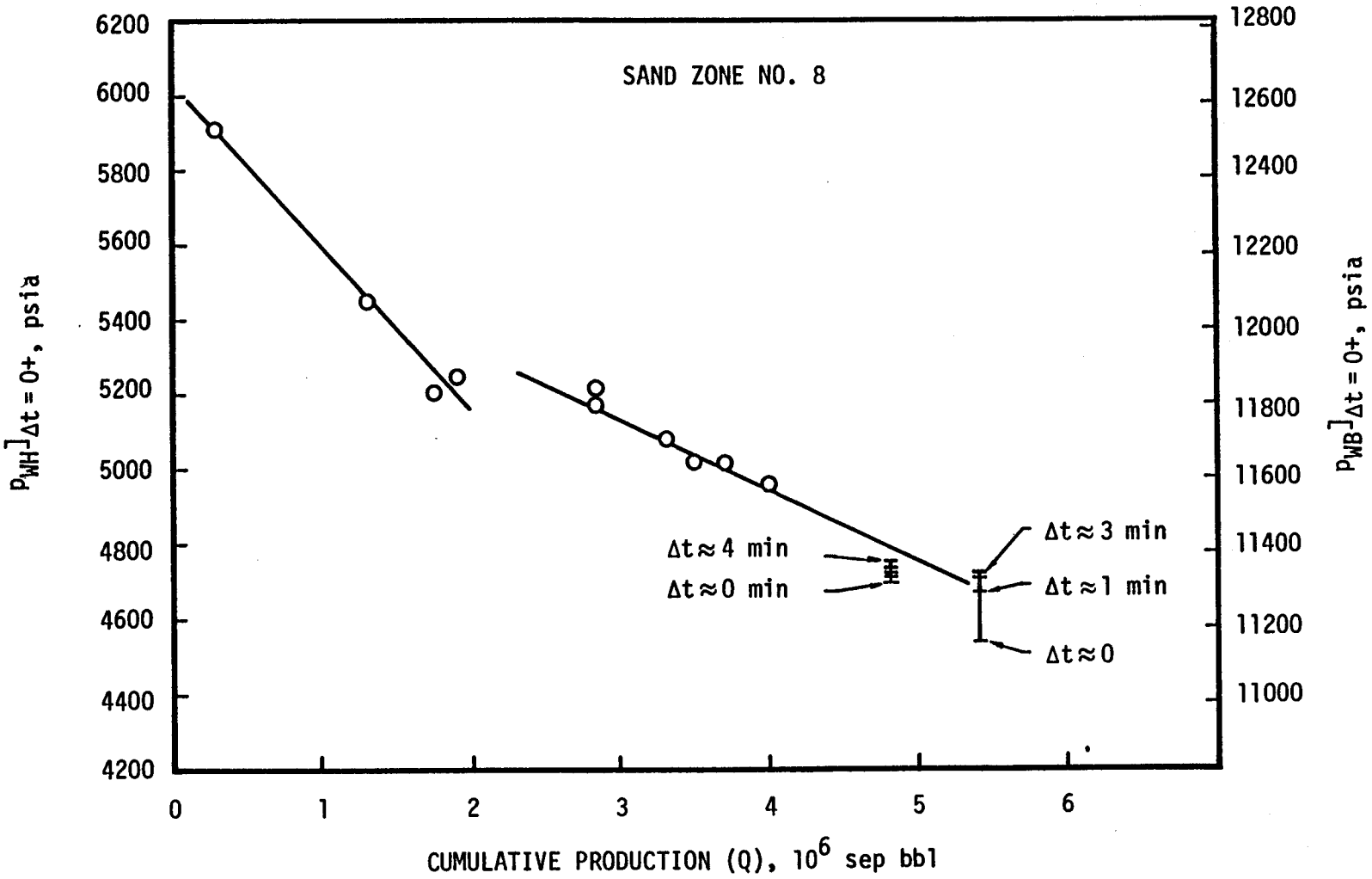

Figure 5.6. Wellhead and estimated wellbottom (15,100 ft) shutin pressures during production testing of Sand Zone No. 8.

in Figure 5.6. The production history implies that there may be additional reservoir recharge that was not evident during the Reservoir Limits Test of Sand Zone No. 8.

There have been a number (see Figure 5.1) of rather long periods during which the production was sustained at a rate q ~ 15,000 sep bbl/day. Since semi-steady state is approximately towards the end of each of these periods, Equation (5.2) may be used to estimate the wellbottom flowing pressure just prior to shutin:

$$p_{WB}]_{\Delta t = 0-} = p_{WH}]_{\Delta t = 0-} + (\Delta p_{fric} + \Delta p_{hydr})$$

During the Reservoir Limits Test (prior to scale buildup) q = 14,200 sep bbl/day and $(\Delta p_{fric} + \Delta p_{hydr})$ ~ 6992 psi; the value of $(\Delta p_{fric} + \Delta p_{hydr})$ subsequent to scale buildup will increase by the amount that Δp_{fric} increases. To illustrate the increase in Δp_{fric} we have plotted (points denoted by * in Figure 5.7) the values of

$$p_{WH}]_{\Delta t = 0-} + 6992 \text{ psi}$$

for drawdown periods for which q ~ 15,000 sep bbl/day. As shown in Figure 5.7, the deviation of these estimates from the corresponding calculated wellbottom flowing pressures increases up to the time (~ 13 x 10^6 sec) when the first acid treatment was conducted by T-F&S.

5.2 SIMULATION OF PRODUCTION TESTING

To test the adequacy of the reservoir simulation model presented in Section 4.2 (which gives an excellent match to the detailed downhole pressure history measured during the Reservoir Limits Test of Sand Zone No. 8 as shown by Figure 4.12), it has been employed to calculate the downhole pressure variations during the sand's production history. The reservoir configuration (Figure 4.11) and reservoir fluid and formation properties presented in Section 4.2 were not changed, but the calculation was continued

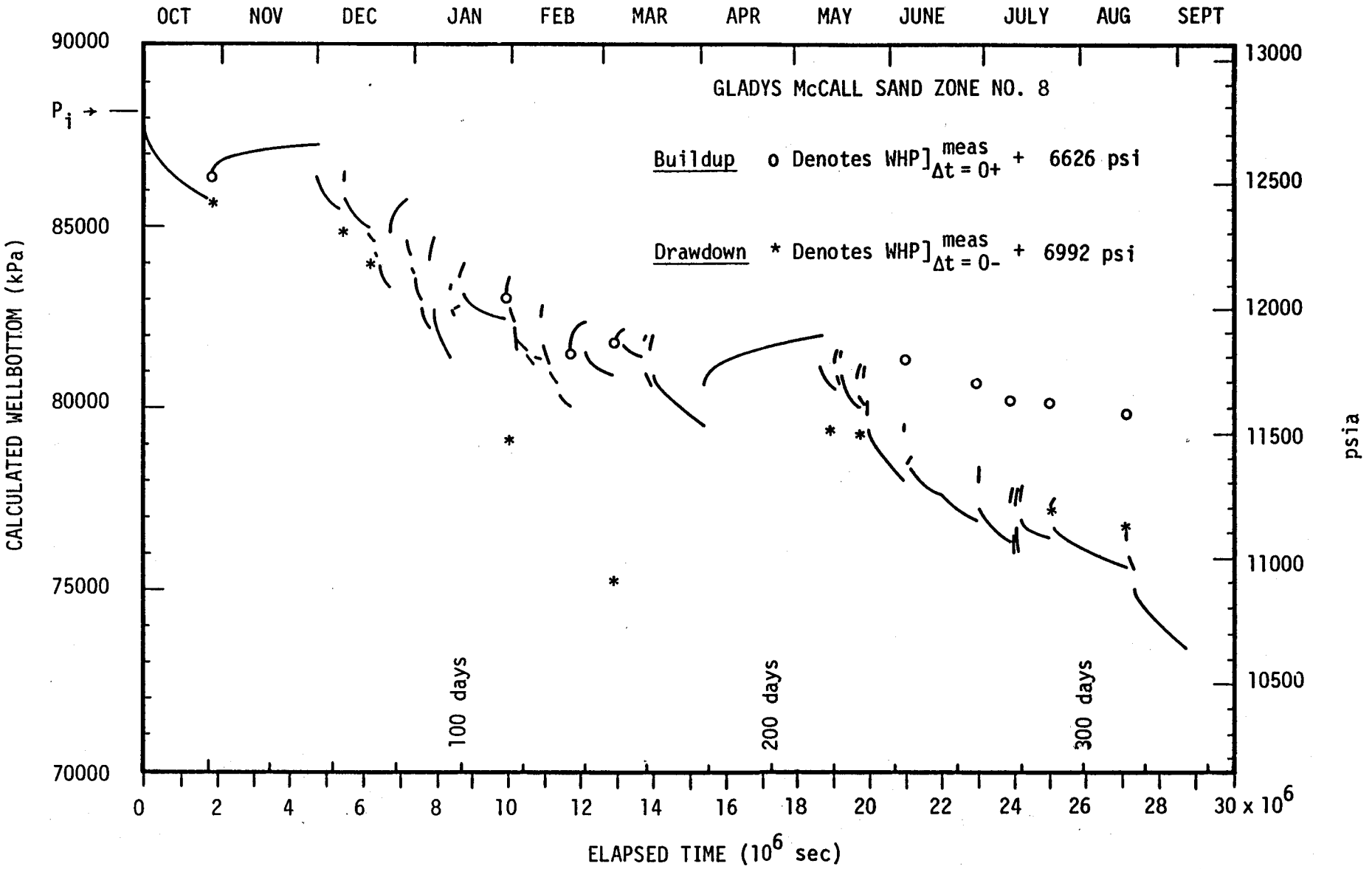

Figure 5.7. Calculated bottomhole pressure (segmented curve) during production testing of Sand Zone No. 8 using model based solely on downhole data for Reservoir Limits Test. Points denoted by o and * are values estimated from wellhead measurements.

through the over 60 rate changes that occurred during the approximately one year production period. The rate variations imposed in the simulation are illustrated in Figure 5.1; the detailed time variations of the production history used in the simulation are presented in Appendix A.

Figure 5.7 depicts the bottomhole drawdown and buildup pressure history that is predicted by the reservoir model over the simulated production period (from initiation of the Reservoir Limits Test of Sand Zone No. 8 through September 4, 1984). The nine values of

$$\text{Estimated } p_{WB}]_{\Delta t = 0^+} = p_{WH}]_{\Delta t = 0^+} + 6626 \text{ psi}$$

listed in Table 5.1 for the production period simulated are also plotted in Figure 5.7 (points denoted by o). The first four of these estimates are in excellent agreement with the simulated initial buildup values; the last five estimates lie several hundred psi above the wellbottom pressures produced by the simulation. The late-time discrepancy corresponds to the late-time deviations in the average pressure decline curve discussed above in reference to Figure 5.6.

It is apparent that either the reservoir volume estimate (Equation 4.16) based on the Reservoir Limits Test of Sand Zone No. 8 is too small, or there is some other operative reservoir response mechanism not considered in the simulation. Alternate conceptual models have been described earlier (see Figure 4.12) but we will simply assume that the volume is larger. Since the model provides an excellent fit for the earlier portion of data, the required increase in the reservoir volume of the model is "remote" from the production interval of the Gladys McCall No. 1 well.

5.3 REVISED RESERVOIR MODEL

Figure 5.8 illustrates the reservoir simulation configuration employed in a series of calculations made to provide a match to the entire production history. Since there is no information on the location of the hypothesized remote additional reservoir volume, half is added to each end of the configuration to maintain symmetry. The series of simulations employed the reservoir formation fluid and rock properties presented in Section 4.2. It was found that a match to the production history could be obtained by assuming that the "near-well" permeability (k_1 = 160 md) extends to a distance of 1100 meters (3609 ft) as before and that the "reduced" permeability (k_2 = 20 md) applies for all of the reservoir volume that lies beyond a distance of 1100 meters. The reservoir thickness was taken as 100 meters or 328 ft (as before) out to 3500 meters 11,483 ft distance from the well, but the additional "remote" volume beyond this distance was characterized by 400 meters (1312 ft) reservoir thickness. The extent of the remote reservoir volume was varied in the series of simulations by changing the single parameter L (see Figure 5.8).

The plot in Figure 5.9 illustrates the calculated wellbottom pressure histories for the seven different simulations in which only the dimensional parameter L was varied. The corresponding total reservoir volumes for the seven cases are listed in Table 5.2. Case A (L = 0) is essentially the same reservoir configuration as used in Section 4.2 to match the Reservoir Limits Test of Sand Zone No. 8. Figure 5.9 shows that all seven cases give the same results over the duration of both the drawdown and buildup portions of the Reservoir Limits Test of Sand Zone No. 8. Even after an elapsed time of 150 days the maximum difference in the calculated bottomhole pressures for the seven cases (i.e., between Cases A and G) is only about 3 bars (~ 40 psi). All seven curves may be considered to equally match the production history up to this point in time since 3 bars approximates the likely error in the values for the bottomhole buildup pressures estimated from the wellhead values. For elapsed

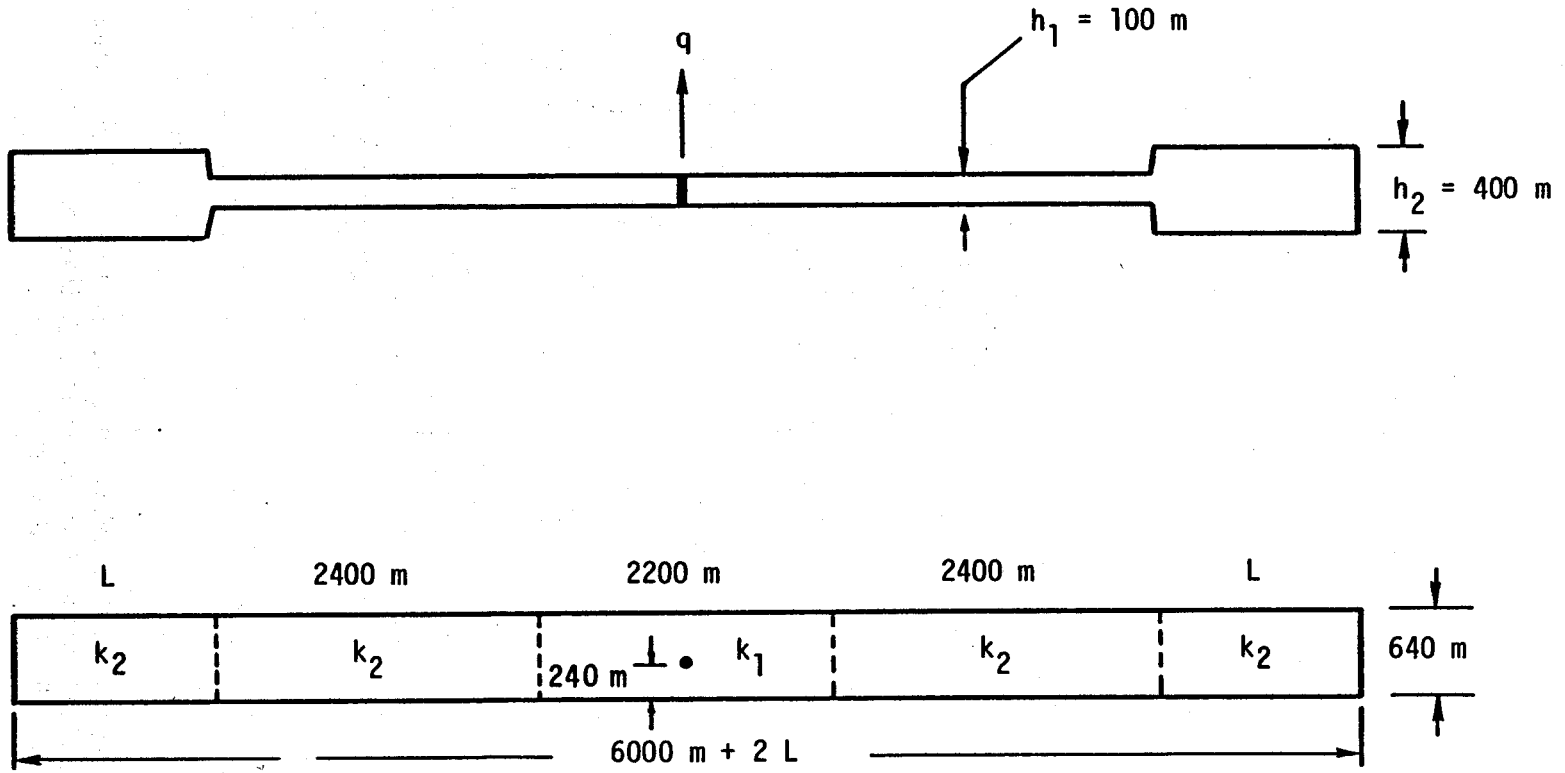

Figure 5.8. Simulation model for Sand Zone No. 8 production history matching.

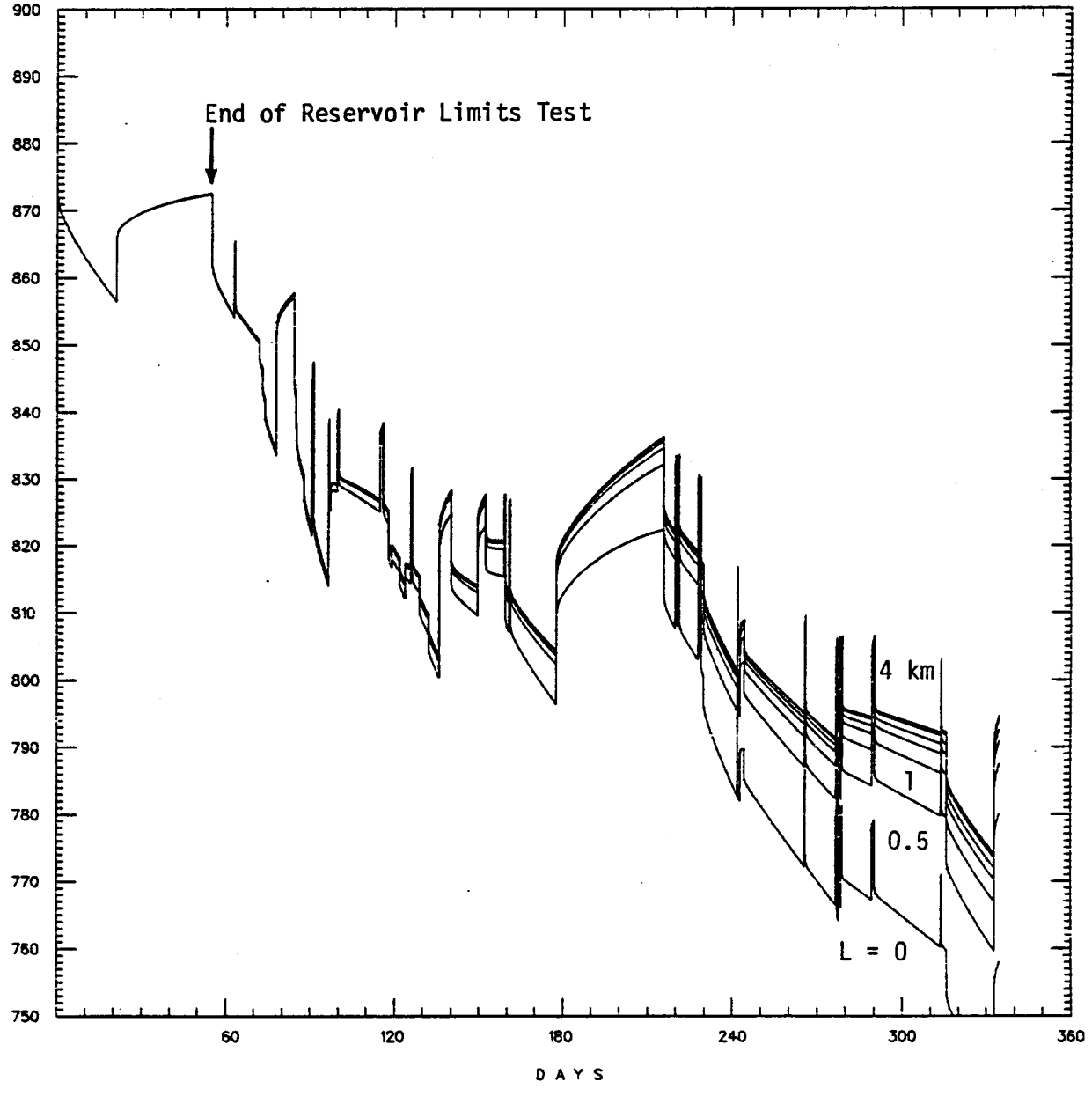

Figure 5.9. Simulated bottomhole pressures for various values of added remote volumes (Cases A through G); L = 0, 0.5, 1, 1.5, 2, 3 and 4 km.

Table 5.2

Reservoir Volumes of Seven Simulations in Which Only the Dimensional Parameter L Was Varied

Simulation No.	L 10^3m	V $10^6 m^3$	øV	
			$10^6 m^3$	10^6bbl
A	0	448	71.68	451
B	0.5	704	112.64	708
C	1.0	960	153.60	966
D	1.5	1216	194.56	1224
E	2.0	1472	235.52	1481
F	3.0	1984	317.44	1996
G	4.0	2496	399.36	2512

times greater than 150 days, however, the effect of the remote volume becomes increasingly important. The simulated wellbottom pressures for $L \geq 1.5$ km (Cases D, E, F and G) are within 3 or 4 bars (40 - 60 psi) of each other for the full production history. On the other hand, the difference between Case A (L = 0) and Case G (L = 4 km ~ 2.5 mi) exceeds 35 bars (500 psi) at the end of the simulated production history.

The late-time discrepancy between the simulated wellbottom pressures and the estimated wellbottom buildup pressures (see Figure 5.7) is eliminated by choices of $L \geq 1.5$ km. Figure 5.10 is a computer plot of the calculated bottomhole pressures over the production history of Sand Zone No. 8 for Case D (L = 1.5 km = 4921 ft). The superposed nine estimates for the downhole buildup pressures are seen to be in good agreement with the simulated buildup pressures. Figure 5.11 presents a comparison of the simulated drawdown/buildup pressures with the downhole values measured during the Reservoir Limits Test of Sand Zone No. 8. This is another form of Figure 4.12. A more detailed comparison for the individual drawdown and buildup portions of the Reservoir Limits Test is presented in Figures 5.12 and 5.13, respectively.

Cases E, F and G provide matches to the available pressure history data that are almost as good as that provided by Case D. The value of L = 1.5 km for Case D is therefore considered a lower bound and the revised estimate for the connected pore-volume is (Table 5.2)

$$V_p = \phi V > \sim 195 \times 10^6 m^3 \ (1224 \times 10^6 \text{ res bbl}) \qquad (5.7)$$

This is approximately three times the pore-volume estimated solely on the basis of the data from the Reservoir Limits Test of Sand Zone No. 8.

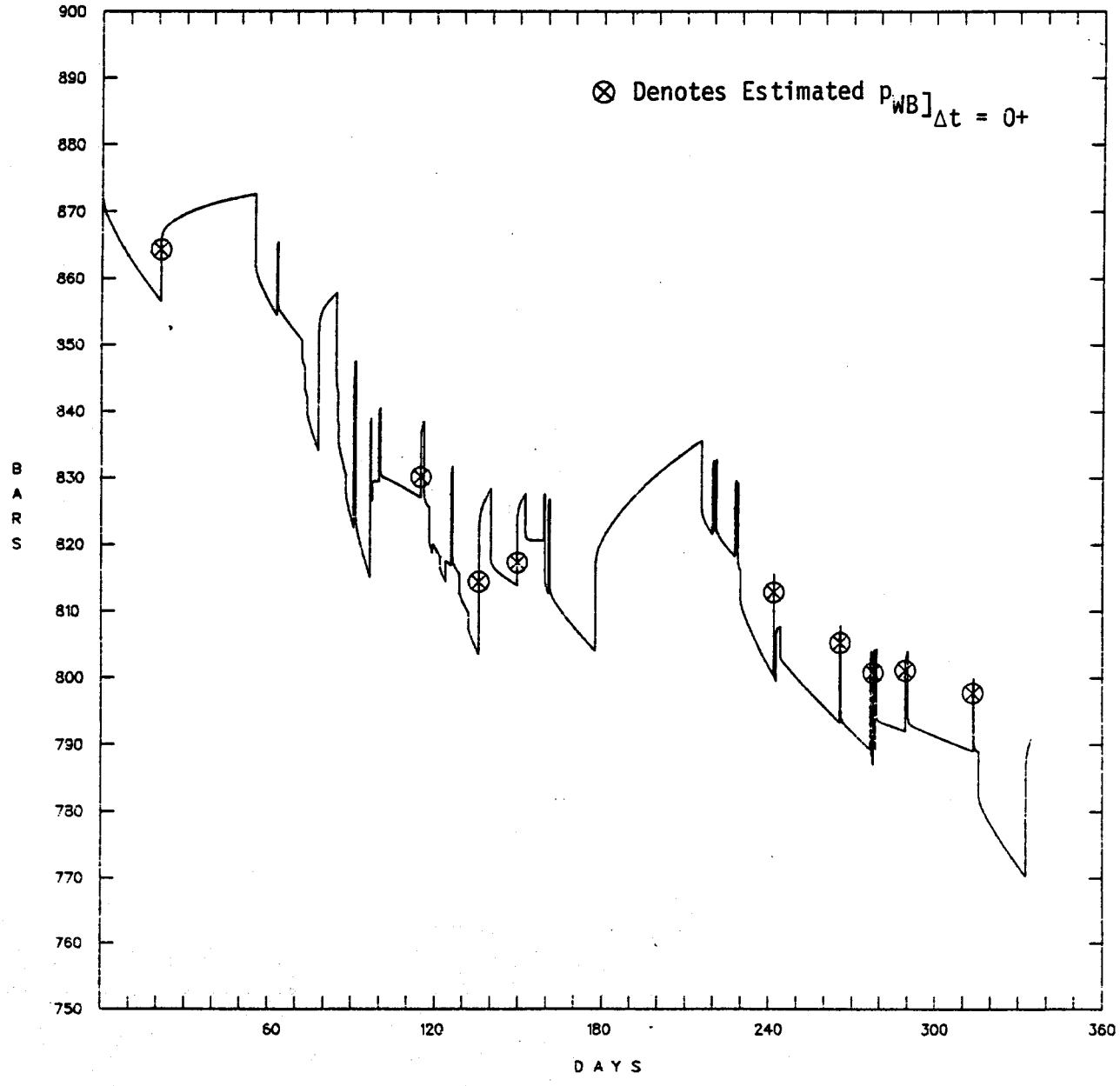

Figure 5.10. Comparison of simulated (Case D) bottomhole pressures with values estimated from wellhead measurements over the production history of Sand Zone No. 8.

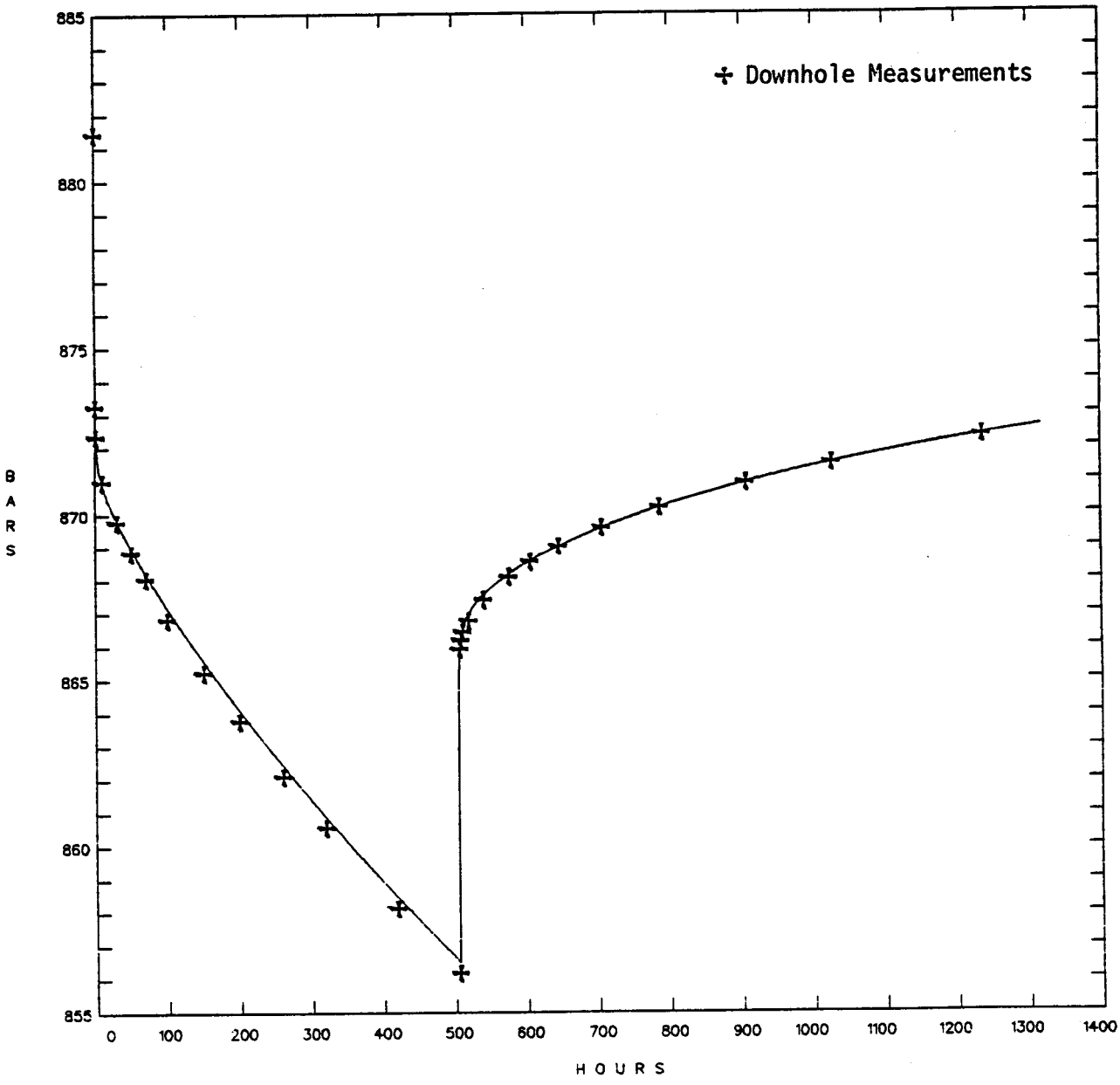

Figure 5.11. Comparison of simulated (Case D) bottomhole pressures with measured downhole drawdown/buildup pressured during Reservoir Limits Test of Sand Zone No. 8.

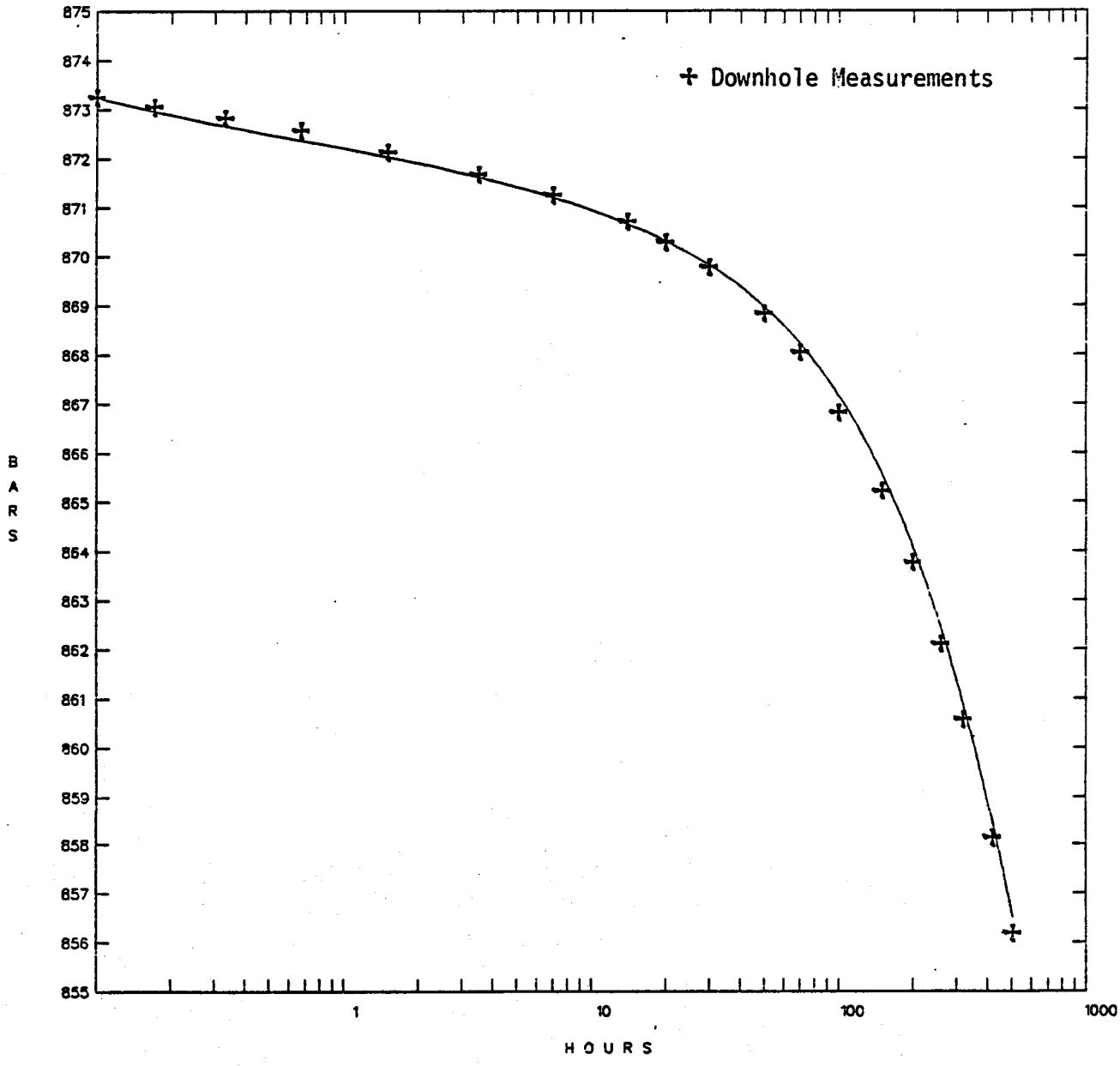

Figure 5.12. Detailed comparison of simulated (Case D) and measured bottomhole drawdown pressures during Reservoir Limits Test of Sand Zone No. 8.

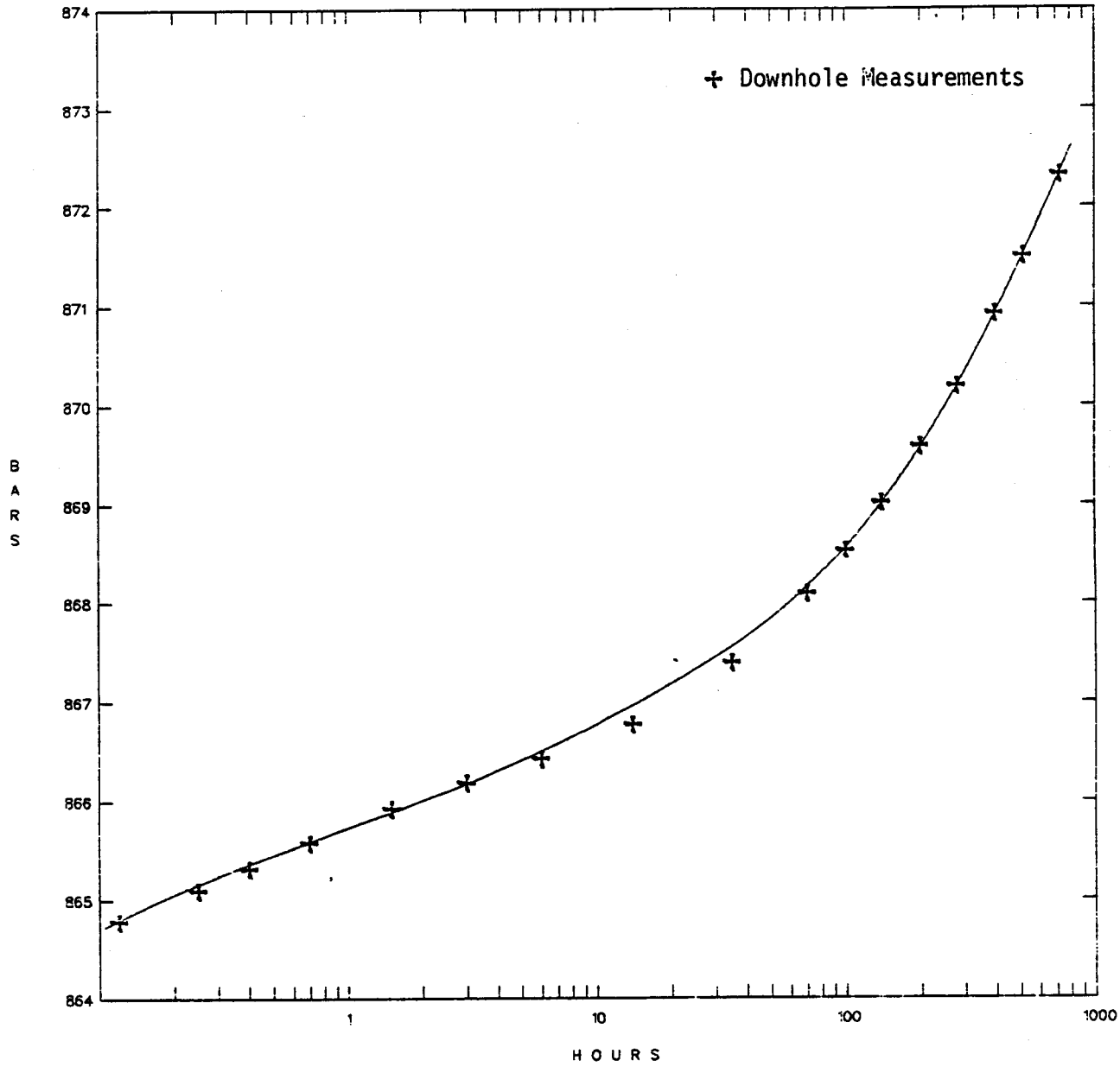

Figure 5.13. Detailed comparison of simulated (Case D) and measured bottomhole buildup pressures during Reservoir Limits Test of Sand Zone No. 8.

5.4 RECOVERABILITY PROJECTIONS

The total recoverable fluid mass from a closed reservoir of volume V is given by

$$M = \rho \phi V C_T \Delta p \tag{5.8}$$

where Δp is the allowable drop in the reservoir pressure from its initial value p_i. Assuming semi-steady state flow, Δp is approximated by

$$\Delta p = p_i - p_{WH} - \Delta p_{fric} - \Delta p_{hydr} - \Delta p_{res} \tag{5.9}$$

where

p_{WH} ~ Wellhead pressure required.

Δp_{fric} ~ Pressure loss due to wellbore friction.

Δp_{hydr} ~ Pressure loss due to elevation.

Δp_{res} ~ Pressure drop in reservoir.

The value of the pressure drop depends on the assumed constant flow rate during the semi-steady state.

The ultimate recoverability is computed by assuming that the flow rate is very small and that the production is continued until the wellhead pressure drops to 1×10^5 Pa (14.5 psia). In this case

$$\Delta p_{max} \sim p_i - p_{WH} - \Delta p_{hydr}$$

With $p_i = 881.43 \times 10^5$Pa (12,784 psia) and $\Delta p_{hydr} = 457 \times 10^5$Pa (6626 psi), we compute $\Delta p_{max} \sim 423 \times 10^5$Pa (6143 psi). Using $\rho = 1030.5$ kg/m^3, $(\phi V) = 195 \times 10^6$m^3 and $C_T = 9.1 \times 10^{-10}$Pa^{-1}, we obtain the following estimate for the ultimate recoverable fluid mass

$$M_{max} = (1030.5)(195 \times 10^{6})(9.1 \times 10^{-10})(423 \times 10^{5}) \tag{5.10}$$

$$\sim 7.74 \times 10^{9}\text{kg} .$$

The corresponding ultimate recoverable fluid volume is

$$Q_{max} = \frac{M_{max}}{\rho} B = (7.74 \times 10^{9})(0.984)/(1030.5) \tag{5.11}$$

$$= 7.38 \times 10^{6}\text{m}^{3}(46.5 \times 10^{6} \text{ sep bbl}) .$$

At a flow rate of 14,170 sep bbl/day, an estimate for the frictional pressure drop (prior to scaling) is available from (5.4), $\Delta p_{fric} \sim 25.23 \times 10^{5}$Pa(366 psi). From the reservoir simulation (Case D) we have $\Delta p_{res} \sim 18 \times 10^{5}$Pa(261 psi). If we assume that Sand Zone No. 8 is produced until the wellhead pressure drops to $p_{WH} = 68.94 \times 10^{5}$Pa (1000 psia), then Equation (5.8) yields

$$\Delta p \sim 312 \times 10^{5}\text{Pa}(4530 \text{ psi}) .$$

The corresponding estimates for the recoverable fluid mass and recoverable fluid volume at q = 14,170 sep bbl/day are as follows:

$$M \sim 5.70 \times 10^{9}\text{kg} \tag{5.12}$$

$$Q \sim 5.44 \times 10^{6}\text{m}^{3}(34.2 \times 10^{6} \text{ sep bbl}) .$$

VI. CONCLUDING REMARKS

The downhole pressure data measured during both the drawdown and buildup portions of the Reservoir Limits Test of Sand Zone No. 8 are closely matched using a reservoir model with linear formation properties (Section 4.2). The downhole measurements (for Sand Zones No. 8 and No. 9) available give no indication of any nonlinear processes operating in the reservoir. The total production during the Reservoir Limits Test of Sand Zone No. 8, however, was less than two percent of the production to date (December 1984) and no further downhole measurements have been made in the Gladys McCall No. 1 well.

Estimated values for the downhole pressures in Sand Zone No. 8 (based on wellhead measurements) during the production period indicate an apparent change in the slope of the pressure decline curve after a pressure drop of $\Delta p \sim 1{,}000$ psi (Figure 5.6). In the absence of any direct evidence of nonlinear reservoir behavior, we have chosen to retain the assumption of linear formation properties in the reservoir model and to match the full production history by hypothesizing a larger reservoir volume; an extra remote reservoir volume is added to the original reservoir model (Figure 5.9). An excellent match to the measured (Reservoir Limits Test) and estimated (Production History) downhole pressure history is obtained using the resulting simulation model (Section 5.3). The simulation model is not unique, however, and equally satisfying history matches might be obtained using alternate models.

We first note that, even in the context of a linear model, the location of the added reservoir volume cannot be determined on the basis of limited data from a single well. The added "remote reservoir volume" may actually be from neighboring sands that immediately overlay or underlie Sand Zone No. 8. These neighboring sands may provide vertical recharge to Sand Zone No. 8 at some distance where intervening shale layers are pinched out. The fluids produced from Sand Zones No. 8 and No. 9 are indeed almost identical.

Alternatively, the apparent change in the slope of the pressure decline curve could be the result of a nonlinear reservoir response mechanism. We note that the reservoir pressure drop at which the slope change occurs is essentially the same value as the pressure drop in the DOW/DOE L. R. Sweezy No. 1 well ($\Delta p \sim 900$ - 1,100 psi) at which there was an apparent change in the pressure decline curves (Garg and Riney, 1984). The L. R. Sweezy geopressued-geothermal design well, however, also displayed nonlinear response mechanisms in the short-term flow test downhole measurements.

The production testing of Sand Zone No. 8 is still in progress. It is strongly recommended that additional downhole pressure transient measurements be made in the Gladys McCall No. 1 well while this sand is still being tested. The downhole drawdown and buildup response should be monitored sufficiently long that boundaries are detected so that any changes both in permeability and/or compressibility can be determined. Such changes apparently occurred in the formation properties tested by the L. R. Sweezy No. 1 Well (Garg and Riney, 1984).

Table 6.1 summarizes the results available from the four geopressured-geothermal Design Wells (reservoirs description and permeability data are taken from analyses performed by S-CUBED). The pore fluids from three wells (Sweezy, Pleasant Bayou and Gladys McCall) are close to saturation; the Amoco Fee reservoir, on the other hand, appears to be undersaturated with respect to dissolved gas. Reservoir temperatures vary from a low of 237°F (Sweezy well) to a high of 306°F (Pleasant Bayou). Fluid salinities lie in the range of 100,900 mg/L to 165,000 mg/L. The Pleasant Bayou and Gladys McCall wells produce from large reservoir volumes (more than 0.4 cubic mile for Pleasant Bayou Sand C and more than 0.3 cubic mile for Gladys McCall Sand Zone 8, respectively). The formation permeabilities tested by both wells are also relatively high. The Sweezy well was designed to deplete a reservoir of limited volume. The Amoco Fee well exhibited a much larger and more rapid pressure drawdown during flow testing than anticipated.

Table 6.1 Results from Design Wells Tested Under the Department of Energy's Geopressure Program (Status as of December 1984)

	WELL (YEAR TESTED)	FORMATION	PRODUCING INTERVAL DEPTH, FT	GROSS (NET) SAND THICKNESS (FT)	RESERVOIR PRESSURE PSIA	TEMPERATURE (^{o}F)	SALINITY TDS (MG/L)	LABORATORY GAS/WATER SOLUTION RATIO SCF/BBL	POROSITY (%) PERMEABILITY (MD)	MAXIMUM FLOW RATE BBL/DAY	PRODUCING GAS/WATER RATIO SCF/BBL	RESERVOIR DESCRIPTION AND COMMENTS
1.	PLEASANT BAYOU NO.2 (1979,1980) [1]	FRIO OLIGOCENE	14,644-14,704	(60)	~11,168	~306	~130,000	~27* *FROM CORRELATIONS	~17.6 ~192	~19,000	~23* *SEPARATOR VALUE (300 PSIA)	ONE BARRIER AT ~3000 FT FROM WELLBORE. RESERVOIR VOLUME ~0.4 MI^3.
2.	MG-T/DOE AMOCO FEE NO. 1 WELL (1981) [2]	MIOCYP SAND FRIO UPPER OLIGOCENE	13,367-13,414	(27)	~12,082	~299	~165,000	~24* *RECOMBINATION MEASUREMENT (WEATHERLY LABORATORIES) ~24** **CORRELATIONS	22 162 FOR R ≤ 200 FT; ~12 FOR R ≥ 200 FT	~16,000	23-27	TWO ALTERNATIVE RESERVOIR INTERPRETATIONS: (1) LOW PERMEABILITY BEYOND 250 FT (2) FLOW ANGLE ~26 DEG.
3.	DOW-DOE SWEEZY NO.1 WELL (1981-1982) [3]	UPPER FRIO OLIGOCENE	13,349-13,386 13,395-13,406	(56)	~11,410-11,447	~237	~160,000	UNAVAILABLE	27 133	~11,000	±20	RESERVOIR AREA ~830 ACRES. SOME EVIDENCE OF RECHARGE
4.	T-P&S/DOE GLADYS MCCALL NO.1 WELL (1982, PRESENT)	MIOCENE SAND	15,158-15,490 (SAND ZONE NO. 8)	(332)	~12,784	~289	~97,000	~30* RECOMBINATION MEASUREMENT (WEATHERLY LABORATORIES)	~16 ~160	~14,000	~30* *SEPARATOR VALUE (500 PSIA)	RESERVOIR VOLUME ~0.3 MI^3 SOME EVIDENCE OF RECHARGE

[1] GARG, S.K., T.D. RINEY AND J.M. FWU, "ANALYSIS OF PHASE I FLOW DATA FROM PLEASANT BAYOU NO 2 GEOPRESSURED WELL," PROCEEDINGS 5TH CONFERENCE GEOPRESSURED-GEOTHERMAL ENERGY, BATON ROUGE, LOUISIANA, PP. 97-100, OCTOBER 1981.

[2] GARG, S.K., "ANALYSIS OF FLOW DATA FROM THE MG-T/DOE AMOCO FEE NO. 1 WELL," DOE REPORT NO. DOE/NV/10150-3 JANUARY 1982.

[3] GARG, S. K. AND T. D. RINEY ANALYSIS OF FLOW DATA FROM THE DOW/DOE L. R. SWEEZY NO. 1 WELL, DOE REPORT NO. DOE/NV/10150-5, MARCH 1984.

[4] THIS REPORT.

Sufficient pressure drawdown data are available during the depletion of the flow tests of the Sweezy and Gladys McCall wells to conclude phase that unanticipated reservoir drive mechanisms are operative; in both cases the pressure is maintained at a higher value than expected. The long-term pressure maintainance may be the result of stress-dependent compressibility, long-term formation creep, shale-water recharge, cross-flow from overlying/underlying sands, or leakage across boundary faults. Long-term testing with at least intermittant downhole pressure transient tests are required to provide data for distinguishing between these possibilities. Since the Sweezy well has been plugged and abandoned, it is strongly recommended that the future test program for the Gladys McCall well include downhole pressure measurements.

REFERENCES

Ancell, K. (1984), "Reservoir Analysis - Gladys McCall No. 1," Dowdle Fairchild and Ancell, Inc. Report, May.

Durrett, L. R. (1982), "Technodril-Fenix and Scisson Gladys McCall Project," Presentation at DOE/Industry Geopressured Geothermal Resource Development Program Working Group, Houston, Texas, Minutes Prepared by C. K. Geo Energy Corporation, December 2.

Durrett, L. R. (1983), "Technodril-Fenix and Scisson Gladys McCall Project," Presentations at DOE/Industry Geopressured Geothermal Resource Development Program Working Group, Houston, Texas, Minutes Prepared by C. K. Geo Energy Corporation, June 9.

Durrett, L. R. (1984), "Technodril-Fenix and Scisson Gladys McCall Project," Presentation at DOE/Industry Geopressured Geothermal Resource Development Program Working Group, Houston, Texas, Minutes Prepared by C. K. Geo Energy Corporation, January 10.

Garg, S. K., T. D. Riney and J. M. Fwu (1981), "Analysis of Phase I Flow Data from Pleasant Bayou No. 2 Geopressured Well," Department of Energy Report No. DOE/NV/10150-1, March.

Garg, S. K. (1982), "Analysis of Flow Data from the MG-T/DOE Amoco Fee No. 1 Well," Department of Energy Report No. DOE/NV/10150-3, January.

Garg, S. K. and T. D. Riney (1984a), "Analysis of Flow Data from the DOW/DOE L. R. Sweezy No. 1 Well," Department of Energy Report No. DOE/NV/10150-5, March.

Garg, S. K. and T. D. Riney (1984b), "Brine and Gas Recovery from Geopressured Systems: I. Parametric Calculations," Department of Energy Report No. DOE/NV/10150-4, February.

Kelkar, S., C. Coley, J. Schatz and T. Borschel (1982), "Core Handling, Testing and Analysis for DOE/T-F S Gladys McCall No. 1 Well, Cameron Parish, Louisiana, Terra Tek, Inc. Report TR 82-64, September.

Technodril-Fenix and Scisson (1982), "Geopressured-Geothermal Drilling and Testing Plan: T-F&S/DOW Gladys McCall No. 1 Well, Cameron Parish, Louisiana," Vol. II - Testing Plan, U. S. Department of Energy, Nevada Operations Office, Report No. NVO-229, January.

Weatherly Laboratories, Inc. Report (1983a), "Reservoir Fluid Analysis for Technodril-Fenix and Scisson, Inc., Gladys McCall Well No. 1, Sand 9, East Crab Lake Field, Cameron Parish, Louisiana," April 30.

Weatherly Laboratories, Inc. Report (1983B), "Reservoir Fluid Analysis for Technodril-Fenix and Scisson, Inc. Gladys McCall Well No. 1, Sand 8, East Crab Lake Field, Cameron Parish, Louisiana," October 23.

APPENDIX

FLOW RATE DATA USED IN SIMULATION OF SAND ZONE NO. 8 PRODUCTION HISTORY

Date	Time	Elapsed Time (hrs)	Elapsed Time 10^6 sec	Cumulative Production (sep bbl)	Flow Rate sep bbl/day	Flow Rate kg/sec
10/7/83	13:14:40	0	0	0	14,162	26.03
10/28/83	13:16:10	505.5	1.8198	297,783	0	0
12/1/83	10:10	1316.92	4.7409	297,783	15,648	28.76
12/9/83	9:20	1508.09	5.4291	422,428	0	0
12/9/83	16:20	1515.09	5.4543	422,428	14,269	26.23
12/18/83	13:00	1727.76	6.2199	548,869	18,665	34.31
12/19/83	13:00	1751.75	6.3063	567,534	23,601	43.38
12/20/83	11:00	1773.75	6.3855	589,169	27,279	50.14
12/24/83	10:25	1869.17	6.7290	697,626	0	0
12/30/83	18:00	2020.75	7.2747	697,626	19,803	36.40
12/31/83	9:00	2035.75	7.3287	710,003	25,832	47.48
12/31/83	15:00	2041.75	7.3503	716,461	29,747	54.68
1/3/84	9:00	2107.75	7.5879	798,266	34,271	62.99
1/6/84	5:00	2175.75	7.8327	895,353	0	0
1/6/84	18:30	2189.25	7.8813	895,355	34,325	63.09
1/12/84	2:05	2316.83	8.3406	1,077,820	0	0
1/12/84	6:45	2321.50	8.3574	1,077,820	18,752	34.47
1/12/84	17:00	2331.75	8.3943	1,085,829	14,865	27.32
1/15/84	3:00	2389.75	8.6031	1,121,753	0	0
1/15/84	14:00	2400.75	8.6427	1,121,753	14,427	26.52
1/30/84	7:00	2753.75	9.9135	1,333,944	0	0
1/31/84	12:00	2782.75	10.0179	1,333,944	16,630	30.57
2/2/84	9:00	2827.75	10.1799	1,365,126	24,097	44.29
2/3/84	15:00	2857.75	10.2879	1,395,247	21,973	40.39
2/6/84	9:00	2923.75	10.5255	1,455,673	24,715	45.43
2/8/84	9:00	2971.75	10.6983	1,505,203	20,222	37.17
2/10/84	7:00	3017.75	10.8639	1,543,869	0	0
2/10/84	19:00	3029.75	10.9071	1,543,869	20,548	37.77
2/13/84	11:00	3093.75	11.1375	1,598,732	24,900	45.77
2/16/84	15:00	3169.75	11.4111	1,677,589	28,415	52.23
2/20/84	8:44	3259.48	11.7341	1,783,834	0	0
2/24/84	14:00	3360.75	12.0987	1,783,834	15,672	28.81
3/5/84	3:00	3589.75	12.9231	1,933,346	0	0
3/8/84	1:00	3659.75	13.1751	1,933,346	9,477	17.42
3/14/84	13:00	3815.75	13.7367	1,994,944	0	0

Date	Time	Elapsed Time (hrs)	Elapsed Time 10^6 sec	Cumulative Production (sep bbl)	Flow Rate sep bbl/day	Flow Rate kg/sec
3/14/84	23:00	3825.75	13.7727	1,994,944	19,489	35.82
3/16/84	6:00	3856.75	13.8843	2,200,124	0	0
3/16/84	16:45	3867.50	13.9230	2,020,124	19,709	36.23
4/2/84	5:00	4263.75	15.3495	2,345,515	0	0
5/10/84	7:30	5178.25	18.6417	2,345,515	15,287	28.10
5/14/84	7:30	5278.25	18.9873	2,406,661	0	0
5/14/84	19:00	5285.75	19.0287	2,406,661	14,942	27.46
5/15/84	5:00	5295.75	19.0647	2,412,892	0	0
5/15/84	17:20	5308.08	19.1091	2,412,892	15,386	28.28
5/22/84	7:00	5465.75	19.6767	2,513,979	0	0
5/22/84	19:45	5478.50	19.7226	2,513,979	14,989	27.55
5/23/84	7:00	5489.75	19.7631	2,521,024	0	0
5/23/84	23:15	5506.00	19.7784	2,521,024	17,995	33.08
5/24/84	9:00	5515.75	19.8567	2,528,330	24,634	45.28
6/5/84	10:10	5804.92	20.8977	2,825,143	0	0
6/5/84	10:31	5805.27	20.8990	2,825,143	24,634	45.28
6/6/84	9:00	5827.75	20.9799	2,848,571	13,703	25.19
6/7/84	17:00	5862.75	21.1059	2,868,577	20,293	37.30
6/29/84	6:00	6376.75	22.9563	3,303,263	0	0
6/29/84	12:45	6383.50	22.9806	3,303,263	20,281	37.28
7/10/84	6:00	6640.75	23.9067	3,520,674	0	0
7/10/84	16:45	6651.50	23.9454	3,520,674	23,913	43.95
7/11/84	6:30	6665.25	23.9949	3,534,376	0	0
7/11/84	18:00	6676.75	24.0363	3,534,376	21,124	38.83
7/12/84	6:00	6688.75	24.0795	3,544,938	0	0
7/12/84	15:00	6697.75	24.1119	3,544,938	15,421	28.34
7/22/84	21:45	6944.50	25.0002	3,703,469	0	0
7/23/84	20:30	6967.25	25.0821	3,703,469	15,118	27.79
8/16/84	7:10	7529.92	27.1077	4,057,832	0	0
8/16/84	15:00	7537.75	27.1359	4,057,832	15,197	27.93
8/18/84	8:00	7578.75	27.2835	4,083,794	25,162	46.25
9/4/84	7:08	7985.88	28.7492	4,510,634	0	0